**Laboratoire de Mécanique, Matériaux et Structures**

*Laboratory of Mechanics, Materials and Structures*

# Nonlinear Pounding and Engineering Failure Analysis of Non-smooth Structural Systems Subjected to Stochastic Excitations

*Thesis submitted in partial fulfillment of the requirements for the award of the degree of Doctor of Philosophy (Ph.D.) in Physics,*
Specialty: **Fundamental Mechanics and Complex Systems**

By

**PAUL NDY VON KLUGE**

Registration Number: **96S567**

*Master of Science in Physics*

Under the Supervision of

**Germaine DJUIDJE KENMOE épouse ALOYEM KAZE**

*Professor*

*University of Yaoundé I*

**KOFANE Timoléon Crépin**

*Professor*

*University of Yaoundé I*

**2021**

**DEPARTEMENT DE PHYSIQUE**
DEPARTMENT OF PHYSICS

# ATTESTATION DE CORRECTION DE LA THESE DE DOCTORAT/Ph.D

Nous, Professeur **NANA NBENDJO Blaise Roméo** et Professeur **WOAFO Paul**, respectivement Examinateur et Président du jury de la Thèse de Doctorat/Ph.D de Monsieur **Paul NDY VON KLUGE** Matricule **96S567**, préparée sous la direction du Professeur **Germaine DJUIDJE KENMOE épouse ALOYEM KAZE** et sous la supervision du Professeur **KOFANE Timoléon Crépin**, intitulée : « **Nonlinear pounding and engineering failure analysis of non-smooth structural systems subjected to stochastic excitations**», soutenue le **Jeudi, 29 Avril 2021**, en vue de l'obtention du grade de Docteur/Ph.D en Physique, Spécialité **Mécanique, Matériaux et Structures**, attestons que toutes les corrections demandées par le Jury de soutenance ont été effectuées.

En foi de quoi, la présente attestation lui est délivrée pour servir et valoir ce que de droit.

Fait à Yaoundé le .... **1 8 MAY 2021** ......

**Les Examinateurs**

**Le Président du Jury**

**Pr. NANA
NBENDJO Blaise**

**Pr. WOAFO Paul**

Le Chef de Département de Physique

*Ndjaka Jean-Marie
Bienvenu
Professeur*

# Nonlinear pounding and engineering failure analysis of non-smooth structural systems subjected to stochastic excitations

Submitted in partial fulfillment of the requirements
for the degree of Doctor of Philosophy (Ph.D.) in Physics
at the University of Yaoundé I

By

**PAUL NDY VON KLUGE**

Postgraduate School of Science, Technology and Geosciences,
University of Yaounde I, P.O. Box 812, Yaounde, Cameroon
*Registration Number:* **96S567**

Under the supervision of

**Prof. Germaine DJUIDJE KENMOE épouse ALOYEM KAZE**
*Professor, University of Yaounde I*

and

**Prof. Timoléon Crépin KOFANE**
*Professor, University of Yaounde I*

*"Le commencement de la sagesse, c'est la crainte de l'Eternel ; Et la science des saints, c'est l'intelligence."*

**Proverbes 9:10**

# Dedications

*To my late Father MBARGA Ndy Auguste, my late Mother BILO'O Marinette and grandmother BESSE'E Moline*

# Acknowledgments

- First of all, I thank the Almighty Lord for the strength he is providing me with and the mercy he is having on me since my childhood.

- Many thanks to Pr. DJUIDJE Kenmoe Germaine épouse ALOYEM Kaze, for her time, patience, for her constant encouragement and invaluable direction in the preparation of this thesis. This work wouldn't have made even a half as formidable door-stop without her pointed advices and valuable suggestions. Her rectitude, her sympathetic attitude and her encouragements enabled me to broaden my knowledge and improve my research skill and capability.

- I am also very grateful to Pr. KOFANE Timoleon Crepin. This thesis certainly would not have been possible without his offer of worthwhile research environment within the Laboratory of Mechanics, Materials Science and Structures. Thank you, Pr. KOFANE for the opportunity to undertake a postgraduate studies in this team you gave me and for this, I am very grateful.

- I would like to thank each member of jury who has accepted to evaluate the present work.

- I express my gratitude to Pr. BEN Boli, Pr. Thomas BOUETOU Bouetou, Pr. NJANDJOCK Nouck Philippe, Pr. NANA Nbendjo Blaise Roméo and Pr. FEWO Serge Ibraid , for many fruitful discussions on different aspects of nonlinear physics. I can not forget their senses of availability and help.

- I would like to sincerely thank all those who have dedicated their time to teach me a part of what they knew, from the primary school to the University, with a particular

emphasis on the teaching staff of the Departments of Physics of the Universities of Yaounde I.

- I am particularly impressed and grateful to my teachers Pr. TCHAWOUA Clement, Pr. WOAFO Paul, Pr. NDJAKA Jean-Marie, Pr. ZEKENG Serges, Pr. BIYA Motto Frédéric, Pr. TCHOFFO Martin and Dr. WOULACHE Rosalie for their teaching and permanent encouragements.

- I wish to express my deepest obligations to my late father MBARGA NDY Auguste, my late mother BILO'0 Marinette and my late grandmother BESSE'E Moline who always pray for my success in all aspects of life. It is indeed because of their prayers and their financial supports that I have been able to achieve this work.

- Particular thanks to my grandfather NSOLO Beh Salomon, my uncle NGAMENGAME Monembama Georges, Mr. NLENG, my elders brothers MESSI Etienne, NDY Amougou Hermann, MBARGA Hector and my elder sister BIKIE Régine for their encouragements.

- I thank all my own family particularly my love wive MBALLA Christelle Tatiane, my children BILO'O Ndy Marinette G., ABODO Ndy Ingrid R., MBARGA Ndy Auguste D., NDY Amougou Israel, and MBALLA Ndy Abigaelle.

- Fruitful discussions with my present Ph.D mates are also to be appreciated: SEN-GHA Ghislain gérard, Dr. NDJOMATCHOUA Frank Thomas, Dr. Takoutsing Cédric Simplice, Dr. MOKEM Fokou Igor, Dr. DJOMO Mbong Thierry, Dr. Temgoua Djouatsa Diane, Dr. FOPOSSI André-Marie, Dr. FOKOU Kenfack Wilson, GNINZANLONG Carlos Lawrence and my late Ph.D mate MFOUMOU Guy Serges.

- I sincerely thank my friends and classmates ODJO'O Emmanuel Polycarpe, MANGA Andre.

- My profound gratitude goes to my whole family (brothers, uncles, nieces, nephews, cousins, ...).

Those whose names are not here mentioned shouldn't feel omitted.

# Contents

# List of Figures

# List of Tables

# Abstract

Under the influence of seismic hazards, the interaction between adjacent structures at insufficient distance can cause resonance effects due to hammering which is likely to lead to damage and destruction of said structures. In this work, we analyze the pounding problem in systems modeled by nonlinear differential equations of Filippov type. Three systems are studied, namely a Smooth and discontinuous oscillator (SD), a spillway colliding with the dam (the pillar) and a building model subjected to an earthquake-type excitation. We focus on the study of the influence of noise, geological soil structure, impact points or discontinuity points on the dynamics of the system when it enters the inelastic phase. The analytical method of Dormant Prince is used to detect discontinuity points. Runge Kutta's fourth order numerical algorithms, Subset Simulation and Thom's conditional probabilities or catastrophe theory are used to solve the equations governing the dynamics of the system and to detect intermediate faults. Emphasis is put on the estimation of the probabilistic distribution of impact forces due to pounding and on the theory of stochastic bifurcation. We obtained in these discontinuous systems, the stochastic bifurcation (p-bifurcation) which identifies the instability zones as areas where the hammering presents a higher intensity. This instability shows the pounding effect even at low amplitude of stochastic excitations. We have noted that certain relationships emerge between instantaneous contact (impact), continuous contact of finite duration and pounding which refers to repetitive contacts. When the time of continuous contact of finite duration is higher than that of impact at low noise intensity, the probability density is high and a lot of damage is observed in the colliding structures. It is also shown that the analysis of impact distribution points promotes the physical understanding of meso-macroscopic slip.

***Keywords:*** *Impact; Filippov systems; Pounding; P-bifurcation; Structural failure; Seismic hazard; discontinuity.*

# Résumé

Sous l'influence des hasards sismique, l'interaction entre les structures adjacentes insuffisamment distants peut causer les effets de résonance dus au martèlement qui est susceptible de conduire à des dommages et des destructions des dites structures. Dans ce travail, nous analysons le problème de martèlement dans des systèmes modélisés par des équations différentielles non linéaires de type Filippov.

Trois systèmes sont étudiés, à savoir un oscillateur lisse et discontinu (SD), un évacuateur de crues entrant en collision avec la digue (le pilier) et un modèle de bâtiment soumis à une excitation de type séisme. Nous nous focalisons sur l'étude de l'influence du bruit, de la structure géologique du sol, des points d'impact ou de discontinuité sur la dynamique du système lorsqu'il entre dans la phase inélastique.

La méthode analytique de Dormant Prince est utilisée pour détecter les points de discontinuité. Les algorithmes numériques de Runge Kutta de quatrième ordre, le " Subset Simulation " et les probabilités conditionnelles ou théorie catastrophe de Thom sont utilisées pour résoudre les équations gouvernant la dynamique du système et détecter les défauts intermédiaires. L'accent est mis sur l'estimation de la distribution probabiliste des forces d'impact dues au martèlement et sur la théorie de la bifurcation stochastique. Nous avons obtenu dans ces systèmes discontinus, la bifurcation stochastique (p-bifurcation) qui identifie les zones d'instabilité comme zones où le martèlement présente une plus forte intensité. Cette instabilité montre l'effet de martèlement même à une faible amplitude des excitations stochastiques. Nous avons noté que certaines relations s'en dégagent entre contact instantané (impact), contact continu de durée finie et martèlement qui fait référence à des contacts répétitifs. Lorsque le temps de contact continu de durée finie est plus élevé que celui d'impact à une faible intensité de bruit, la densité de probabilité est élevée et beaucoup de dommages sont observés dans les structures en collision.

Il en ressort également que l'analyse des points de distribution des impacts favorise la compréhension physique du glissement méso-macroscopique.

***Mots clés:*** *Impact; Modèle de type Filippov; Martèlement ; P-bifurcation; Dommages structurels; Hasard sismique; discontinuité.*

# General Introduction

### 0.0.1 Background

Stochastic dynamics was originated from an effort to describe Brownian motion quantitatively a century ago. There are some results about these different kinds of stochastic systems. The first kind of stochastic dynamical systems are the systems driven by stochastic parameter excitation or external noise excitation idealized as Gaussian white noise processes. The second kind of stochastic systems are the systems with only internal random parameter considered as time-invariant and that served as random fields or as random variables. However, there also exist other stochastic systems with both random fields and external noise processes.

The theory of structural pounding risk analysis may be considered as a branch of applied probability theory. The main issue of this theory is to define an event called "structural pounding" and to set up a "probability space" that contains that event. This modeling part of structural pounding risk analysis is based on statistical information about the uncertainty of the relevant parameters or knowledge about the inherent stochastic nature of the applied earthquake loads. A major reason leading to interactions between adjacent insufficiently separated structures results from the differences in their dynamic properties.

The earthquakes are stochastic events, so in most of the studies each single seismic event is defined as a sample function of a stochastic process that models the earthquake ground motion occurring in a specific area. This stochastic process modelling the earthquake occurring in an area is defined through the characteristics of the strong ground motions recorded in that area. The stochastic-based approach is the most suitable to model earthquake records owing to the complex nature of the release of the seismic waves

and their propagation in the soil.

In evaluation of the pounding risk of buildings, *Lin and Weng* [1] proposed a spectral approach to investigate the seismic pounding probability of adjacent buildings based on random vibration theory and total probability theory, assuming linear elastic structure responses. Recently, *Lin, J. H. et al.* [2] investigated the probability distribution of the required separation distance of buildings with steel moment resisting frame (SMRF), which exhibit elasto-plastic behavior in the form of a hysteretic restoring force displacement characteristic, by the Kolmogorov Smirnov test that considers the quality of fit between a hypothesized distribution function and an empirical distribution function, based on data obtained by the Monte Carlo simulation method. The results indicated that the separation data fit almost perfectly with extreme value distribution. This dissertation considered stochastic bifurcation (p-bifurcation) as instability zone. This instability increases pounding effect with weak noise, hence high probability density function (PDF).

Safety analysis of structures subjected to stochastic excitations, such as earthquake, wind or wave loading, is a primary goal of structural engineering [3]. Therefore, prediction of the structural response under uncertain conditions, either in the structural characteristics or in the input excitations, is a more realistic approach for the civil engineering field. The earthquakes are stochastic events, hazardous phenomenon due to insufficient clear spacing often called pounding effects. Noises due to internal friction of colliding bodies could include either architectural or severe structural damage in both spillway structures, bridges and dam during strong ground motion vibrations. Due to discontinuities in soil conditions along the propagation earthquake excitation, there are both evident randomness and strong nonlinearity owing to the evaluation norms of seismic intensity but also the site soil classification. A realistic analysis and design of structural systems subjected to such earthquake excitations must account for the uncertainty arising from randomness, impact and friction.

In recent years, many damages in structures have occurred at the past earthquakes because of insufficient gaps between adjacent buildings. Especially, significant damage of pounding occurred after 1971 San Fernando, 1994 Northridge, 1989 Loma Prieta earthquakes in United States of America; 1985 Mexico City earthquake in Mexica, 1999 Athens earthquake in Greece, 1999 Kocaeli (Izmit) and 2011 Van earthquakes in Turkey. The

recent investigations have reported that pounding effects due to relative displacements of neighboring buildings should not be ignored. Pounding effects could include either architectural or severe structural damage in both building structures and bridges during strong ground motion vibrations. In the case of closely spaced buildings, the damages appear in the form of infill wall damage, column shear failure and collapse due to pounding [4]. Pounding between structures could produce large acceleration demands on the floors which are directly involved in collisions [5].

Events like earthquakes are likely to induce pounding between adjacent structures with different dynamic characteristics and insufficient separation distance. In particular, dynamic impacts represent a problem in densely built-up area, where adjacent structures can be in a full or partial contact with each other. Many cases related to structural damages due to impacts in neighboring buildings have been reported [6–8]. The same phenomena can affect different typologies of structural systems or structural elements [9, 10]. For example, structural damages due to the pounding have been reported in several bridges in past seismic events, such as in *the* 1995 *Kobe earthquake* [11]. *Taflanidis* [12] has shown that pounding forces lead to high impact stresses in the bridge deck, the support bearings, and the substructures, and the non-uniform seismic excitation in long bridges exacerbates the problem. Pounding action may also result in areas of damage located around the corners of the deck or in large differential settlements on the abutments side with a consequent presence of cracks [13]. Dynamic impacts can occur even between base-isolated buildings and the surrounding moat walls [14–16], leading to a significant increase in the superstructure response. Impact phenomena can also represent an issue in the nuclear field. *Pellissetti et al.* [17] have studied how plastic deformations, due to impacts between fuel assemblies in a nuclear reactor, can affect the reliability of a safety shutdown for increasing seismic intensity levels.

## 0.0.2 Motivation, Goals and Scope of the Project

Theory of nonlinear stochastic dynamics was developed mainly since the 1960$s$ due to mathematicians, engineers and physicists. The results up to the 1980$s$ were summarized in many review papers [18, 19]. However, the theory of piecewise-smooth SDEs is only in its infancy compared to its noiseless counterpart. From the previous disconnected studies,

it is not clear how non-smooth SDEs can be studied with techniques developed and used for smooth systems. More efforts need to be done to understand the interrelation between noise and discontinuities. Thus, understanding the interplay between discontinuities and noisy perturbations is a great challenge in many applications. Dynamical systems with discontinuities are frequently used by piecewise-smooth differential equations, the study of which is a relatively recent topic in the field of dynamical systems. The dynamics generated by these equations displays many unexpected phenomena, including stick-slip transitions associated, for instance, with dry friction forces [20], and bifurcations that do not appear in the standard classification of catastrophes of smooth dynamical systems. They also show, in the case of systems with discontinuous derivatives or forces (so-called Filippov systems [21]), multi-valued solutions for a given initial condition, leading to a loss of determinism.

Stochastic bifurcation theory is consisting in a qualitative change of the stationary probability distribution. However, the p-bifurcation studies the mode of the stationary probability density function or the invariant measure of the stochastic process. The stochastic p-bifurcation takes place when the mode of the stationary probability density function changes in nature. It indicates the jump of the distribution of the random variable in probability sense. Over the last fifteen years, an important research activity has been devoted to the studied of stochastic p-bifurcation in the smooth systems [22]. However, the study of stochastic bifurcation phenomena is still immature, precisely in non-smooth systems. Overviews of this literature models are presented in [23, 24].

In engineering practice, to estimate seismic gap between buildings, nonlinearities in the structure are to be considered when the structure enters into inelastic range during devastating earthquakes exhibiting restoring forces that depend on the response history [25]. This kind of behaviour is described in the literature by the term hysteresis. To consider this nonlinearity effects, inelastic time history analysis is a powerful tool for the study of structural seismic performance. The reliability should be evaluated considering the inherent randomness of the structural parameters.

In this thesis, we focus on dynamical properties of piecewise-smooth SDEs with respect to three interesting topics:

(i) Stochastic bifurcations of SD oscillator with dry friction.

(ii) non-linear structural pounding in non-smooth stochastic systems.

(iii) Structural failure analysis.

The reason to consider these three topics is explained as follows. Firstly, the SD oscillator is particularly interesting from a physical point of view because a piecewise-smooth system does not necessarily behave continuously with the magnitude of a force or noise and therefore may behave in a non-trivial way in the limit of vanishing noise. While noise in self-excited oscillator has been widely used for smooth systems, it is not clear how to apply noise in SD oscillator for non-smooth systems. Moreover, the validity of a weak-noise for non-smooth systems needs to be checked. This type of nonlinear dynamical systems are usually called piecewise-smooth or non-smooth dynamical systems. The terms are used interchangeably in this thesis. Secondly, in dynamic of structures, the explanation and understanding of the impact model focuses on the usual case of two bodies. The impact forces and consequences between two colliding bodies depend on their masses and their acceleration. Since all the structures can exhibit dramatic movements when they vibrate under earthquakes, building pounding is a special event for engineers to investigate and to assess the numerical study of collision. If adjacent buildings do not have sufficient separation distance from each other, earthquake can be provided large lateral displacement and buildings can be damaged considering building pounding, even if they are well designed and well-constructed. Due to the high number of degrees of freedom and the nonlinearity as well as non-smoothness of the contact problem, the evaluation of the multiple structure pounding is time-consuming. Thirdly, safety analysis of structures subjected to stochastic excitations, such as earthquake, wind or wave loading, is a primary goal of structural engineering. Therefore, prediction of the structural response under uncertain conditions, either in the structural characteristics or in the input excitations, is a more realistic approach for the civil engineering field. The factor of safety is typically a ratio of strength to stress, thus an accurate estimation of strength and stress is required for a safe and good design. The organization of the work is as follow:

## 0.0.3 Thesis Outline

◇ Chapter 1 presents the background, literature review and some consequences of pounding phenomenon. The inherent nonlinear nature of non-smooth (discontinuous)

systems leads to phenomenologically rich dynamical behaviors could be significantly different from continuous nonlinear dynamical systems.

◇ In chapter 2, we deal with the numerical methods used in the study of the dynamics of stochastic bifurcations of discontinuous systems. The study of the effects of earthquakes subjected to Gaussian white noise of relatively high intensity, filtered through a Kanai-Tajimi filter.

◇ Then in chapter 3, the main findings of this thesis are presented. In fact, we analyze the dynamics of some civil structures and examine numerically the generation of the probability density function (PDF) of those Non-smooth Systems.

◇ The present thesis ends with a general conclusion along with prospects. We summarize our results and give some future directions that could be investigated.

# Chapter 1

# Literature review and problem statement

## Introduction

      This chapter aims to insert the object under consideration in this thesis, i.e. pounding which introduces impact loads that have to be superimposed on those caused by the ground acceleration itself. It introduces basic concepts to be used in the remainder (subsequent chapters) of this dissertation.

We will consider the impact-friction phenomena in engineering structures in order to illustrate the structural pounding, preventing earthquake-induced pounding, describe the impacts in engineering structures, define various contact mechanisms for impact and then point out general information on non-smooth systems. We will then analyze the effects of structural failures; stochastic processes and the problem statement in conclusion. The goal of this dissertation is to illustrate the potential of non-smooth analysis in modelling of various problems in real-life problems. The emphasis will be laid on the completeness and mathematical correctness of the presentation, although several industrial applications will be presented.

## 1.1  Impact-friction phenomena in engineering structures

In the framework of a comprehensive study on the seismic risk of historical lands, large attention should be paid to the assessment of the vulnerability of constructions, of the seismic hazard and of the exposure, the latter representing the number of assets (economic damages, damaged constructions and loss of human lives) exposed to risk. Instead, the seismic hazard is dependent on both the event physical characteristics and the geological characteristics of the area in which the event occurs: the higher is the frequency and intensity of events characterizing geographical area, the greater is the hazard. In fact, the seismic hazard is related to a natural phenomenon typically aleatory in terms of occurrence probability and frequency, which can affect areas with different geological characteristics.

### 1.1.1  Structural Pounding

The first mention of structural pounding in the literature may have been as early as 1926 [26] in which the pounding of non-structural components against the structural elements of a building was discussed and the provision of a sufficient separation gap and proper detailing were recommended. Since then, the increase in urban development and the associated increase in real-estate values have compelled developers and designers to maximize land usage.

Although *the Mexico City earthquake of* 1985 is often cited as the most important single event in which extensive pounding damage was reported [27], the actual severity of the damage attributed directly to pounding may have been overstated [28], it counts about 15 percent of the failure case (U.S. Dept. of commerce 1990). Nonetheless, the potential structural and non-structural damage due to pounding should be assessed during the design stage or in the seismic assessment of structures. Sufficient provisions should be implemented to minimize the potential threat to human life (caused by falling debris, e.g. glass or concrete, loss of a structural element, e.g. failure of a column due to sustained pounding at its mid-height and to the worst condition of total collapse of the structure) and to limit the resulting financial losses which may be incurred by the owner(s).

Cases of structural pounding have been reported in more recent earthquakes such as the 1994 *Northridge earthquake* [29] (pounding of base-isolated buildings against their stops),

*the* 1995 *Hyogo-ken-Nanbu (Kobe) earthquake of* 1995 [38] (collision of pedestrian bridges between buildings) and *the* 1998 *Colombia earthquake*.

As population of a country increase land become the scarcest resource, because of the land cost wise utilization of the space becomes not a choice rather an obligation. Owners want to build their structure aligned with their property line ignoring adjacent structure that lead to pounding.

## 1.1.2 Preventing of earthquake-induced pounding

Earthquake is a set of vibrations on the Earth's surface, ranging from faint tremor to wild motion. These are caused by sudden release of energy stored beneath the Earth. In most of the cases checking the minimum pounding free distance, for future earthquake problem that will be applied according to the need, will solve pounding problems. Before design and construction of any structure it is necessary to step out and check the surrounding space of the structure to avoid future pounding problem.

Structural pounding is mainly attributed to the difference in the dynamic properties of adjacent structures. The disparities in mass, stiffness, and/or strength result in out-of-phase lateral displacements under external excitations. Impacts will occur if these out-of-phase displacements exceed the available separation gap between the structures. The magnitude of the impact force and the location of impact along the height of the structures depends on the magnitude of the existing separation gap, the extent of the disparity between the dynamic properties of the impacting structures, and the characteristics of the excitation. It is therefore apparent that, under certain conditions, the properties of the supporting soil must also be taken into consideration due to its influence on the above aspects.

Many suggestions were made to reduce the destructive effects of pounding in the past. *Westermo* [30] recommended connecting of buildings by beams. The transmittance of the forces between buildings in this case could eliminate pounding's effects. Another advantage of this method is the energy absorbance property [30]. According to the study of *Anagnostopoulos* [31], filling the gap distance between two adjacent structures by energy absorbing materials can reduce the destructive effects of pounding [31]. Application of bumpers, variable dampers and crushable devices is another idea which has been proposed

by *Jankowski et al.* to reduce the destructive effects of pounding in bridges [32]. Recently, *Sheikh et al.* presented an analytical investigation on the use of magneto-rheological (MR) dampers in reducing the pounding effect of base-isolated multi-span RC highway bridges [33]. Although the results of several analytical studies are available vastly in pounding problem, few experiments have been conducted to investigate its destructive effects. The experiment of *Van Mier et al.* [34], which was implemented on concrete to concrete collisions, is one of them. Besides, *Papadrakakis and Mouzakis* [35] and *Chau et al.* [36] conducted shaking table tests with considering different cases for pounding analysis. As a new attempt, *Jankowski* determined the coefficient of restitution (e), for different materials based on the experimental analysis [37]. Seismic pounding is essentially a problem of dynamic impact.

### 1.1.3  Impacts in engineering structures

Impact implies a sudden and brief rise in forces exerted on a body colliding with another object and is a strong nonlinearity when viewed from a dynamical systems perspective. It is therefore natural to model impacts in the piecewise-smooth framework. For impacts where the duration of contact is relatively long, a compliant impact model is appropriate. This is typically modelled as contact with a stiff spring and a damper. On the other hand, if the time duration of the impact is relatively short, an instantaneous jump in velocity according to Newtons impact law

$$v_{rel} \mid after = -ev_{rel} \mid before \tag{1.1}$$

where $e$ is called the coefficient of restitution and $v_{rel}$ is the relative velocity of the colliding bodies, is usually sufficient. $e \in [0,1]$ is a measure of the amount of kinetic energy dissipated in the collision. For further discussions of modelling impacts see [40]. Eq. (1.1) together with the law of conservation of momentum defines the state of the system after the impact. *Ivanov* in [42] writes; "*The choice of this or other impact model for exact problem solution is connected with compromise between simplicity and realistic approach. However, one can achieve it rarely at practice*". The use of Hertz contact force allows to determine both impact duration and impact force value and to find the law of its time change. There are generally two different approaches to modelling of structural pounding. The first one

applies the classical theory of impact, called stereo mechanics, which is based on the laws of conservation of energy and momentum and does not consider transient stresses and deformations in the impacting bodies. The theory focuses on determination of post impact velocities of colliding bodies based on the approaching velocities prior to contact and a coefficient of restitution which accounts for the energy dissipation during impact incorporating response non-linearities. The second model to simulate structural pounding is the contact element approach. The stereo-mechanical theory is not appropriate for developing a time-history analysis of multi-degree-of freedom structural systems, as it does not simulate the structural response during contact, by assuming a negligible duration of it. The contact element approach offers a straightforward idealization of the pounding problem, as it corresponds to the intuitive interpretation of the phenomenon. Impact is simulated by a contact element that is activated when the separation gap between the structures shrinks, which allows solving the problem within the framework of an ordinary response analysis. The formulae for the post-impact velocities $v'_1$ and $v'_2$ of two non-rotating bodies with masses $m_1$ and $m_2$ in the case of the central impact are given by [44]

$$v'_1 = v_1 - (1+e)\frac{m_2 v_1 - m_2 v_2}{m_1 + m_2}; \qquad v'_2 = v_2 + (1+e)\frac{m_1 v_1 - m_1 v_2}{m_1 + m_2}; \qquad (1.2)$$

where $v_1$ and $v_2$ are approaching velocities and $e$ is a coefficient of restitution which can be obtained from the equation

$$e = \frac{v'_2 - v'_1}{v_1 - v_2} \qquad (1.3)$$

the coefficient of restitution which is a measure of energy loss during each impact.

A value of $e = 1$ deals with the case of a fully elastic collision, and a value of $e = 0$ with a fully plastic one. The value of the coefficient of restitution can be determined experimentally by dropping a sphere on a massive plane plate of the same material from a height $h$ and observing the rebound height $h^*$. Then, the following formula is used:

$$e^2 = \frac{h^*}{h} \qquad (1.4)$$

It has been assessed that the coefficient of restitution used to simulate real collisions between structures ranges usually from 0.5 to 0.75 (see Reference [45]). Based on the experimental results, *Azevedo and Bento* [46]) suggested that $e = 0.65$ should be used for

typical concrete structures. In fact, this value has been used by a number of researchers in the analysis of pounding between different types of structures (see, for example, References [47,48]). Some of the studies indicate, however, that collisions between structural members can be more plastic in some cases. *Zhu et al.* [49], for example, obtained the value of $e = 0.4$ based on the results of the experiments conducted on a steel bridge girder model. *Owing* to its macroscopic approach, the classical theory of impact is rather not recommended when a precise pounding-involved structural response is required, especially in the case of multiple impacts. Moreover, since it does not trace the structural response during contact, assuming that it lasts a negligibly short time, its application is usually limited to the analysis of pounding between two structures modelled as single-degree-of-freedom systems [50]. In the case when the structures are simulated by multi-degree-of-freedom models or when the study on the pounding of buildings in series or between several segments of a bridge is conducted, the structural response during the time when contact takes place is essential. This is due to the fact that, when the structural members rebound after collision they might come into contact with other members. Moreover, it may also happen that at the time of contact between two given structural members other members may collide with each other. The energy dissipation during the pounding process is dependent on the differences between approaching and separative velocities of colliding bodies. Structural pounding is a complex phenomenon involving plastic deformations at contact points, local cracking or crushing, fracturing due to impact, friction, etc. Forces created by collisions are applied and removed during a short interval of time initiating stress waves which travel away from the region of contact. The process of energy transfer during impact is highly complicated which makes the mathematical analysis of this type of problem difficult.

### 1.1.4 Various contact mechanisms for impact

The forces produced during collision act over a short period of time, where energy is dissipated as heat due to random molecular vibrations and the internal friction of the colliding bodies. Usually, contact is modeled using either a continuous force model by using contact element approach or via a stereo-mechanical (coefficient of restitution) approach. The contact element approach has been widely used by the researchers because of

its easy adaptableness and reasonable accuracy. The impact forces generated during the collision of two adjacent structures can readily be thought as being provided by a contact element, which is activated only when the structures come into contact. The collision forces are assumed to act in a continuous manner. The contact element is usually a spring of very high stiffness, which may be used in combination with a damping element. The high spring stiffness is necessary to provide a realistic estimate of the impact force, ensure small impact duration and limit the penetration or overlapping of the colliding structures. The contact element is linear or nonlinear based on the stiffness of spring element and the damping properties of dashpot. The stereo mechanical model, which works on the principle of momentum conservation and coefficient of restitution, is rather not recommended when a precise pounding involved structural response is required especially in the case of multiple impacts with longer duration. The stereo mechanical approach uses the instantaneous impact for which the duration of impact should be very small, which is not possible in the case of building pounding. Furthermore, this approach cannot be easily programmed in widely used commercially available software.

### 1.1.4.1    Linear spring contact element
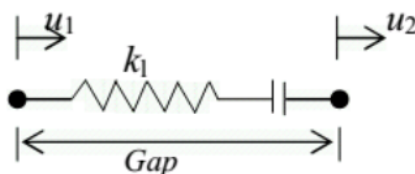


**Figure 1.1**: *Contact elements for impact simulation: Linear spring element*

A linear impact of stiffness ($k_l$) can be used to simulate impact once the gap between adjacent structures closes. The impact force at time t is provided by

$$F_c(t) = k_1 \delta(t) \tag{1.5}$$

Where, $\delta(t)$ is the interpenetration depth of the colliding bodies. This approach is relatively straightforward and can be easily implemented in commercial software. However, in the formulation the energy loss during impact is not taken into account. This model

---

is shown in Fig.1.1 which has been extensively used for impact simulation by *Maison and Kasai* [54].

### 1.1.4.2 Kelvin-Voigt element contact element
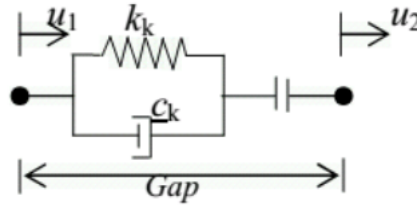


**Figure 1.2**: *Contact elements for impact simulation: Kelvin-Voigt element*

A linear impact spring of stiffness $(k_k)$ is used to be in conjunction with a damper element $(c_k)$ that accounts for energy dissipation during impact. The model shown in Fig.1.2 has been widely used in some studies reported by *Anagnostopoulos* [45]. The impact force penetration relation can be represented as

$$F_c(t) = k_k \delta(t) + c_k \dot{\delta}(t) \tag{1.6}$$

Where, $\dot{\delta}(t)$ is the relative velocity between the colliding bodies at time t. The damping coefficient $c_k$ can be related to the coefficient of restitution $e$, by equating the energy losses during impact:

$$c_k(t) = 2\xi \sqrt{k_k \left( \frac{m_1 m_2}{m_1 + m_2} \right)} \tag{1.7}$$

$$\xi = -\frac{lne}{\sqrt{\pi^2 + (lne)^2}} \tag{1.8}$$

The damping force in the Kelvin-Voigt model causes negative impact forces that pull the colliding bodies together, during the unloading phase, instead of pushing them apart. To avoid the tensile impact forces, slight modification is proposed by *Komodromos et al.* [55]. The modified equation for the next time interval is written as

$$F_c(t + \Delta t) = \begin{cases} k_k \delta(t) + c_k \dot{\delta}(t), & F_c(t) > 0; \\ 0, & F_c(t) \leq 0. \end{cases} \tag{1.9}$$

### 1.1.4.3   The modified Kelvin-Voigt contact element
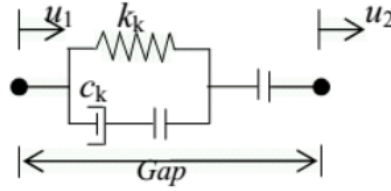


**Figure 1.3**: *Contact elements for impact simulation: modified Kelvin-Voigt element*

This model is developed by *Pant and Wijeywickrema* [56]. Here, the impact force $F_c(t)$ is expressed as

$$F_c(t + \Delta t) = \begin{cases} k_k \delta(t) + c_k \dot{\delta}(t), & F_c(t) > 0; \\ 0, & F_c(t) \leq 0. \end{cases} \tag{1.10}$$

Where, $k_k$ is the stiffness of spring element, $c_k$ is the damping coefficient, indentation at contact surface is $\delta$ and relative velocity of impact is $\dot{\delta}$ .

$$c_k = \xi \delta \qquad and \qquad \xi = \frac{3k_k(1 - e^2)}{2r^2 \dot{\delta}_0} \tag{1.11}$$

Where, $\xi$ is damping ratio. In expression, $e$ is the coefficient of restitution and $\dot{\delta}_0$ is the relative velocity just before the impact. This model is depicted in Fig.1.3.

### 1.1.4.4   Hertz contact element
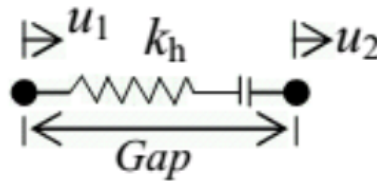


**Figure 1.4**: *Contact elements for impact simulation: Hertz contact element*

In pounding, it is expected that the contact area between neighboring structures should be increased as the contact force grows, leading to a non-linear stiffness. In order to model highly non-linear pounding more-realistically, Hertz impact model has been adopted by

various researchers [57, 58]. This model uses the Hertz contact law: a non-linear spring in an impact oscillator. The force in the contact element as shown in Fig. 1.4 can be expressed as:

$$F_c = \begin{cases} k_h \delta(t)^{\frac{3}{2}}, & \delta(t) > 0; \\ 0, & \delta(t) \leq 0. \end{cases} \tag{1.12}$$

Where, $\delta(t)$ is the relative displacement. Assuming that the colliding structures are spherical of density $\rho$ and the radius $R_i$ estimation can be calculated as:

$$R_i = \sqrt{\frac{3m_i}{4\pi\rho}}; i = 1, 2 \tag{1.13}$$

The nonlinear spring stiffness $k_h$ is linked to the material properties and the radii of the colliding structures as stated through the eq.1.14 and eq.1.15:

$$k_h = \frac{4}{3\pi(h_1 + h_2)} \left[\frac{R_1 R_2}{R_1 + R_2}\right]^{\frac{1}{2}} \tag{1.14}$$

Where, $h_1$ and $h_2$ are the material parameters defined by the eq.1.15:

$$h_i = \frac{1 - \gamma_i}{\pi E_i}; i = 1, 2 \tag{1.15}$$

Here, $\gamma_i$ and $E_i$ are the Poisson's ratio and Young's Modulus respectively. The coefficient $k_h$ depends on material properties and geometry of colliding bodies. The Hertz contact law, is incapable of taking into account energy dissipation during impact phenomenon.

Results of the experiments indicate that for impacts between concrete elements, it ranges typically from 40 to $80kN/mm^{\frac{3}{2}}$, $(1.2 \times 10^9 - 2.6 \times 10^9 N/m^{\frac{3}{2}})$ depending mainly on the contact surface geometry [59]. The impact stiffness parameter for steel-to-steel impacts takes usually higher values [51]. The formulae to calculate values of $k_h$ for certain special impact cases, such as impacts between two spheres or between a sphere and a massive plane surface, have been given by Goldsmith [51]. The disadvantage of the Hertz contact law model is that it is fully elastic and does not account for the energy dissipation during contact due to plastic deformations, local cracking, friction, etc.

### 1.1.4.5 Hertz damp contact element model
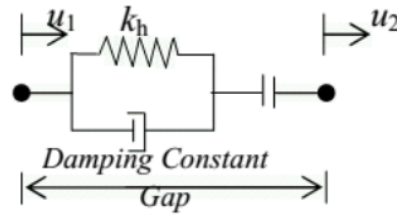


**Figure 1.5**: *Contact elements for impact simulation: Hertz-damp contact element*

An improved version of the Hertz model, called Hertz damp model, has been considered by *Muthukumar and Des Roches* [60], where in a non-linear damper is used in combination with the Hertz spring. The pounding force for the model shown in Fig.1.5 is written as

$$F(t) = \begin{cases} k_h \delta^{\frac{3}{2}}(t)[1 + \frac{3(1-e^2)}{4(v_1 - v_2)}\dot{\delta}(t)], & \delta(t) > 0; \\ 0, & \delta(t) \leq 0. \end{cases} \tag{1.16}$$

Where, $e$ is the coefficient of restitution and $\dot{\delta}(t)$ is the relative velocity during contact and $v_1 - v_2$ is the relative approaching velocities prior to contact.

### 1.1.4.6 Nonlinear viscoelastic model
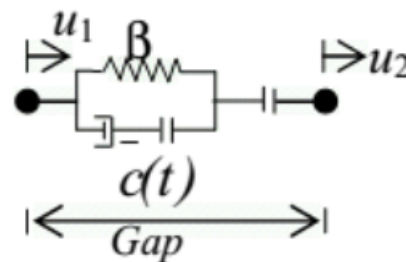


**Figure 1.6**: *Contact elements for impact simulation: Nonlinear viscoelastic element*

Another improved version of the Hertz model has been introduced by *Jankowski* [61] as shown in Fig.1.6 by connecting a nonlinear damper in unison with the nonlinear spring. The contact force for this model is expressed as:

$$
F(t) = \begin{cases}
\beta\delta^{\frac{3}{2}}(t) + \bar{c}(t)\dot{\delta}(t), & \delta(t) > 0 \text{ and } \dot{\delta}(t) > 0; (Approach \quad period) \\
\beta\delta^{\frac{3}{2}}(t), & \delta(t) > 0 \text{ and } \dot{\delta}(t) < 0; (restitution \quad period) \\
0, & \delta(t) \leq 0.
\end{cases} \tag{1.17}
$$

Where, $\beta$ is the impact stiffness parameter and $\bar{c}(t)$ is the impact element damping. Here $\xi$ is an impact damping ratio corresponding to a coefficient of restitution $e$ which can be defined as;

$$
\xi = \frac{9\sqrt{5}}{2}\frac{(1-e^2)}{e(e(9\pi - 16) + 16)}; \bar{c}(t) = 2\xi\sqrt{\beta\sqrt{\delta(t)}\frac{m_1 m_2}{m_1 + m_2}} \tag{1.18}
$$

In addition to the above contact element models, recently various contact element models have been added in the pounding simulation contact element dictionary by the researchers from all around the globe [62, 63].

### 1.1.5  Non-smooth systems

Roughly speaking, non-smooth systems are those systems whose solutions are not everywhere differentiable, and may even possess discontinuities. Their study requires quite specific tools that people working with smooth systems are usually not familiar with. Mechanical Engineers and Applied Mathematicians have long studied this class of dynamical systems (Lagrangian systems with impacts, friction, variational inequalities, differential inclusions). Dynamical systems with discontinuities in the time evolution of their state space trajectories - due to such phenomena as impact, friction or state dependent switches - are defined as non-smooth systems. The inherent nonlinear nature of such systems leads to phenomenologically rich dynamical behavior characterized by bifurcations and routes to chaos which could be significantly different from continuous nonlinear dynamical systems. Before proceeding we should clarify what we mean with the term 'discontinuous dynamical system'. Physical systems can often operate in different modes, and the transition from one mode to another can sometimes be idealized as an instantaneous or discrete transition. Examples include mechanical systems with dry friction, impact and backlash. Discontinuous dynamical systems can be divided in three types according to their degree of discontinuity: The mathematical modeling of non-smooth dynamical systems involves

ordinary differential equations with discontinuous right hand sides. Depending on the type of discontinuity, these systems are categorized as follows:

1. Systems in which the vector fields are continuous at a discontinuity boundary but their Jacobian is discontinuous i.e., systems with continuous but non-smooth vector fields. Systems with purely elastic one-sided supports fall into this category.

2. Systems in which the vector fields governing the motion are discontinuous at a discontinuity boundary, called Filippov systems. Systems involving dry friction and viscoelastic supports fall into this category.

3. Systems involving jumps in state space resulting from impacts between various system components in a mechanical system. Impact micro actuators and gear rattle are a few examples of systems with jumps. These are also called impact oscillators.

In all three cases a kind of switching is involved and those systems are therefore often called switching systems or differential equations with switching conditions. In the field of systems and control theory, the term hybrid system is frequently used for systems composed of continuous differential equations and discrete event parts. Nowadays, the term hybrid system is used for any system which exposes a mixed continuous and discrete nature, even if the system is not controlled. Discontinuous (or switching/hybrid) systems can be considered as dynamical extensions of Linear Complementarity Problems, which gives another term: complementarity systems. Application of *the Amontons-Coulomb* model to dynamical models of systems with dry friction results in differential equations of Filippov-type. Filippov systems form a class of discontinuous systems described by differential equations with a discontinuous right-hand side. To the class of Filippov systems do not only belong mechanical systems with Amontons-Coulomb friction but also electrical circuits with diode elements, controlled systems with switching control laws, mechatronical systems with encoders and many other systems, being mechanical or non-mechanical, where a kind of switching is involved.

**Figure 1.7**: *Examples of the Kobe earthquake aftermath. Picture on the right shows damage: Partial collapse or total collapse of civil structures caused by liquefaction: (a) building, (b) landslides/creep (c) bridges/tunnel, (d)scupper-hole, (e) Building pounding (New Zealand 2009) [11], (f) Pounding effect between two buildings [43]*

# 1.2 Consequences of non-smooth geomechanics and natural hazards assessment

The earth's crust is a rocky layer of variable thickness; crust comprises of portions called plates which vary in size from a few hundred to thousands of kilometers. When these plates contact each other, stress occurs within the crust. The peripheries of the plates pull away from each other, push against one another or slide sideways relative to each other; these are the major causes for the occurrences of earthquakes. The main disasters of geological origin are earthquakes, landslides, tsunamis and volcanic eruptions. Earthquake is a form of energy, which originates in a limited region and then spreads in the form of waves in all directions from the source of disturbance.

Natural hazards failure are represented in Fig. 1.7. We can see failure in foundations caused by liquefaction, foundation movements, creep, shrinkage, cracking, cumulative damage (Fig. 1.7(a, b)). Fig. 1.7(e, f) shows pounding of two adjacent concrete buildings with no sufficient gap size. When two structures are close together, it is expected that they will pound against each other. Pounding of adjacent structures increases the damage of structural components. It may even cause collapse of structures. Fig. 1.9(b) leads to failure occurred during volcanic eruption. Therefore, in Fig. 1.9(c), we can see Beam-column joint or infill wall failure. But Fig. 1.9(d) illustrates the overflow in rail transport. Earthquake is the most dangerous among the disasters of geological origin. The destruction caused by an earthquake is directly related to its source (size) and indirectly related to the path travelled by the seismic waves. In order to mitigate the destruction, the knowledge of its source and path travelled by seismic waves is very important. The understanding of these attributes of earthquakes is important for carrying various development activity such as, river valley projects, bridges and other construction works. The basic physical mechanisms which are responsible for the loss of energy of propagating seismic waves are intrinsic absorption from inelasticity of rocks and scattering due to heterogeneities present in the path of seismic waves. The seismic energy is converted into the heat by intrinsic absorption and redistributed due to the internal heterogeneous medium though which the seismic wave passes. The higher frequency component of seismic waves attenuates more

**Figure 1.8**: *Examples or traffic disruption due to key network component failures: (a) The landslide at Gouache, Bafoussam. (b) landslide at Gouache (c) In Bafoussam, in western Cameroon, a landslide in early November caused large cracks on a tarmac track; (d) The erosion has washed away part of the sidewalk from the track.*

rapidly than the low frequency components resulting in resolution loss in seismograms. Therefore, the attenuation of seismic waves in the lithosphere is an important property for studying the regional earth structure in relation to seismicity.

On the night of Monday October $28, 2019$, in the Gouache $IV$-Block 6 district in the Arrondissement of Bafoussam $III$, Western region, a natural disaster occurred. On a night that was apparently calm and punctuated by severe weather, the worst happened suddenly at around 10 p.m. On the side of these clay hills of Gouache, a strong shock accompanied by a landslide and a deafening noise wake up the peaceful citizens. The concern spontaneously gives way to cries of distress that resonates. The landslide buried 11 houses and their occupants. The balance sheet shows 43 dead Fig.1.8(a, b).

Two weeks after a landslide in a district of the city of Bafoussam, in the west of Cameroon, left forty people dead, another ground movement, without victims this time, cut a tarmac road in two. People are worried Fig.1.8(c, d). When they woke up on the morning of November 5, residents of Bafoussam noticed, in amazement, large faults over several hundred meters on the bitumen of a bypass road very popular with motorists to avoid traffic jams in the city center. Since then, it is no longer possible for the populations of Bafoussam to take this section of asphalted track between the crossings Evêché and $Cami - Toyota$ which allows to join the National 6 in the first arrondissement of the commune.

## 1.3   Analysis of structural failures

This section outlines the common observed damage patterns of different types of buildings in engineering structures induced by the earthquake and their constructional deficiencies. Both un-reinforced masonry buildings and reinforced masonry structures suffered low to heavy destruction. The construction and structural deficiencies were identified to be the major cause of failure, however local soil amplification, foundation problems, liquefaction associated damages and local settlement related damages were also significantly observed during this earthquake. Failure event can be classified in several types according to many factor ranging from natural hazards, materials assessment to designers errors.

**Classification of failures**

(a)

(b)

(c)

(d)

**Figure 1.9**: *Examples or traffic disruption due to key network component failures: (a) bridges. (b) slopes or roads; (c) beams, columns and infill walls failure (Commercial Rd collapse, London,* 2007*); (d) overflow in rail transport* [11]

(a) Structures, the behaviour of which are reasonably well understood by the designers (and consequently, the calculation procedural models are good), but which fail because a random extremely high value of load or extremely low value of strength occurs (e.g. excessive wind load, imposed load, inadequate beam strength);

(b) Structures which fail due to being overloaded or to being under strength (as (a)), but where the behaviour of the structure is poorly understood by the designer and the system errors in the calculation procedural models are as large as the random errors in the parameters describing the model; the designer here is aware of the difficulties (e.g. foundation movements, creep, shrinkage, cracking, cumulative damage, durability generally);

(c) Structural failures where some independent random hazard is the cause, e.g. earthquake, fire, floods, explosion, vehicle impact; the incidence of this type can be obtained statistically;

(d) Failures which occur because the designers do not allow for some basic mode of behaviour inadequately understood by existing technology (this mode of behaviour has probably never before been critical with the type of structure under consideration; a basic structural parameter may have been changed so much from previous applications that the new behaviour becomes critical, or alternatively, the structure may be entirely of a new type or involve new materials or techniques; it is possible, however, that some information concerning the problem may be available from other disciplines or from specialist researchers, and this will be information which has not generally been absorbed by the profession);

(e) Failures which occur because the designer fails to allow for some basic mode of behaviour well understood by existing technology;

(f) Failures which occur through an error during construction; these would be the result of poor site control, poor inspection procedures, poor site management, poor communications leading to errors of judgement, the wrong people taking decisions without adequate consultation etc., and may also occur through a lack of appreciation of critical factors and particularly through poor communications between designers and constructors;

(g) Failures which occur in a deteriorating climate surrounding the whole project; this climate is defined by a series of circumstances and pressures on the personnel involved; pressures may be of a financial, political or industrial nature, and may lead directly to a

shortage of time or money with the consequent increased likelihood of errors during both design and construction processes; they may also result in rapidly deteriorating relationships between those involved in the project;

(h) Failures which occur because of a misuse of a structure or because the owners of the structure have not realized the critical nature of certain factors during the use of a structure; associated failures are those where alterations to the structure are improperly done. We can identify damage and failure mode either in Reinforce Concrete (RC) buildings, un-reinforce masonry (URM) buildings, the deck and the abutment, Local failures in RC Buildings, or Non-Structural Damage of Buildings. The tables: 1.1, 1.2, 1.3, 1.4 illustrated these cases.

## 1.4    Stochastic processes

Noise or random excitations are the words that are used to define stochastic processes. The oldest experiment concerning a noise in physical system is the Brownian particle. In our case, we will be dealing with mechanical noise. Noise can be classified in two different ways. Based on the spectral properties, we can distinguish white noise and colored noise.

### 1.4.1    Spectral properties of white noise

A white noise is a realization of random process in which the power spectral density is the same for all the frequencies. Since white noise is a totally random process, there is no relation between the values taken by it at the different instant. Similarly, there is no relation between the values taken at any two instants by two different white noises. The consequence is that the autocorrelation function of a white noise is a Dirac function, while the correlation function of two different noises is the null function.

$\langle \xi_1(t)\xi_2(t') \rangle = Cte\delta(t - t')$

$\langle \xi_1(t)\xi_2(t') \rangle > 0$

Moreover, a noise is said to be colored when it is not white. The difference can be as much on its Fourier spectrum as on its autocorrelation function. In the majority of physical systems, there is no ideal white noise as described above. This is the case, for example,

**Table 1.1**: *Damage and failure mode in Reinforce Concrete (RC) buildings*

| Failure mode | Types of damages | Causes |
|---|---|---|
| Soft story failure | Sinking of lower stories, sinking of intermediate stories | ✓ Omitting infill masonry wall for parking, shopping, lobby, etc. purpose<br>✓ Omitting infill masonry wall for architectural needs like creating big halls (even omitting middle column), irregular sizing of rooms, etc. |
| Pounding failure | Displacement, plumb out of the buildings, severe damage of the adjacent buildings, total collapse of the adjoining buildings | ✓ Lack of gap between adjoining buildings<br>✓ Stiffness different within the adjoining buildings<br>✓ Floor height different between adjoining buildings, stiffness and mass irregularities<br>✓ Excessive load transfer from higher buildings to lower height buildings<br>✓ Drastic decrease in stiffness in the higher buildings from the roof level of lower building to top of higher building |
| Structural irregularity failure (plan and mass) | Overturning of massive floor, tilting of the building, separation of massive story from the building | ✓ Relatively higher deflection of massive floor to other light floor<br>✓ Stress concentrate in the floor level and ultimately may separate (poor ductile detailing in joints |

| Failure mode | Types of damages | Causes |
|---|---|---|
| Failure due to ground rupture | Tilting or shifting of the building, structural elements damages or total collapse | ✓ Built building in the poor soil strata<br>✓ Build in the land pooling area<br>✓ Lack of important of soil testing<br>✓ Built in the fault area |
| Pancake | Total collapse | ✓ Weak column-strong beam<br>✓ Poor workmanships<br>✓ Worst ductile detailing<br>✓ Poor quality of construction material<br>✓ Built for selling purpose |

of the external force acting on a Brownian particle. In reality, in this physical system, the values taken by the external force are correlated. However, the time after which the correlation function begins to take almost zero values, reflecting the fact that there is no relationship between the values taken at the time t and at the time $t+\tau$ is very small. It is of the order of the intermolecular distance divided by the mean velocity of the molecules $(10^{-13}s)$. However, in the limit where the correlation time tends to 0, this force can be assimilated to an ideal white noise. This type of approximation is often done in the modeling of many physical systems, which facilitates their analytical and/or numerical study. In the literature, noise with a constant probability density function is said to be uniform and we have [64]

$$f(y) = \frac{1}{2A_m} \tag{1.19}$$

Where $A_m$ is the maximum amplitude of the noise. While noise with a Gaussian probability density function are called Gaussian noises.

<div align="center">

**Table 1.2**: *Local Failures in RC Buildings.*

</div>

| Failure mode | Types of Damages | Causes |
|---|---|---|
| Beam failure; Shear failure | (Cracks developed at $45^o$, angle normally), spallation of concrete at the middle or near the joints) | ✓ Stirrups provided in the Beams are not sufficient (spacing of rebar 175 mm to 300 mm) <br> ✓ Rebar size that is used is of minimum diameter (5 mm to 7 mm) <br> ✓ Hoop provided is $90^o$ with minimum hoop length (20 mm to 50 mm) <br> ✓ Stirrups are not placed correctly <br> ✓ Main rebar provided in the beam are not sufficient (using four bars of diameter ranging from 10 mm to 12 mm) <br> ✓ Overlapping length is minimum (usually 150 mm to 300 mm) <br> ✓ Overlapping location is also not appropriate (major problem) <br> ✓ Confinement reinforcement are not provided <br> ✓ Size of the beam is 230 mm by 230 mm (including slab thickness) |
| Beam-column | (Joints failure) | ... |

| Failure mode | Types of Damages | Causes |
|---|---|---|
| Shear failure | (Cracks develop at the beam- column joint, crumble of concrete at the joints) | ✓ Lack of use of confinement rebar near the joints<br>✓ Lack of use of confinement rebar inside the beam-column junction<br>✓ Use of poor quality concrete |
| Brittle failure | (Separation of beam from column, crumble of concrete) | ✓ Adequate anchorage length of the beam is not provided (major problem)<br>✓ Main bar provided in the beam and column is not sufficient<br>✓ Extra bar that need to provide in the beam column joints are omitted |
| Shear failure | (Diagonal cracks of the column near joints and at the middle of the column, crushing of the column majorly near the joints) | ✓ Stirrups provided in the column are not sufficient (Single hoop)<br>✓ Rebar size that is used is of minimum diameter (usually 5 mm to 7 mm)<br>✓ Hoop provided is $90^o$ with minimum length (20 mm to 50 mm) |

| Failure mode | Types of Damages | Causes |
|---|---|---|
| Flexural failure | (Crumble of concrete, yielding of rebar, racks near the joints, formation of hinge (ultimate condition)) | ✓ Main rebar provided in the column are not sufficient (normally four bars of diameter ranging from 10 mm to 12 mm)<br>✓ Overlapping length is minimum (usually 150 mm to 300 mm)<br>✓ Overlapping location is also not appropriate (major problem)<br>✓ Confinement reinforcement are not provided<br>✓ Size of the column is 230 mm by 230 mm majorly<br>✓ Orientation of the column is not appropriate |
| Buckling failure | (Buckling of column, spalling of the concrete, bending of the rebar) | ✓ Main rebar is not sufficiently layout<br>✓ Meshing of the rebar is same for any kind of slab size<br>✓ Thickness varies (100 mm to 175 mm)<br>✓ Lack of proper detailing of the slab rebar<br>✓ Poor concrete quality |

**Table 1.3**: *Non-Structural Damage of Buildings.*

| Failure mode | Types of Damages | Causes |
|---|---|---|
| Infill wall | (Out of plan damage, crushing of wall diagonally or at toe and heel, shearing of bed joints, separation between the wall and the frame) | ✓ Lack of sill band and lintel band<br>✓ Diagonal strut action<br>✓ Due to strong infill surrounded by a strong frame<br>✓ Weak joints and strong members<br>✓ Strong infill and strong frame but vibrate differently |
| Water tank failure | (Bare framed supporting polythene tank collapsed, formation of plastic hinges in the upper and lower edges of column) | Large inertia forces due to water tank mass |
| Staircase | (Damage at the junction of the landing and the flight, sagging or drop down of the landing, total collapse) | ✓ Rebar detailing problems<br>✓ Minimum use of main bar (8 mm to 10 mm)<br>✓ Short column effect<br>✓ Deck thickness varies from 75 to 125 mm |
| Parapet failure | (Partial and totally collapsed) | ✓ No anchorage is provided<br>✓ Built as secondary element with no proper design |

| Failure mode | Types of Damages | Causes |
|---|---|---|
| Poor quality of materials | (Cop-outs and spalling of concrete, material deteriorates effortlessly, breakage of corroded rods, loss in capacity of rods, corrosion can to spread to other parts, possibility of vanish of rods due to corrosion) | ✓ Pilling out/cop out the cover of the concrete in structural components <br> ✓ Breakage of the rod due to size reduction of rebar due to corrosion |

$$f(y) = \frac{1}{\sqrt{2\pi\sigma^2}} exp(-\frac{(y - \langle y \rangle^2)}{2\sigma^2}) \qquad (1.20)$$

One also says that the random variable y follows a normal distribution.

### 1.4.2 Techniques for the production of random number sequences: Box-Muller Transformation

This transformation created in 1958 by *Georges Edward et al.* [64] states that if $y_1$ and $y_2$ are two independent random variables uniformly distributed between 0 and 1, then the variables:

$$z_1 = \sqrt{-2ln(y_1)}cos(2\pi y_2); \quad z_1 = \sqrt{-2ln(y_1)}sin(2\pi y_2) \qquad (1.21)$$

are Gaussian random variables each having a zero mean and a variance equal to unity. This transformation will be used in the simulations to produce random variables representing the Gaussian white noises.

### 1.4.3 Stochastic bifurcations.

Many engineers believe that, for instance, probability theory will be of little help in understanding the basic causes of structural failures. Arnold proposed two kinds of stochastic

**Table 1.4**: *Damage and Failure Mode of un-reinforce masonry (URM) buildings.*

| Failure mode | Types of Damages | Causes |
|---|---|---|
| Shear failure | (Diagonal cracks at corner of openings and at center of wall segment) | ✓ Stress concentration at corners of windows and doors <br> ✓ Absent of sill and lintel band |
| Tension failure | (Vertical cracks at the center, ends or corners of the walls) | ✓ Walls too high and too narrow <br> ✓ Openings too close to corners |
| Out-of-plane failure | (End masonry walls failure, bulging of masonry wall, delamination of wall leaf) | ✓ Lack of structural integrity <br> ✓ Deficient bond at corners continuous vertical joints (wall to wall connection) <br> ✓ Flexible floor diaphragm <br> ✓ Trusting nature of sloping roof <br> ✓ Ineffective or lacking passing through connections in multi leaf masonry assemblages |
| Spandrel failures | (Cracks between two openings one above the other) | ✓ Flexible floor diaphragm <br> ✓ Absent of sill and lintel band |

| Failure mode | Types of Damages | Causes |
|---|---|---|
| Pounding | (Cracks at the floor level, sway of buildings) | ✓ Lack of space between two buildings |
| Torsion and warping Failure | (Larger damage occurs near the corner of the building, excessive cracking due to shear in all walls) | ✓ Unsymmetrical in plan and elevation of building<br>✓ Imbalance in the sizes and positions of openings in the walls |
| Mixed mode failure | (Partial collapse or total collapse) | ✓ Accumulation of in plane out of plane and corner effects<br>✓ Corner buildings in row housing |
| Roof failure | (Dislodging of roofing material, separation of roof truss from supports) | ✓ Improperly tied roofing material<br>✓ Lack of tie rod or tie beam<br>✓ Weak support connection<br>✓ Heavy roof material |
| Overturning failure | (Sliding of the whole building) | ✓ Weak foundation design |

bifurcations: D-bifurcation and P-bifurcation. The so-called dynamical bifurcation (D-bifurcation) examines the sudden change of sign of the largest Lyapunov exponents, and the phenomenological bifurcation (P-bifurcation) studies the sudden change of the shape of the stationary probability density. First, the model is reduced to a one-dimensional Ito averaged equation by using the stochastic averaging method. Then, the relationship between the qualitative behavior of the stationary probability density and the qualitative behavior of the diffusion process is established. The results show that stochastic P-bifurcation occurs when the system parameter varies in the response analysis and the stationary PDF evolves from bimodal to unimodal along the unstable manifold during the bifurcation.

## 1.5   Problem statement

This chapter has given an overview on the generalities concerning the natural hazard impact-friction phenomenon and the effects induced by those non-smooth vibrations on engineering structures. An important issue which has seen somewhat less attention in the friction and dynamic systems literature is the stochastic nature of dynamic surface interactions. The source of the random excitation is the environmental changes, such as earthquakes and wind loads exciting for example high rise buildings or wave motions at sea exciting for example offshore structures. Alternatively, the randomness of the excitation may stem from material properties, such as the distribution of imperfections or defects. The analysis of nonlinear non-smooth stochastic systems is studied. Friction under nominally constant sliding conditions can be described by a constant value plus broadband noise. Different control strategies used to mitigate those pounding phenomena due to external excitations have been also presented. To reduce the effects of pounding, small separation distances needs to be maintained and these gaps needs to be filled up with a special shock absorbing material (bumper dampers for instance). So that where the structures are subjected to pounding action, there will not be any damage to the main structure. The bumper damper element in the form of rubber shock absorber can be placed between the structures, but connected only to one of the structures. Bumper dampers are the energy dissipation links that are activated when the gap is closed. The presence of the

bumper damper element will reduce the impulsive forces transmitted from one structure to the other. Other options to minimize the effect of pounding have to do with the decreasing of lateral motion by joining adjacent buildings at critical positions so that their motion could be in-phase. The nonlinear dynamics of mechanical Filippov systems is explored in this thesis. The following chapter will be devoted to the description of mathematical tools used to model a network of adjacent engineering structures. Analytical and numerical formalisms used to solve the problem of the thesis are presented.

# Chapter 2

# Methodology: Analytical and numerical methods

## Introduction

The previous chapter has introduced the phenomenon of structural pounding and some analysis of structural failure. The topic is interesting because it is a more realistic approach for the prediction of the structural response under uncertain conditions, either in the structural characteristics or in the input excitations in the civil engineering. This chapter deals with the models, the analytical and numerical methods that will be used to solve the problems that thesis addresses. We will consider a model of smooth-and-discontinuous (SD) oscillator, a model of a bridge or a spillway which interacts with an abutment under the influence of noise or external excitation. The last model is a practical example of building subjected to natural hazard excitation.

## 2.1 Smooth -and -discontinuous oscillator model

Consider a non-deformable moving belt, moving with a constant velocity $v_0$, the block of mass $m_1$ moving in the lying flat surface and connected to a damping capacity C (or damping function $\Phi(x_1(t), \mu))$) and a fixed backing by an inclined linear spring of stiffness coefficient K, which is capable of opposing both tension and compression (see Fig. 2.1. (a)). The block can either ride on the belt, with zero relative velocity with respect to it,

or slip on it because friction is added as a constraint on a rough surface between the mass and the belt. We then suppose large displacements of the mass same as large deformations in continuum mechanics so that the system is strongly nonlinear. $X_1$ is the displacement from the rest state. The kinetic energy and the potential energy of the system can be written as:

$$T = \frac{1}{2}m_1\dot{X}_1^2; \qquad V = \frac{1}{2}K(\sqrt{X_1^2 + H_1^2} - L)^2 \tag{2.1}$$

which follow the Lagrangian formulation
$\frac{dL}{dt}\left(\frac{\partial L}{\partial \dot{X}_1}\right) - \left(\frac{\partial L}{\partial X_1}\right) = 0$ where $L = T - V$. The presence of damping, restoring and external forces in the system leads to the following perturbed system:



(a)

(b)
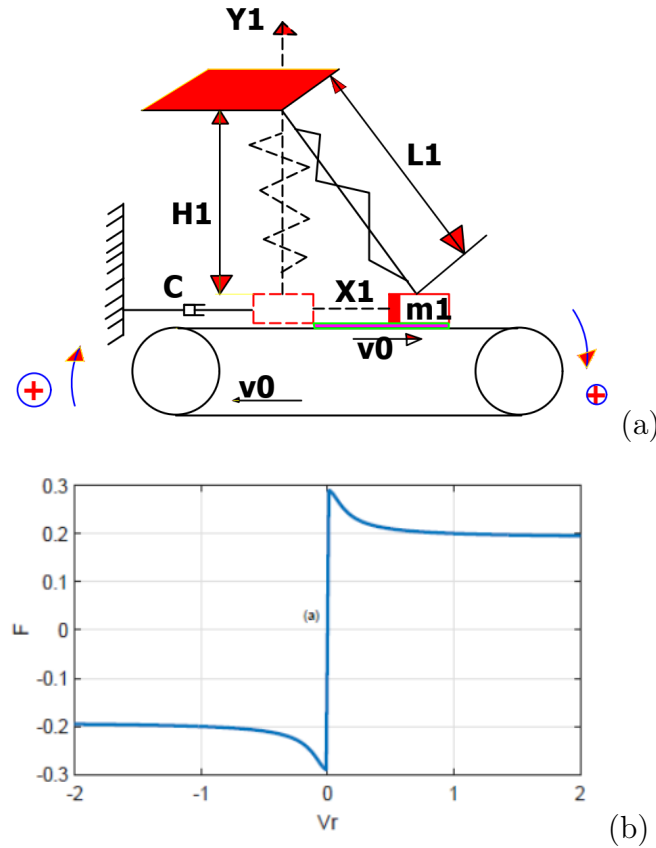
**Figure 2.1**: *The mechanical model of the system: (a): the self-excited SD oscillator (b): Coulomb friction Eq. 2.4 with: $\alpha = 0.1$ ; $g_1 = 2.0$; $\mu = 0.1$; $v_0 = 0.0$*

$$m_1\frac{d^2X_1(t)}{dt^2} + C\frac{dX_1(t)}{dt} + KX_1(t)\left(1 - \frac{L}{\sqrt{X_1^2 + L_1^2}}\right) + G_s = F_e cos(wt) + \xi(t) \tag{2.2}$$

where $L_1$ is the original length of the spring, $H_1$ is the distance between fixed point and belt, and $\xi(t)$ is the normalized source of Gaussian white noise satisfied:

$$\langle \xi(t)\xi(t')\rangle = 2D\delta(t-t'), \qquad \langle \xi(t)\rangle = 0 \tag{2.3}$$

where $D$ is the noise intensity. The dry friction force $G_s$ is due to the surfaces in contact and can be defined during the slip mode. We use the friction force $G_s$ modeled as Stribeck friction between objects in contact. It is determined by the material characteristics of the block and the belt and is described as

$$G_s = -\mu(C_0 + C_1|X_1| + C_2|(\dot{X}_1)|)sgn(\dot{X}_1)) \tag{2.4}$$

So that $X_1$ and $\dot{X}_1$ are the sliding displacement, and correspondent velocity, $C_0$ is the vertical contribution of the spring force, coefficients $C_1$ and $C_2$ are respectively the friction interface amplitudes , with the correspondent velocity. $\mu$ is the friction coefficient depending on the relative velocity of the contact $V_r = (\dot{X}_1 - V_0)$ as:

$$\mu = \begin{cases} \mu_k & (\dot{X}_1 \neq V_0), \\ \mu_s & (\dot{X}_1 = V_0), \end{cases} \tag{2.5}$$

Where $V_0$ is the belt velocity. $C_0 = F_N$ is the contribution of the weight in the friction force and can be expressed as $F_N = Mg - KH_1(1 - \frac{L}{\sqrt{X_1^2+H_1^2}})$; where the condition $Mg > KH_1$ is satisfied.

The coefficient of the kinematic friction characteristic $\alpha_0 = \mu F_N$ is determined by the material characteristics of the block and the belt.

If the moving load acceleration is equal to zero, i.e. $\ddot{X}_1 = 0$ when the load sticks on the belt, $\dot{X}_1 = V_0$, thus the value of the friction force $(G = -KX_1(t)(1 - \frac{L}{\sqrt{X_1(t)^2+H_1^2}}))$ is confined to the interval $(-G_{max} < G < G_{max})$. Knowing that $G_{max} = \mu(Mg - KH_1(1 - \frac{1}{\sqrt{X_1^2+H_1^2}}))$ is the maximum static friction force derived from the product of the friction coefficient with the normal force.

Hence the Coulomb friction force $G_s$ between the mass and the belt is illustrated in Fig. (2.1)(b). We have described the intermittent behaviour (or the set-valued extension) of

the system in the differential inclusion of Filippov type as:

$$sgn(X_1) = \begin{cases} 1 & if \quad (X_1 > 0), \\ \in [-1, 1] & if \quad (X_1 = 0), \\ -1 & if \quad (X_1 < 0), \end{cases} \tag{2.6}$$

without loss of generality, the equation of motion Equation (2.2) can be normalized using the non-dimensional variables and parameters as follows: $x_1 = \frac{X_1}{L_1}$; $w_0^2 = \frac{K}{m_1}$; $c = \Phi(x_1, \mu) = \frac{C}{m_1 w_0}$ ie., (damping capacity C (or damping function $\Phi(x_1, \mu)$))); $\tau = w_0 t$ ; $\alpha = \frac{H_1}{L_1}$; $v_0 = \frac{V_0}{L_1 w_0}$; $g_1 = \frac{g}{L_1 w_0^2}$.

Then, substituting these variables into Equation (2.2), the non-dimensional equation of motion for this system is:

$$\ddot{x}_1 + (\Phi(x_1, \mu))\dot{x}_1 + x_1(t)(1 - \frac{1}{\sqrt{x_1^2 + \alpha^2}}) - \mu(C_0 + C_1|x| + C_2|(\dot{x}_1)|)sgn(\dot{x}_1)) = fcos(wt) + \xi(t) \tag{2.7}$$

Where $C_0 = [g_1 - \alpha(1 - \frac{1}{\sqrt{x_1^2 + \alpha^2}})]$, and (.) denotes the differentiation with respect to the non-dimensional time $\tau$. The motion of the mass can be characterized into two qualitatively different modes, the slip and stick modes.

Physically, this oscillator is similar to a snapthrough truss system. The smoothness parameter $\alpha$ not only defines the geometry of the oscillator, but also has physical meaning. For $\alpha > 1$, the system represents a pretensioned discrete elastic string, while if $\alpha = 0$, the model corresponds to an oscillating mass supported by two parallel vertical springs. When $\alpha > 0$, the nonlinearity associated with the system is continuous and for $\alpha = 0$, the system nonlinearity is discontinuous. The dynamics of the SD oscillator has been investigated randomly in the two domains. The equation of motion of the SD oscillator for the discontinuous case is given by:

$$\ddot{x}_1 + (\Phi(x_1(t), \mu))\dot{x}_1 + (x_1 - zsgn(x_1)) - dsgn(\dot{x}_1) = fcos(wt) + \xi(t) \tag{2.8}$$

Where $d = -\mu(C_0 + C_1|x_1| + C_2|(\dot{x}_1)|)$.

At least one coefficient will be null in practical case (one between $z$ and $d$ will be zero). Thus, for the two intermittent modes "$sgn(x_1)$" and "$sgn(\dot{x}_1 - v_0)$", one could have the excited SD oscillator when $(z = d = 0)$ and the dry friction model when $(z = 0; d = 1)$. Other phenomena such as clearance, vibro-impacts, and preloaded compliance can occur

when $(z = 1; d = 0)$. A Filippov (or piecewise smooth) system [65] is composed of different smooth ODEs defined in open non-intersecting domains $S_i$ separated by smooth discontinuity boundaries. Filippov representation for the discontinuous SD oscillator is given by:

$$
F_1(x_1, x_2) = \begin{cases}
\dot{x}_1 = x_2, & v_r = x_2 - v_0 < 0; \\
\dot{x}_2 = -(\Phi(x_1(t), \mu))x_2(t) & \\
-x_1(t)(1 - \frac{1}{\sqrt{x_1^2 + \alpha^2}})+ & \\
-\mu(g_1 - \alpha(\frac{1}{\sqrt{x_1^2+\alpha^2}}) + C_1|x_1| + C_2|(x_2)|)sgn(x_2))+ & \\
+f cos(x_3) + \xi(t) & v_r = x_2 - v_0 < 0.
\end{cases}
$$

$$
F_2(x_1, x_2) = \begin{cases}
\dot{x}_1 = x_2, & v_r = x_2 - v_0 > 0; \\
\dot{x}_2 = (\Phi(x_1(t), \mu))x_2(t) & \\
-x_1(t)(1 - \frac{1}{\sqrt{x_1^2 + \alpha^2}})+ & \\
+\mu(g_1 - \alpha(\frac{1}{\sqrt{x_1^2+\alpha^2}}) + C_1|x_1| + C_2|(x_2)|)sgn(x_2))+ & \\
+f cos(x_3) + \xi(t) & v_r = x_2 - v_0 > 0.
\end{cases}
$$

(2.9)

Where $v_r = x_2 - v_0$; $C_0 = [g_1 - \alpha(1 - \frac{1}{\sqrt{x_1^2+\alpha^2}})]$; $\mu$ is the friction coefficient (see Eq.2.5). A solution of this equation should be continuously differentiable. This equation describes many physical systems collectively called SD Van der Pol$-$Duffing oscillators.

## 2.1.1  Generic Filippov system analysis

The oscillator slides or rests on the horizontal belt surface traveling with a constant speed $v_0$. If a self$-$excited SD oscillator is pulled by a stage and it starts to slide, then, because of the variation of position $X_1(t)$, the sliding process destroys the limit cycle setting up a stick-slip dynamics. Consider $x \in R^n$, and $f^{(i)} : R^n \to R^n$, $i = 1, 2$, are smooth functions. A generic Filippov system of the form:

$$
x = \begin{cases}
f_+(x) & (for \quad x \in S_1), \\
f_-(x) & (for \quad x \in S_2),
\end{cases}
$$

(2.10)

is defined in Fig. 2.2. Moreover, the discontinuity boundary $\Sigma$ separating the two regions is described as

$\Sigma = \{x \in R^n : H(x) = 0\}$, where H is a smooth scalar function with non vanishing gradient $H_x(x) = \frac{\partial H(x)}{\partial x}$ on the discontinuity boundary $\Sigma$, and

$$S_1 = \{x \in R^n : H(x) < 0\},$$

$$S_2 = \{x \in R^n : H(x) > 0\}, and$$

$$\Sigma = \{x \in R^2/n(x) = \dot{x} - x_v = 0\}. \tag{2.11}$$

(a)

(b)

(c)
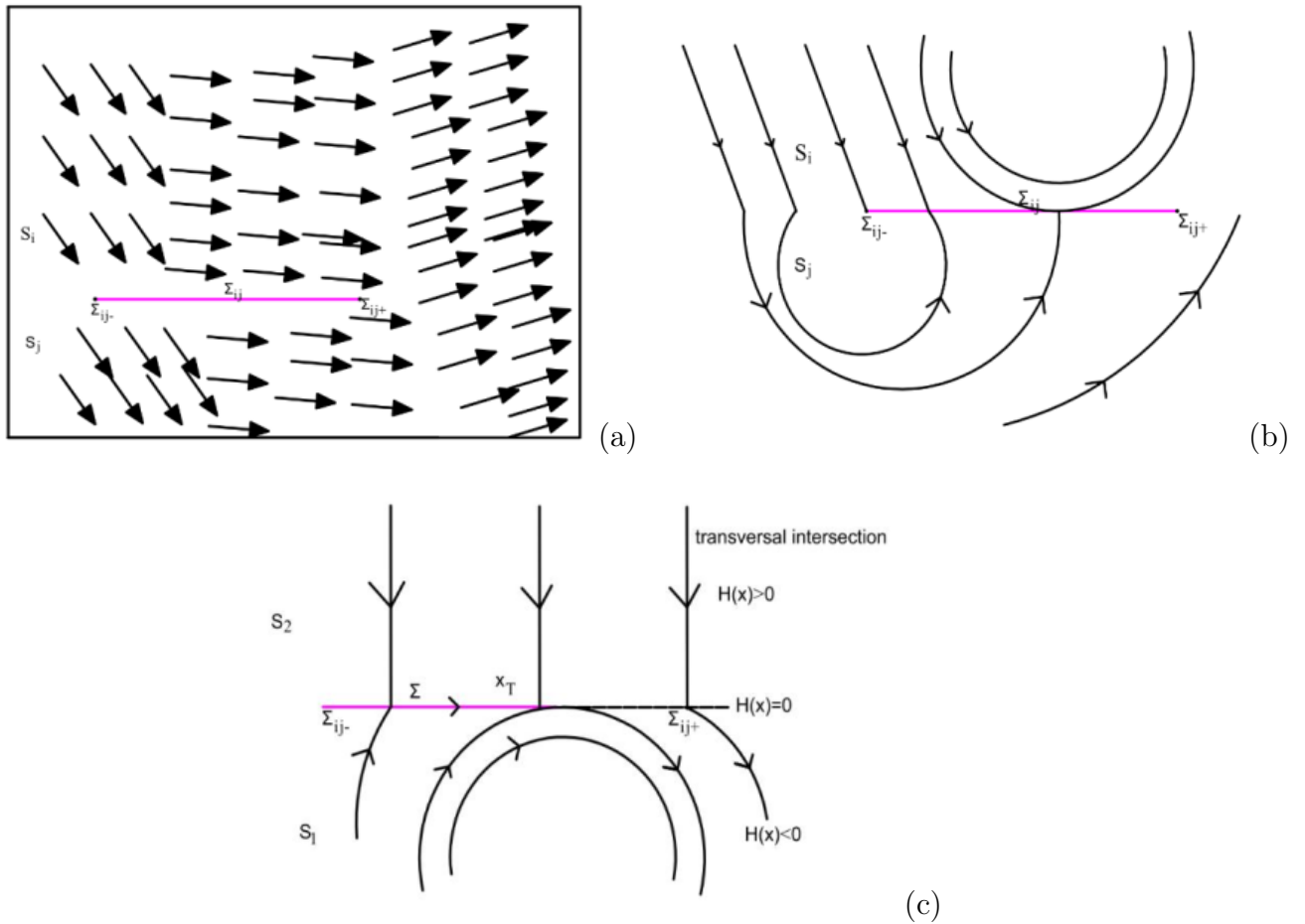
**Figure 2.2**: *Filippov representation: (a) Two vector fields $F_i$ and $F_j$ and an open $\Sigma_{ij}$ (left), of the corresponding trajectories (right-hand side,(b)). (c) Filippov' Piecewise Smooth System*

The boundary $\Sigma$ is either closed or goes to infinity in both directions and $f^{(+)} \neq f^{(-)}$ on $\Sigma$. By concatenating standard solutions in $S_{1,2}$ and sliding solutions on $\Sigma$ obtained with the well known Filippov convex method, it is possible to construct the desired general solutions of Eq. 2.9.

Let $\sigma(x) = \langle H_x(x), f^{(+)} \rangle \langle H_x(x), f^{(-)} \rangle$, be the definition of switch control function in which $\langle .,. \rangle$ denotes the standard scalar product in $R^n$. The crossing set $\Sigma_c \subset \Sigma$ is defined as: $\Sigma_c = \{x \in \Sigma : \sigma(x) > 0\}$, which is the set of all points $x \in \Sigma$, where at these points the orbit of system Eq.2.9 crosses the boundary $\Sigma$ i.e., the orbit reaching x from $S_i$ concatenates with the orbit entering $S_j$, $i \neq j$, from x. The complement to $\Sigma_c$ in $\Sigma$: $\Sigma_s = \{x \in \Sigma : \sigma(x) \leq 0\}$, where at these points $x \in \Sigma_s$, the orbit of system Eq.2.9 which reaches x does not leave $\Sigma$ and will therefore have to move along $\Sigma$. The crossing set is open, while the sliding set is the union of closed sliding segments and isolated sliding points. In general, the orbit of system Eq.2.9 crosses $\Sigma$ at points $x \in \Sigma_c$, while it slides on $\Sigma$ when points $x \in \Sigma_s$. Notice that, a sliding segment is delimited either by a boundary equilibrium $x_B$, or by a point $x_T$ (called tangent point) in which one of the vectors $f^{(i)}(x_T)$ is tangent to $\Sigma$ and both of them are nonzero. Therefore, the following definition of the tangent points $x \in \Sigma_s$ holds: $\langle H_x(x_T), f^i(x_T) \rangle = 0$, $i = 1, 2$. In the discontinuous differential system Eq.2.9 with switching conditions, $f(x)$ is not well defined when $x$ is on the discontinuity surface $\Sigma$. A way to define the vector field on $\Sigma$ is to consider the Filippov approach, that is the set valued extension $F(x)$ below:

$$\dot{x} \in F(x) = \begin{cases} f_+(x, \mu), & x \in S_1; \\ \overline{co}\{f_+(x, \mu), f_-(x, \mu)\}, & x \in \Sigma; \\ f_-(x, \mu), & x \in S_2. \end{cases} \tag{2.12}$$

where $(f_+(x), f_-(x))$ are given by the smooth functions, and $\overline{co}\{A\}$, is a vector field along the separation boundary, (the closure of the convex hull) denotes the smallest closed convex set containing A.

$\overline{co}\{f_+, f_-\} = \{f_F : x \in R^n \to R^n : f_F = (1 - \alpha)f_+ + \alpha f_-, \quad \alpha \in [0, 1]\}$, then the system vector field can be described by a differential inclusion (systems with multi-valued right-hand sides)

---

### 2.1.2 The convex approach of non-smooth dynamics

Consider a piecewise smooth dynamical system

$$\frac{dx}{dt} = f(x) = \begin{cases} f_+(x) & (for \quad v(x) > 0), \\ f_-(x) & (for \quad v(x) < 0), \end{cases} \tag{2.13}$$

we can extend such a model across $v(x) = 0$. In the standard Filippov approach prominent in variable structure control and in piecewise smooth dynamical systems theory, when a system switches between two systems as in Eq.2.13, we form their convex combination

$\frac{dx}{dt} = f(x, \lambda) = \frac{F_+(x) + F_-(x)}{2} + \lambda \frac{F_+(x) - F_-(x)}{2}$

(or a similar form $\frac{dx}{dt} = f(x, \lambda) = [F_+(x) + F_-(x)] + u[F_+(x) - F_-(x)]$, with $\lambda = 2u - 1$ where

$$\lambda \in \begin{cases} sgn(v) & (if \quad v \neq 0), \\ [-1, +1] & (if \quad v = 0), \end{cases} \tag{2.14}$$

Thus $f(x, +1) \equiv f_+(x)$; $f(x, -1) \equiv f_-(x)$ . The standard approach then seeks so-called sliding modes which satisfy $\frac{dv}{dt} = 0$ at $v = 0$.

## 2.2 Model of a bridge or a spillway which interacts with an abutment
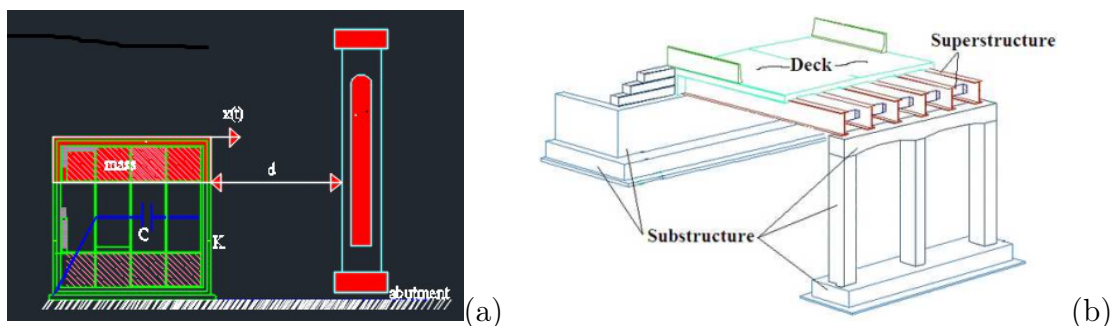


**Figure 2.3**: *Model of a spillway which interacts with an abutment.*

## 2.2.1 General formulation

James H. Dieterich et al., [66] described the phenomenon to model the friction between the crustal plates of Earth . J. R. Rice et al., [67] have analyzed a special friction model in the stability of tectonic sliding. The model has also been used in connection with control, see James R. Rice et al., [68]. Due to discontinuities in soil conditions along the propagation earthquake excitation, there are both evident randomness and strong nonlinearity owing to the evaluation norms of seismic intensity but also the site soil classification. A realistic analysis and design of structural systems subjected to such earthquake excitations [69,70] must account for the uncertainty arising from randomness, impact and friction.

Let us consider an n-degree-of-freedom nonlinear structural system governed by the Eq.2.15

$$m_1 \frac{d^2 q(t)}{dt^2} + c_1 \frac{dq(t)}{dt} + k_1 q(t) = f(t) \tag{2.15}$$

In which $m_1$ is the mass matrix and consistent $c_1$ is a viscous damping matrix (which is normally selected to approximate energy dissipation in the real structure) and $k_1$ is the static stiffness matrix for the system of structural elements. Forces $f(t) = p_j(t)$ acting on each point mass $m_j$ has a resisting force $f_s$ and the damping force $f_d$ acting against them. Newton's second law of motion gives for each mass:

$$m_j \ddot{u}(j) + f_{sj} + f_{dj} = p_j(t). \tag{2.16}$$

Where $m_j \ddot{u}$ is the inertia force and the damping force $f_d$ is related to the velocity $\dot{u}$ across the linear viscous damper i.e. ($f_d = c_1 \dot{u}$; $f_s = k_1 u$, $k_1$ is the lateral stiffness of the system). The column $q(t) = u(t)$ represents the degrees of freedom of the system. The first and second derivative of the column $q(t)$, with respect to time t, are $\dot{q}(t)$ and $\ddot{q}(t)$, respectively. The column $f(t)$ denotes the external excitation of the system with intermittent characteristics due to friction. The mass is able to move or vibrate in one direction, perpendicular to the column. It is considered to have certain amount of damping, $c_1$ [71,72], see table.2.1.

**Table 2.1**: Damping ratios of the fixed -base eigenfrequencies of the dynamic model

| mode no. | 1 | 2 | 3 | 4 | 5 | 6 and higher |
|---|---|---|---|---|---|---|
| eigenfrequency [Hz] | 0.46 | 1.27 | 1.98 | 2.98 | 4.10 | 4.25 and higher |
| damping ratio [-] | 0.03 | 0.04 | 0.05 | 0.06 | 0.08 | 0.10 |

While earthquakes are recurrent and aperiodic on a continuum time scale, the stick-slip of spring-block oscillations has mostly been periodic on a short time scale(see Fig. 2.3). In this model, the excitation exists of gravity; earthquake ground motion and noise due to friction. The relatively complex phenomenon of friction has a discontinuous behaviour caused by the fact that the friction force always opposes the relative velocity between two contacting surfaces which are subjected to friction. Then, friction may be a function of the relative velocity during sliding. Furthermore, dynamic effects, such as pre-sliding and varying break-away level, may be present.

## 2.2.2 Stationary stochastic process modelling the seismic ground motion

A simple model used to represent an earthquake accelerogram is a filtered stationary noise $w(t)$. This signal has the real frequency content of the earthquake acceleration. In this kind of model a White Noise (WN) models the earthquake acceleration at the bedrock, while a Single Degree of Freedom (SDoF) system defines the filtering effects of the soil layer crossed. Indeed the soil filters the frequency content of the signal. Two parameters characterizes this SDoF system: the damping ratio $\xi_g$ and the circular frequency $w_g$ . The ground acceleration $a_{st}$ is defined as the absolute acceleration of the filter:

$$\ddot{x} + 2\xi_g w_g \dot{x} + w_g^2 x = -w(t) \tag{2.17}$$

$$a_{st} = \ddot{x} + w(t) = -(2\xi_g w_g \dot{x} + w_g^2 x) \tag{2.18}$$

The power spectral density function of the filtered WN is

$$s(w) = s_0 |H(iw)^2| \tag{2.19}$$

where $H(iw)$ is the complex frequency response function of the filter and $s_0$ is the Power Spectral Density (PSD) of the WN excitation. This filter is a linear second order one, so the PSD of the filtered process is

$$s(w) = s_0 \frac{[1 + \xi_g^2 (\frac{w}{w_g})^2]}{[1 - (\frac{w}{w_g})^2]^2 + 4\xi_g^2 (\frac{w}{w_g})^2} \tag{2.20}$$

This model to estimate the PSD of the earthquake acceleration is known as the Kanai-Tajimi one. From Eq. 2.16, we get Eq. 2.17 as

$$\ddot{u} + 2\xi_g w_g \dot{u} + w_g^2 u = -\ddot{u}_g \tag{2.21}$$

such that, $\ddot{u}_g$ denotes the ground acceleration: horizontal motion of bedrock. The bedrock acceleration is related to the earth surface motion through the above differential equation.

u: vector of all translational and rotational degrees-of-freedom relative to earth surface. The dynamic effects of the sublayer deposit are specified by a Kanai-Tajimi filter with the parameters $\xi_g$ and $w_g$.

$\{\ddot{u}_g(t), t \in [0, \infty]\}$ is modelled as a modulated Wiener process.

$$\ddot{u}_g dt = \beta(t) dB(t) \tag{2.22}$$

$\beta(t)$ is a deterministic intensity function.

$\{B(t), t \in [0, \infty]\}$ is a unit Wiener process, which is a Gaussian process with the incremental properties.

$$E[dB(t)] = 0, \qquad E[dB(t_1)dB(t_2)] = \begin{cases} 0, & t_1 \neq t_2; \\ dt, & t_1 = t_2. \end{cases} \tag{2.23}$$

The integrated system of differential equations consisting of the structural system equations Eq. 2.15, and the filter equation Eq. 2.21 can then be written as the Stratonovich differential equations. Appearance of the resonant effect is in an amplification of ground motions, which can be as large as a factor ten relative to the rock sites [73] at different frequencies between 0.3 to $15Hz$.

## 2.2.3 Non-linear viscoelastic model: Numerical modeling of colliding structures to estimate the induced pounding forces

The proposed model is a nonlinear spring following the Hertz law of contact [74]. An other complex phenomenon involving plastic deformations at contact points is structural pounding. It causes local cracking or crushing, fracturing due to impact, friction, etc. Forces created by collisions are applied and removed during a short interval of time initiating stress waves which travel away from the region of contact. The process of energy transfer during impact is highly complicated which makes this type of problem difficult in the mathematical analysis. In general, to calculate impact force during contact we use the formula:

$$F_{im}(t) = k_{st}\delta^n(t) + c_{im}\dot{\delta}(t) \tag{2.24}$$

such that $k_{st}$ represents the stiffness of impact, $\delta$ represents the relative displacement, $\dot{\delta}$ represents the relative velocity, and $c_{im}$ denotes the damping coefficient. For $n = 1$, we are talking about linear systems, but in this thesis, $n = 1.5$ because of the nonlinearity of our systems. We should obtained $k_{st}$ by iteration of experimental and numerical simulation of the peak pounding force. And then $c_{im} = 2\zeta_{im}\sqrt{k_{st}\sqrt{\delta(t)}m_e}$ for nonlinear systems. Where $m_e = \frac{m_1 m_2}{m_1 + m_2}$; $m_i$ (i=1,2): masses of colliding structures.

The deformation $\delta(t)$ is expressed as $\delta(t) = x(t) - d$ where $d$ is the initial separation gap between the spillway and the abutment and $x(t)$ is the displacement of the spillway for example.

### 2.2.4 Law of the conservation of momentum and Newton's collision rule govern in collision between two systems.

Let us consider for example the collision between $m_1$ and $m_2$. Suppose $v_i$ and $v_i^+$ to be the velocity just before and just after the impact between the masses, respectively. Therefore, Newton's collision rule implies that

$$v_1^+ - v_2^+ = -\epsilon(v_1 - v_2) \tag{2.25}$$

where $\epsilon$ is the coefficient of restitution. It can be obtained from that eq.2.26.

$$\epsilon = \frac{v_2^+ - v_1^+}{(v_1 - v_2)} \tag{2.26}$$

The case of a fully elastic collision is $\epsilon = 1$. Hence $\epsilon = 0$ represents a fully plastic one. The rule of conservation of momentum determines the velocities just after the collision:

$$m_1(v_1^+ - v_1) = m_2(v_2 - v_2^+) \tag{2.27}$$

A collision between $m_1$ and $m_2$ happens when $x_1 \geq x_2$ and $v_1 > v_2$. In this case, the post-collisions velocities are

$$v_1^+ = v_1 \frac{m_1 - \epsilon m_2}{m_1 + m_2} + v_2 \frac{1 + \epsilon}{m_1 + m_2} \tag{2.28}$$

and

$$v_2^+ = v_1 \frac{m_1(1 + \epsilon)}{m_1 + m_2} + v_2 \frac{(m_2 - \epsilon m_1)}{m_1 + m_2} \tag{2.29}$$

The state variables of the system are represented by the position and velocity of each mass. Friction between the colliding bodies takes place during the whole time of impact. For the reasons of simplicity, in the model, during the restitution period the minor energy loss is neglected.

We recognize that the equation of motion for a single degree of freedom (SDOF) system under seismic action is generally expressed as:

$$m\ddot{u} + c\dot{u} + ku = -m\ddot{u}_g \qquad (2.30)$$

We reminder that $\ddot{u}_g$ denotes the ground acceleration. The bedrock acceleration is related to the earth surface motion through the above differential equation.

u: vector of all translational and rotational degrees-of-freedom relative to earth surface. We can divided the Eq.2.30 by the mass, m, it results Eq.2.21, which demonstrates that the response of a system due to an earthquake induced ground acceleration only depends on the natural frequency, $w_n$, of the system and its critical damping ratio, $\xi$.

### 2.2.4.1 Adjacent deck segments of bridge model: a spillway/bridge which interacts with an abutment

Let us consider the model of structural pounding as illustrated in Fig.2.3, used in the study of the effects of earthquakes. At each instance of collisions, the structures are subjected to short duration high magnitude lateral impulsive impact forces for which structures are not generally being designed as per the conventional design structural codes. In the past, it is noticed that the pounding forces can be much higher than the seismic forces calculated as per conventional design codes [75]. Pounding in bridges have lead to local crushing and spalling of pier bents, abutments, shear keys, bearing pads and restrainer, and also contributed to the collapse of decks. Parameters of interest in earthquake analysis, are relative displacement and velocity, and total acceleration, which is simply the sum of relative plus ground accelerations: $\ddot{x}_T(t) = \ddot{x}_g(t) + \ddot{x}(t)$. In a practical case, Eq.2.16 becomes the following equation

$$2\ddot{x} + 4.1\dot{x} + 210.125x + v(x, \dot{x}) + F_f - e(t) = \xi(t) \qquad (2.31)$$

The system consists of a mass $m_1 = 2kg$ (for instance), a frame (or spillway's spans) that provides stiffness to the system for example $k_1 = 210.125$, and a viscous damper that dissipates vibrational energy of the system $c_1 = 4.10$. Each structural member contributes

to the inertia (mass), elasticity (stiffness of flexibility), and energy dissipation (damping) properties. These properties can be considered as separate components (mass component, stiffness component, viscous component ) [77]. For an inelastic system, $v(x, \dot{x})$, is incorporated in the equation. When using Newton's second law (see Eq. 2.15), we deduced Eq. 2.31 including the impact force term, and the friction force term. Moreover, in Eq. 2.31 , $v(x, \dot{x})$ represents the pounding force which is equal to zero if $x(t) < d$ (d is an initial separation gap).

It is illustrated by Eqs. (2.24) when $x(t) > d$, where deformation $\delta(t)$ is expressed as $\delta(t) = x(t) - d$. $t \in [0, 3]$ the displacement time history of the spillway, with $e(t) = 2sin(14t)$ where the external force is acting on the system with a certain frequency, $w = 14$ Hz, and the maximum amplitude of the force is $p_0 = 2$. $v(x, \dot{x})$ is given by the knowledge of peak impact force during collisions and frictions. The friction can be expressed as: $F_f = -\mu N sgn(\dot{x_1})$.

where $\mu$ is the coefficient of sliding friction, N is the weight of elements in friction (N $= \sum_{i=1}^{n} (m_i g)$. $\xi(t)$ is the normalized source of Gaussian white noise Eq. 2.3. The equation of motion is written including the impact force term, $v(x, \dot{x})$, force between two masses

$$v(x, \dot{x}) = \begin{cases} 0, & \text{if } x < \nu; \\ c(x - \nu)^{\frac{3}{2}} + 1.98\sqrt{2c}(x - \nu)^{\frac{1}{4}}\dot{x}, & \text{if } x > \nu, \dot{x} > 0; \\ c(x - \nu)^{\frac{3}{2}}, & \text{if } x > \nu, \dot{x} < 0; \\ c = 2.47e10^6, & \nu = 0.005. \end{cases} \quad (2.32)$$

$\nu$ is the Poisson's ratio of the soil. Recall that the deformation $\delta(t)$ is expressed as $\delta(t) = x(t) - d$ where $d$ is the initial separation gap between the spillway and the abutment. Moreover Eq. 2.32 denotes the pounding force as Eqs.(2.24) [78]. It is a discontinuous nonlinear contact- impact term with friction. This impact force between the spillway and the abutment will be our concerned in the numerical simulation. As is the case for most forced vibration problems, the diffusion vector $e(t)$ is independent of the state vector $x$. Then the associated *Itô* and Stratonovich differential equations of the problem are equivalent. Fig. 2.4 shows the view of the spillway in 3-dimensions. The pounding phenomenon is illustrated in Fig. 2.4(b) with an associated plan scale A. The Key plan

of spillway and flushing sluice is shown in Fig. 2.4(c).
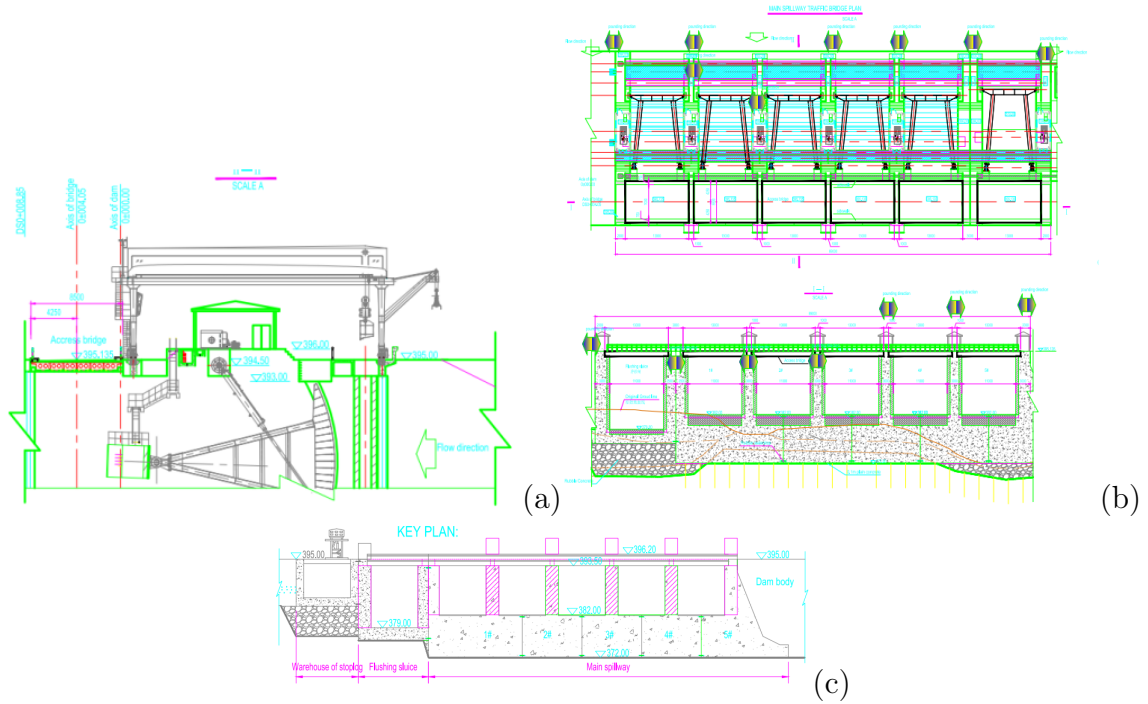


**Figure 2.4**: *view of the 3D spillway: (a): spillway of the project. (b): Main spillway and flushing sluice (associated with plan scale A) (c): Key plan of spillway and flushing sluice*

For piecewise-smooth systems it is important to record the transitions through the discontinuity surfaces, i.e. at impacts or switches between different vector fields of the system. Such transitions are called events and are triggered by zero crossings of scalar valued event functions. Matlab solvers (such as ode45) contains built in routines for detecting zero crossings of event functions have therefore been used here. The structural model defined by eq.2.31 is the basis of the numerical analysis. We present the expression as a first order system (non-smooth, non-stiff differential systems

$y'(t) = f(t, y(t)), \qquad y(0) = y_0 \in R^m, \qquad t \in [t_0, t_f]$ ) with two components:

$$\begin{cases} y_1(t) = x(t), \\ y_2(t) = \dot{x}(t) \end{cases} \tag{2.33}$$

Then

$$\dot{y} = \begin{pmatrix} \dot{y_1} \\ \dot{y_2} \end{pmatrix} = \left\{ \begin{pmatrix} y_2 \\ -4.1y_2 - 210.125y_1 - u(y_1, y_2) - e(t))) \end{pmatrix} = f(t, y) \qquad (2.34) \right.$$

It is assumed that the solution crosses the hyper-surface of discontinuity and a transversality condition is satisfied. However, there are dynamical systems for which the solution reaches the discontinuity surface and stays on it for some time and then goes out again. This happens in the so called sliding mode regime for Filippov systems in which a switching surface attracts, in finite time, nearby dynamics, so that trajectories become constrained to remain on this surface. Such systems appear, for example, in mechanical and electromechanical systems under certain control techniques, ecology and population models.

## 2.3 Application: The dynamic behavior of a n-floor storey

The dynamic behaviour of civil structure, which is shown in Fig. (2.5), needs to be determined concerning pounding and consequently failure of the building. Fig. 2.5 shows the pounding phenomenon in all the building. As an impact of Ntem (River closed to Atlantic Ocean) Fault , local faults and densely jointed zones are found on the banks along Ntem Canyon. The rocks closer to the bank of the Ntem Canyon, the rock may be more fractured, that's means $\nu = 0.0$. Therefore, the building shall be away the bank as far as possible to avoid the adverse effects on foundation excavation and rock support, slope stability due to cross the joints. Structures may be subject to various types of live load caused by events such as earthquakes, high speed winds. Therefore, pounding effect is evident. We can illustrated the displacement of the structure at each floor and the variability effects on the response dispersion. But, the potential damaging effect of pounding remains difficult to estimate. The columns between the floors will be taken as springs and the masses of the floor slabs are lumped at the floor levels. Additionally, a motion exerts a small force on the lumped mass at each floor directly proportional to the velocity of that degree of freedom. The horizontal vibrations of a one-storey building can be conveniently modeled as a single degree of freedom (SDOF) (Fig. 2.5), because each structural member contributes to the inertial (mass), elastic (stiffness or flexibility) and
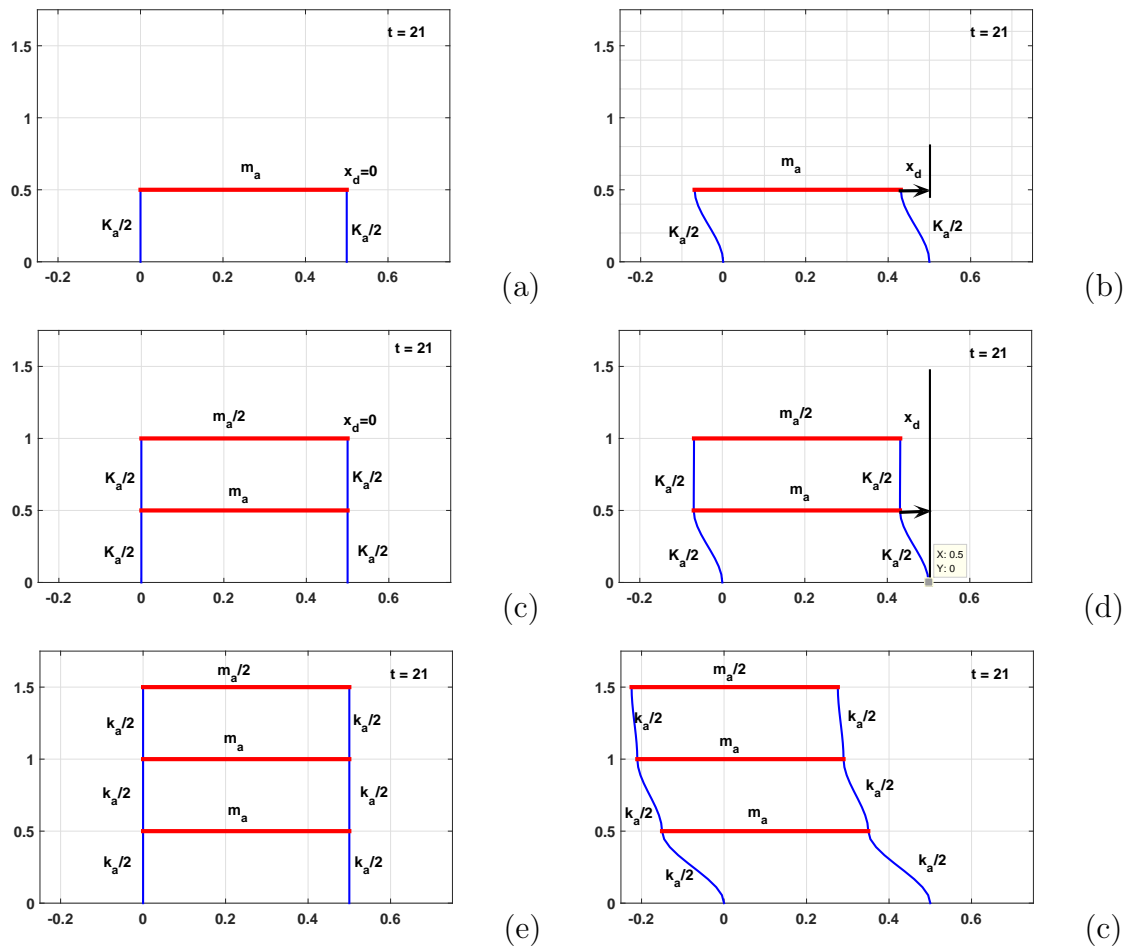
**Figure 2.5**: *Hysteretic (one, two, three)-DOF structural system modelled as mass spring system: Simple vibration model of a building subjected to ground motion (b);(d);(f).*

energy dissipation (damping) properties of the structure. In the analysis, two types of dynamic excitation can be considered:

i). Time-varying forcing function F(t), (Fig. 2.5(b, d, f)) and

ii). Earthquake induced ground motion $\ddot{x}_g(t)$ (Fig. 3.11(c)).

The general mathematical representation of (SDOF) system is expressed using Newton's second law of motion as above. The forces acting on the mass at some time instant include the external force (F(t)), the elastic ($f_s = Kx$) or inelastic ($f_s = f(x, \dot{x})$) resisting force, where K is the lateral stiffness of the system (force/length units), and the damping resisting force ($f_d = C\dot{x}$), where C is the viscous damping coefficient (force · time/length units). The external force, the displacement x, the velocity $\dot{x}$ and the acceleration $\ddot{x}$ are

taken to be positive in the direction of the $x - axis$, therefore the resultant force along the x-axis is $F(t) - f_s - f_d$, and applying the Newton's second law (F = ma): see Eq. 2.16. Based on the given information about the mass of each floor and the stiffness of each column, the mass matrix M, stiffness matrix K and damping matrix C, $3 \times 3$ each matrix can be constructed as the equation of motion Eq. 2.16 under seismic excitation undergoing pounding. Let suppose $f_p(t) = 0$, $n = 1, 2, 3$, we get Eq. 2.16 where $\dot{x}_0 = v_0$ and         $x_0 = x(0)$.

Vectors x and F store the floor displacements and applied loads at each floor, respectively. $x_0$ and $v_0$ give the initial state (displacement and velocity) of the structure at time $t = 0$. We can then illustrated the mass of each floor and the stiffness of each column, the mass matrix, stiffness matrix and damping matrix can be seen as:

$$M = \begin{pmatrix} m_a & 0 & 0 \\ 0 & m_a & 0 \\ 0 & 0 & \frac{m_a}{2} \end{pmatrix};$$

$$K = \begin{pmatrix} 2k_a & -k_a & 0 \\ -k_a & 2k_a & -k_a \\ 0 & -k_a & k_a \end{pmatrix};$$

Obviously, the inter-story yielding strength is random with truncated normal distribution. With the Rayleigh method, in which the damping matrix is assumed to be proportional to the mass and stiffness matrix $C = \alpha_1 M + \beta_1 K$.

Initially, an excitation pulled the first floor with a displacement $s_0$, and suddenly got cut at time $t = 0$ (see fig. 2.5). When a structure is in free vibration, the applied loading is zero.

In case of a free vibration problem, $F = 0$. Initially, $s_0$ is a the first floor displacement, as shown in Fig.2.5, and suddenly got cut at time $t = 0$. The initial conditions of this problem can be described as $\dot{x}_0 = [0 \quad 0 \quad 0]^T$ and $x(0) = [s_0 \quad s_0 \quad s_0]^T$. Convert the given system into standard form:

$\dot{y} = f(t, y)$,

$\dot{y}(t) = f(t, y(t))$

$$y(t) = \begin{pmatrix} y_1(t) \\ y_2(t) \end{pmatrix}$$

$$\begin{pmatrix} y_1(t) \\ y_2(t) = \dot{y_1}(t) \end{pmatrix} = \begin{pmatrix} x(t) \\ \dot{x}(t) \end{pmatrix};$$

and

$$\left\{ \begin{pmatrix} \dot{y_1}(t) \\ \dot{y_2}(t) \end{pmatrix} = \begin{pmatrix} y_2(t) \\ M^{-1}[F(t) - Cy_2(t) - Ky_1(t)] \end{pmatrix} \right. \tag{2.35}$$

For elasto-plastic frames under heavy excitation plastic deformations may accumulate in such a way, that large permanent deflections occur, see fig. 2.5. The variance-response of the storey displacements will be significantly influenced by the state variables (such as the bending moment M for instance) which control the hysteresis are far from being normally distributed.

This section highlight the fact that periodic impacts do not occur for some excitation frequencies. Among many intrinsic material parameter, Poisson's ratio ($\nu$) describe toughness and brittleness of materials. To withstand earthquakes excitation, the natural frequencies of vibration of buildings are not close the ground motion frequency oscillation. We recognized that the natural frequencies of buildings are determined primarily by the masses of its floors, but also by the lateral stiffness of its supporting columns, (these last one acted as horizontal springs). We can calculated these frequencies by solving for the roots of a polynomial called the structure's characteristic polynomial. Fig. 2.5(f) shows the exaggerated motion of the floors of a three-story building. Let us supposed, each floor has a mass m and the columns have stiffness k, the structure's characteristic polynomial is written:

$$(\alpha - f^2)[(2\alpha - f^2)^2 - \alpha^2] + \alpha^2 f^2 - 2\alpha^3 \tag{2.36}$$

Knowing that $\alpha = \frac{k}{4m\pi^2}$. If we found the positive roots of this equation, that's means we got the building's natural frequencies in cycles per second. Hence to find the building's natural frequencies in cycles per second for the case where $m = 1000kg$ and $k = 5 \times 10^6 N/m$. The characteristic polynomial consists of sums and products of lower-degree polynomials. The resulting positive roots and thus the frequencies, rounded to the nearest integer, are 20, 14, and $5Hz$.

The SDOF system is analyzed; with natural frequency $w = 7.85$ rad/s, and damping ratio $\zeta = 0.02$ subjected to the same white noise excitation $W_{tk}$ defined. This system is characterized by the following equation of motion eq.2.21.

Where $\dot{r}_0 = 0; r(0) = 0; z(0) = 0$ (initial conditions) see Fig. 3.11(c).

## 2.3.1 The practical study of seismic vulnerability in the southern plateau area of Cameroon

The ground generally descends from north towards south at an elevation varied between 400 m and 700 m above the Atlantic Ocean level. No seismic study has been carried out since the following analysis. The southern plateau area of Cameroon is a part of Congo Stable Block. Tectonic features in the region mainly comprise folds and faults striking in a generally $NE - SW$ direction. A major fault ( Ntem Fault) runs in $NE - SW$ direction at some 500 m downstream of the proposed dam site. It controls the flow of Ntem river, making the Ntem course bended from northwest to southwest and forming a waterfall of 35 height near the faulted zone, then linearly traced to the "Gorge Du Ntem" about 40 km. Several faults are encountered at Ntem Fault that generally strike $NE30 \sim 40$, dip northwesterly at an angle of $50 \sim 60$, each of limited fractured zone. They are filled with breccia and cataclasite and are well cemented with fair behavior. It might be formed at Mesozoic era to Eogene period. Given the terrain feature and earthquake history, Ntem Fault is considered to be passive.

Since seismic network was built in Cameroon in 1984, there have been in our knowledge only six unfelt events that were recorded. Earthquake data of the area bounded by latitude $(N - 4.33)$ degrees to $(S - 0.33)$ degrees and longitude $(E - 8.25)$ degrees to $(E - 12.25)$ degrees was searched by international seismological center (ISC) in United Kingdom by the request of JICA study team, which indicate no earthquake that may affected to the project site was found out from the ISC historical events in the period of $1904 - 1990$ and ISC comprehensive catalogue in the period of $1964 - 1988$. According to Seismicity of West Africa [79], Ambrasey and Adams studied seismic data near some important projects area. As shown in Table2.2 and Fig.3.8 illustrated, only three events are depicted in the report which might be affected to these projects site.

**Table 2.2**: Historical Earthquakes near the Project Area

| Date | | | Epicenter | $M$ | $r$ | $I$ | $Ah$ |
|------|------|------|-----------|-----|-----|-----|------|
| 1903 | *June* | 10 | $3N10.0E$ | 4.4 | 79.4 | 3.7 | 13.0 |
| 1911 | *March* | 26 | $3.1N11E$ | 5.7 | 119.3 | 4.6 | 24.8 |
| 1913 | *October* | 9 | $3.8N12.3E$ | 5.1 | 280.0 | 1.6 | 3.1 |

Where $M$ is the magnitude, $r$ is the distance from the epicenter of earthquake to the site in kilometer. The Intensity $I$ for the site can be by theoretically calculated using the modified Mercalli Scale

$$I = 8.0 + 1.5M - 2.5lnr \tag{2.37}$$

(by Cornell , [80])

Hence Ah, Acceleration in $cm/sec^2$ theoretically calculated

$$LogAh = 0.014 + 0.30I \tag{2.38}$$

(by Trifunac and Brady, [81])

The analysis for an earthquake coefficient based on the relation between intensity felt at the site as above listed and frequency of occurrence (Nc) in the period for 100 years and 250 years by ISC method, Japan Meteorological Agency (JMA) method and Munich Reinsurance (M.R.) company. The results of the analysis are calculated and summarized as shown in Table2.3

**Table 2.3**: Calculation of Earthquake Coefficient

| Return Period | | $ISCmethod(i)$ | $JMAmethod(ii)$ | $M.R.(i)$ |
|---------------|------|----------------|-----------------|-----------|
| 100 | *years* | $2.5(= 5.8gal)$ | $I - II(2.5gal)$ | ... |
| 250 | *years* | $4.0(= 16.4gal)$ | $III(= 14gal)$ | 5 or blow ($<$ $32.7gal$) |

Where $(i)$ $logAh = 0.014 + 0.30I$ (I: Intensity in ISC scale)

$(ii)$ $a(gal) = 0.45 * 10^{S/2}$ (S: Intensity in JMA scale)

From the above calculated, the earthquake coefficient ($k = gal/980$) is resulted as $k = 0.0006$Ą say; $k = 0.01$ for the return period of 100 years and $k = 0.03$ for 250 years respectively. The value of $k = 0.01$ is the proposed earthquake coefficient for the Nachtigal Amont Hydropower project locating some 350 km northeast of Memve'ele project site.

As defined in American regulation No. $ER1110 - 2 - 1806$, Operating Basic Earthquake (OBE) is an earthquake that can reasonably be expected to occur within the service life of the project, that is with 50-percent probability of exceedance during the service life. ( This corresponds to a return period of 144 years for a project with a service life of 100 years). For conservative design, OBE is currently recommended to be $0.03g$ (corresponding to a return period of 250 years as calculated in 1993) and MCE to be double of OBE, i.e. $0.06g$ for Memve'ele hydroelectric project.

To sum up, Memve'ele hydroelectric power development project is tectonically and seismologically located on a stable block. Therefore, full-scale validation (monitoring) of structural response through recorded wind and earthquake excitation is important. The non-smooth properties can be exploited to design new mechanical devices. As suggested in this work it opens up the possibility of, for example, fast limit switches and energy transfer mechanisms.

### 2.3.2    Thom's theorem in case of the so-called conditional catastrophes; Probability of failure.

Normally, structural failures occur due to extreme loads exceeding the residual strength. The load-carrying capacity of buildings leads to a singular point on the equilibrium surface of structures. Thus, the defect sensitivity can be expressed in terms of the bifurcation set in the catastrophe theory. The conditional probability $p_0$ is used to determine the imperfection sensitivity curves or surfaces from the singularity condition in the catastrophe theory. Therefore in structural reliability, models are established for resistances R and loads S individually and the structural reliability is assessed through the probability of

failure. Probability of failure

$$p_f = P(R - S < 0) \tag{2.39}$$

Reliability:

$$1 - p_f \tag{2.40}$$

Let X be a random variable in an engineering application. The probability density function (PDF) and cumulative distribution function (CDF) of X are denoted by $f_X$ and $F_X$, respectively. Their relationship is

$$f_X(x) = \frac{\partial F_X(x)}{X} \tag{2.41}$$

$$P_f = P(M \leq 0) = P(g(X) \leq 0); X = (x_1, \ldots, x_n).$$

Introduce the joint probability density function $f_X(X)$ for the basic random variables X. Then

$$P_f = \int_0^{w_f} f_X(X) dX \tag{2.42}$$

where $w_f$ is the failure region defined by the limit state function (LSF).The assessment of small failure probability in engineering design field to find intermediate failure events during ground shaking is our motivation. That's why the concept of conditional probability $p_0$ of collapse subjected to static loads is used.

### 2.3.2.1   Illustrative examples

Fig.(2.5) is found in fractured bedrock i.e., $\nu = 0.0$ (poisson's ratio of the soil Eq.(2.32), but for $\nu = 0.20$, the rock is not fractured. The metamorphosed bedrock at depth generally have poor permeability and fracture water is mainly stored in densely jointed zones and faulted zones. From Eq.(2.31), we can illustrated pounding areas i.e. the discontinuous points, see Fig.(3.12) (b). Let us considered the two-bay two-storey frame with their collapses subjected to static loads, including one horizontal load $P_1$ in each storey and

a vertical load $P_2$, as shown in Fig.(3.12). Both $P_1$ and $P_2$ are random and normally distributed. The failure of the each frame is defined by the first-order rigid-plastic hinge theory and then some dominant collapse mechanisms can be illustrated, as shown in Fig.(3.12) as failure modes. The frame fails when any one of these collapse mechanisms occurs. This means that it is a series system in each storey, i.e., the limit state function (LSF) of this frame.

Concludingly, it is noted that the behavior of the system can be described by a response variable y, which may represent, for example, the roof displacement or the largest inter-story drift.

As second application, let us considered now the deviation of a cantilever beam, with a rectangular cross-section, uncertain parameters and subjected to a uniform load. The target failure region is a linear half-space, i.e., $F = h(x) < 0$, and h is a normal variable so that the failure probability is analytically given by:

$$p_f = p(h(x) < 0) = \Phi(-b) \tag{2.43}$$

Where $\Phi(.)$ is the CDF of standard normal distribution; to avoid the failure of the cantilever beam, at the fixed end of the beam, the maximum stress should not exceed the yield strength constant value $\sigma_s$. To illustrate the use of subset simulation (SS function), consider estimating the failure probability of the following LSF: the cost function is:

$$\Phi(b, w, l) = \sigma_s - \frac{6\sigma_x l}{w^2 h} - \frac{6\sigma_y l}{w h^2} \tag{2.44}$$

where l is the length of the beam, w and h are the width and height of the cross section of the beam, respectively. They are uncertain parameters which are supposed to be independent and have normal distribution, as specified in tb.2.4. The force $\sigma_x$, is horizontal and $\sigma_y$, a vertical force. These forces are applied to the end of the beam.

We use $\sigma_s = 100.46154$ N as the threshold for the definition of the failure event, and a failure happens when the cost is larger than threshold.

#### ⬦ **Failure to nonstructural elements:**

Various parameters can expressed the seismic performance of structures under earthquake loading. Some of these parameters can be correlated to the amount of motion of the building and the expected resulting failure to nonstructural elements. Nonstructural elements

---

**Table 2.4**: random input factors.

| Variable | Distribution | values in sample 2 |
|----------|--------------|--------------------|
| l        | ℵ            | 957.64             |
| w        | ℵ            | 94.41              |
| h        | ℵ            | 199.87             |

are often considered, because they experience the same movement as structural ones, but fail at much less deformation. Furthermore, because nonstructural elements consist of a vast group of necessary building items (for instance ceilings, partitions, furniture, lighting, etc.), they usually make up a great percentile of the entire cost of the building [83]. The performance of nonstructural elements is thus of great importance. Collapse mechanisms should occur to nonstructural elements.

Supposed two performance indicators that can be correlated to the amount of failure modes (or damage) to nonstructural elements, are the inter-story drift ratio $IDR_i$ and the horizontal floor acceleration $a[m/s^2]$. The inter-story drift ratio is defined as the ratio of the relative horizontal displacement between two successive floors and the story height:

$$IDR_i(t) = \frac{x_{i+1}(t) - x_i(t)}{h_i} \tag{2.45}$$

Herein, $i$ is the construction level, $x_i$ is the horizontal displacement [m] of the floor of construction level $i$ (the floor of construction level 1 equals the first slab) and $h_i$ is the construction level height [m].

The maximum absolute value of the inter-story drift ratio of construction level i over a time-span t, is called $IDR_i$:

$$IDR_i = max_t \left| \frac{x_{i+1}(t) - x_i(t)}{h_i} \right| \tag{2.46}$$

We can summarized the probability of failure of the inter-story drift ratio of construction level i over a time-span t in tb.2.5.

The floor acceleration $a_i(t)$ is illustrated as the horizontal acceleration of the top of construction level $i$, is another collapse mechanisms that occur to nonstructural elements;

**Table 2.5**: Estimated failure probabilities and the number of samples with different $p_0$

| $p_0$ | 0.10 | 0.15 | 0.20 | 0.35 |
|---|---|---|---|---|
| Failure probability (here $Pfss$) | (0.1000) | 0.1350 | 0.1328 | 0.1533 |
| Number of samples | 950.0 | 925 | 900 | 825 |

measured relative to inertial space:

$$a_i = \ddot{u}_{hor}(t) + \ddot{x}_{i+1}(t) \tag{2.47}$$

$\ddot{u}_{hor}(t)$ equals the horizontal ground acceleration. $\ddot{x}_{i+1}(t)$ denotes the acceleration of the top of construction level $i$.

## 2.4   Numerical simulation of the probability density

Obtaining analytical solution of differential equations is in most cases, the most difficult challenge in continuous time dynamics. Since most ordinary differential equations are not soluble analytically, numerical integration is the only way to obtain information about the trajectory. Different methods have been proposed and used in an attempt to more accurately solve various types of differential equations. However there are a handful of methods known and used universally (i.e., Runge-Kutta, Adams-Bashforth and Backward Differentiation Formula methods). All these methods discretize the differential system to produce a discrete system of equation or map. The methods obtain different maps from the same differential equation, but they have the same aim; that the dynamics of the map should correspond closely to the dynamics of the differential equation. In this work, we use the fourth order Runge-Kutta algorithm and other numerical methods which depend on what we want to find.

### 2.4.1   The fourth order Runge-Kutta algorithm

The fourth order Runge-Kutta is a much more locally accurate method. Let's consider the following problem

$$\begin{cases} \frac{dy}{dt} = f(t, y), \\ y(t_0) = \alpha, \end{cases} \qquad (2.48)$$

and define h to be the normalized integration time step size and set $t_i = t_0 + ih$. Then the following sequence of operations

$$U_o = \alpha$$

$$U_{i+1} = U_i + \frac{h}{6}(k_1 + 2k_2 + 2k_3 + k_4), \qquad for \qquad i = 0, 1, ..., n - 1 \qquad (2.49)$$

computes an approximate solution, that is $U_n \approx y(t_n)$. $k_1, k_2, k_3$ and $k_4$ are the coefficients which have to be evaluated in each stage of the loop (of the fourth order Runge-Kutta algorithm) by the formulas below:

$$k_1 = f(t_i, U_i)$$
$$k_2 = f(t_i + \frac{h}{2}, U_i + \frac{h}{2}k_1)$$
$$k_3 = f(t_i + \frac{h}{2}, U_i + \frac{h}{2}k_2)$$
$$k_4 = f(t_i + h, U_i + hk_3) \qquad (2.50)$$

In the case of differential equation of Filippov's type of which we are particularly concerned with in the framework of this dissertation, the above algorithm is slightly modified to take into account the piecewise definition of the differential equation. Consider the following Filippov type equation

$$\begin{cases} \frac{dy}{dt} = f(t, y) = \begin{cases} f^-(t, y), & \text{if } y < \beta; \\ f^+(t, y), & \text{if } y > \beta. \end{cases} \\ y(0) = \alpha, \end{cases} \qquad (2.51)$$

where $y = \beta$ defined the switching boundary, that is the manifold of the state space on which the right-hand side (f(t, y)) of Eq. 2.54 changes discontinuously. The algorithm used to obtained the approximate solution of this equation (Eq. 2.54) is given as follows:

$$U_0 = \alpha$$

$$U_{i+1} = \begin{cases} U_i + \frac{h}{6}(k_1^- + 2k_2^- + 2k_3^- + k_4^-), & \text{if } U_i < \beta; \\ U_i + \frac{h}{6}(k_1^+ + 2k_2^+ + 2k_3^+ + k_4^+), & U_i > \beta. \end{cases} \qquad (2.52)$$

where

$$k_1^j = f^j(t_i, U_i)$$
$$k_2^j = f^j(t_i + \frac{h}{2}, U_i + \frac{h}{2}k_1)$$
$$k_3^j = f^j(t_i + \frac{h}{2}, U_i + \frac{h}{2}k_2)$$
$$k_4^j = f^j(t_i + h, U_i + hk_3) \qquad (2.53)$$

$j \in -, +$ The Runge-Kutta method is very widely favored as:

⋄ It is easy to use and no equations need to be solved at each stage;

⋄ It is highly accurate for moderate h values;

⋄ It is a one step method, that is; $U_{i+1}$ only depends on $U_i$;

⋄ It is easy to start and easy to code.

In the special case when f(t, y) = f(t), we have

$$y(t) = \int_{t_0}^{t} f(t)dt + y(t_0) \qquad (2.54)$$

and the task of evaluating this integral accurately is called quadrature. To solve any differential equation with the fourth order Runge-Kutta algorithm, we need to put it into the standard form given by Eq. 2.48.

## 2.4.2 Other numerical methods

The other numerical methods used in this dissertation help us to plot the results obtained with the fourth order Runge-Kutta algorithm and other curves such as the dependencies of the period and the amplitude with respect to parameters of the oscillator, the dependencies of the phase differences between coupled oscillators with respect to time or coupling coefficients.

**✓ The pair of explicit RK formulas of Dormand and Prince (DOPRI) [84] of orders 4 and 5, for the numerical solution of PWS systems.**

An adaptive Runge-Kutta code, based on the DOPRI $(5, 4)$ [85] pair for solving Initial Value Problems for differential systems with Piecewise Smooth solutions (PWS) is used and the algorithms used in the code are described. The code automatically detects and locates accurately the switching points of the PWS, restarting the integration after each discontinuity. Further, in the case of Filippov systems, algorithms to handle properly sliding mode regimes in an automatic way are included. The code requires the user to provide a description of the IVP and the functions defining the hypersurfaces where the switching points are located, and it returns the discrete approximated solution together with the switching points.

We consider Initial Value Problems (IVPs) for differential systems with Piece Wise Smooth solutions (PWS) that are defined by

$$\dot{y} = f(t, y); \qquad y(t_0) = y_0 \in R^m; \qquad t \in [t_0; t_f]; \qquad (2.55)$$

where the vector field $f : R \times R^m \rightarrow R^m$ contains bounded discontinuities either in f itself or in some its derivatives on a smooth event hyper surface defined by $g(t, y) = 0$ (switching surface), so that f(t, y) can be locally written in the form:

$$f(t, y) = \begin{cases} f_-(t, y), & \text{for} \qquad g(t, y) < 0; \\ f_+(t, y), & \qquad g(t, y) > 0. \end{cases} \qquad (2.56)$$

with the sufficiently smooth functions $f_-$ and $f_+$ satisfying a local Lipschitz condition with respect to y in a tubular domain around the solution of Eq. 2.55 in their definition domain. These PWS systems are also called switching systems, and some authors consider them as hybrid systems. It is assumed that the solution crosses the hypersurface of discontinuity and a transversality condition is satisfied. However, there are dynamical systems for which the solution reaches the discontinuity surface and stays on it for some time and then goes out again. This happens in the so called sliding mode regime for Filippov systems [86] in which a switching surface attracts, in finite time, nearby dynamics, so that trajectories become constrained to remain on this surface.

**✓ A Variable-Step Fourth-Fifth-Order Runge-Kutta Solver**

For problems in which the time increments are not much shorter than the shortest natural periods involved in the system, and for problems involving hard nonlinearities, such as problems involving impact or friction, fixed-step Runge-Kutta solvers may be numerically unstable. In such cases one may attempt a re-analysis using a shorter time step for every time step, or one may use a solver in which the large fixed time-steps are automatically subdivided only when necessary. A feature of such variable time-step solvers is that a desired level of accuracy may be enforced throughout the simulation, by comparing a fourth-order accurate solution with a fifth-order accurate solution. The implementation of the fourth-fifth order solver discussed here was proposed by *Cash et al.* [87]. The components of the structural system have first-order dynamics (for example, visco-elasticity or Bouc-Wen hysteresis): hence the first order dynamics can be appended to the state vector, and the simulation of the second order structural system coupled with the first order structural components can proceed in the same time.

✓ **Subset Simulation** Subset Simulation is an adaptive stochastic simulation procedure for efficiently computing small failure probabilities. Strictly speaking, it is a procedure for efficiently generating samples that correspond to specified levels of failure probabilities in a progressive manner. *Monte Carlo simulation (MCS)* [88] is robust to the type and dimension of the problem, however it is not suitable for finding small probabilities, because the number of samples, and hence the number of system analyzes required to achieve a given accuracy is proportional to $1/P_f$. A more advanced method is Subset Simulation [89, 90] (SubSim) which compensate this drawback. In this procedure, the failure probability is expressed as a product of conditional probabilities of some chosen intermediate failure events.

## 2.5 Conclusion

This chapter has presented the mathematical formalisms needed for analytical investigations and the numerical methods used to integrate the ordinary differential rate equations of the system. We started by presenting the analytical methods and some mathematical formalisms. After that, the numerical methods and some computational techniques both utilized to solve the ODEs and to characterize dynamical behavior of

the system have been described. The mathematical basis, for the pounding phenomena, on which most of response analysis methods are founded, is discussed. Furthermore, specific nonlinear stochastic response phenomena are encountered, discussed, explained and compared with specific deterministic nonlinear response phenomena. The analytical treatment of these models, which are differential equations of Filippov type, is found to be very cumbersome. Therefore, the main results are based on numerical treatments. The results of numerical simulations are presented in the next chapter with the discussions.

# Chapter 3

# Results and discussions

## Introduction

## 3.1   Introduction

In the previous chapters, we have provided the generalities on non-smooth systems, impact-friction phenomena and failure events in structural buildings. We have also modeled the pounding effects in civil structures and have given failure phenomena in building structures subjected to natural hazard excitations. In the present chapter, we bring out our results. Thus, we present an archetypal self-excited SD oscillator with dry friction under excited stochastic base-driven stick-slip. We investigate the dynamic response, stability, and bifurcation behavior of this non-smooth nonlinear dynamical systems under stochastic excitation. Secondly, we illustrate the impact-friction behavior between a spillway and the abutment and between three floors building with adjacent structures. Thirdly, we present plastic deformation during excitation that is allowed in special parts of the structure, often called plastic hinges, while the rest of the structure remains in its elastic range. The calculation of failure probability associated with inelastic response is performed using a Subset Simulation procedure.

## 3.2 Friction processes upon geometrical nonlinearity with large deformations in the case of SD oscillator

It is evident that a deep analyzing of the role of non-smooth sliding process of our model is of crucial importance in the nature and many engineering cases. Friction processes upon geometrical nonlinearity with large deformations open new windows to observe 'Tom's catastrophic Theory' in SD oscillator. In mathematics, catastrophe theory is a branch of bifurcation theory in the study of dynamical systems; it is also a particular special case of more general singularity theory in geometry. Hence, René Thom calls catastrophe theory the application of specific mathematical results in the field of differential topology and the theory of singularities. The applications of classical catastrophe theory to engineering problems have been pioneered by Michael Thompson. In particular, the books with Giles Hunt [91, 92] serve as standard reference. Our goal was to make this illustration homogeneous and easy to follow in the sense that each bifurcation type is demonstrated as failure event on the same type of structure (continuous beam with supports displacement, shear, buckling, ...), as a result, some illustrations are somewhat due from natural hazards). We have computed Eq. 2.9 numerically to illustrate the theoretical predictions using fourth-order Runge−Kutta algorithm. In all the calculations we assume that: $c = 0.048$, $x_{fk} = 0.25$; $x_{fs} = 1.0$; $f = 0.85$; $\alpha = 0.4$; $C_0 \neq 0$ ($C_0 = [g_1 - \alpha(1 - \frac{1}{\sqrt{x_1^2 + \alpha^2}})]$); $C_1 = C_2 = 0$; $\mu = 0.5$. The stick-slip behavior in friction oscillators is very complicated due to the non-smoothness of the dry friction, which is the basic form of motion of dynamical systems with friction. Furthermore, we introduce a smooth function which approximates the discontinuous drift. The system exhibits different shapes of periodic windows follow by a sudden occurrence of chaotic responses certainly due to the jumps that are characteristics of 'grazing-sliding bifurcations'.

Fig. 3.1 shows the time histories and phase plane plots of the solution with friction coefficients $\mu = (0.0; \quad 0.1; \quad 0.3)$. It shows the influence of friction coefficient in the dynamic of the system. The stick-slip friction and limit cycle oscillation (LCO) are really identified in Fig.3.1(b, c). Therefore, Fig.3.1(d, e) shows a segment of trajectory crosses the sliding region, enter into the slipping region and joins back the sliding surface. The
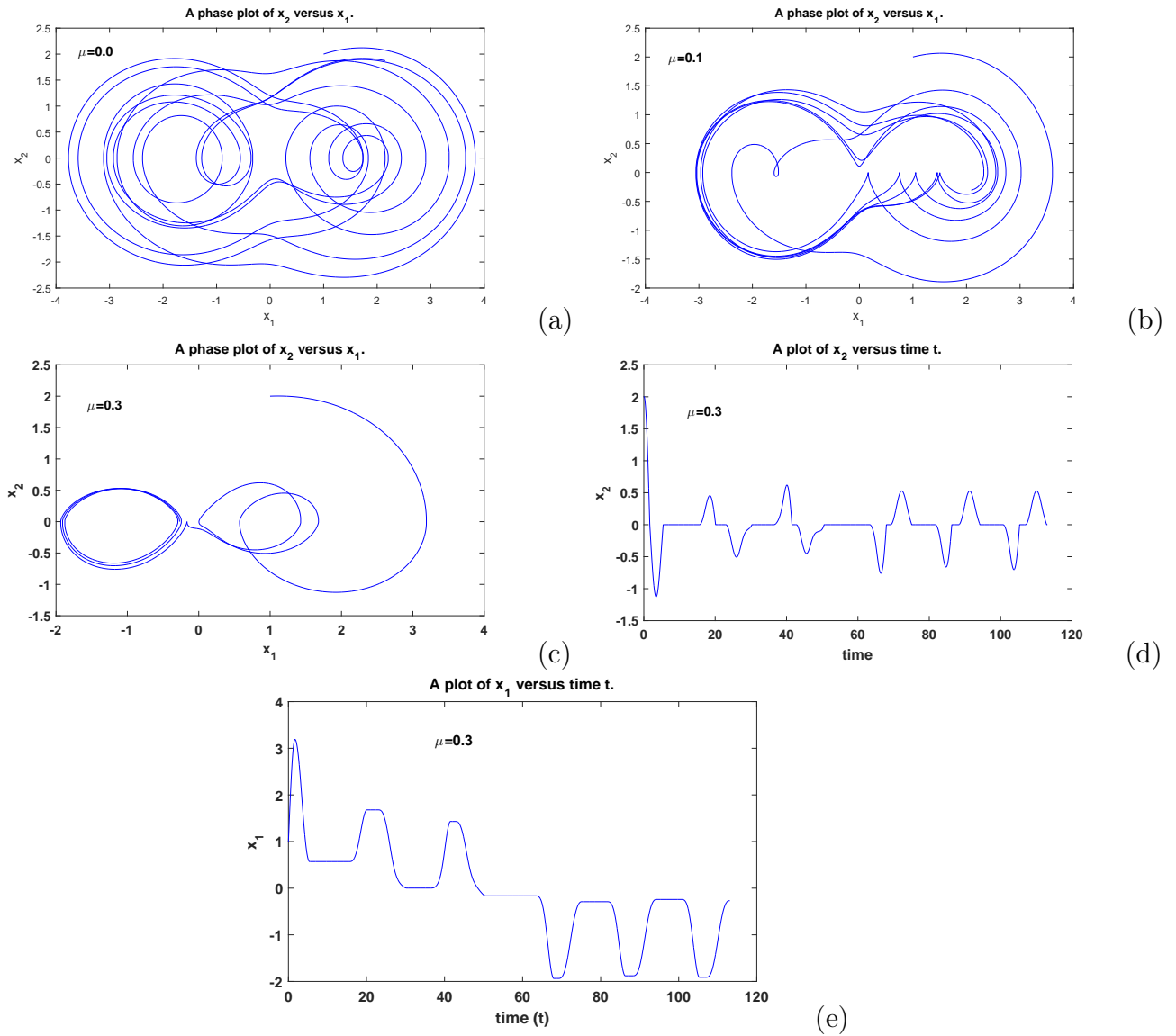
**Figure 3.1**: *Friction oscillator with external excitation: sliding filippov method : $c = 0.048$; $\alpha = 0.4$; $g_1 = 2.0$; $f_0 = 0.85$; $\Omega = 1/3$: (a) Phase plane plot $\mu = 0.0$ (b) Phase plane plot with friction (c) Limit cycle occurred in Phase plane plot as friction increases ((d)-(e)): Dynamics at the transition from stick to slip*

stick and slip phases are consecutive. Thus, to verify directly the dynamical features of the motion patterns transition we focus at the statistic occurrence of sticking and sliding times, i.e., the distribution of time intervals the load spends in states $v_r = 0$ (sticking events) and $v_r \neq 0$ ( sliding events). The transition value from stick to slip is reached at $G_s = \mu F_N$. The slip event finishes for $x_2 = v_0$. Besides, we can count the same number of sticks and slips because the system response ends during a slip mode Fig. 3.1(d, e). We count the first slip just after the first stick. The sliding segment shows the generation of an additional slipping segment at the boundary. Besides, if the system response ends during a slip, the number of sticks is equal or the number of slips. The system response is composed by a random sequence alternating stick and slip-modes. The number of time intervals in which stick or slip occurs, the instants at which they begin, and their duration can be estimated. Considering that base speed is constant in time, knowing the mass position when a stick starts, it is surely possible to predict its duration.

We consider the bifurcations under changes in the driving force and frequency.

From Fig.3.2, both periodic and chaotic responses are showing. Respectively, period$-1$, period-2, period-3 and chaotic responses, are presented. It should also be pointed out that there is an abrupt transition from the periodic to chaotic response and, afterwards, from the chaotic to the periodic response. The presence of 'grazing sliding bifurcations' may cause a sudden jump to chaos. Sliding bifurcations introduce discontinuous transitions between different motions. It is also found that sliding dramatically change the characteristics of the frequency-response curve. From the smooth to discontinuous regime, periodic windows and chaotic responses are found. In a smooth dynamical system that exhibits chaos, in the absence of noise a chaotic attractor is structurally unstable , whereby, the periodic windows are found and occupy open sets in the parameter space (see Fig.(3.2(c, d, e)). It is found that, for a fixed set of parameters, a special chaotic orbit exits there which fills a finite region and connects a series of islands dominated by different chains of fixed points. Indeed, a transition from regular to chaotic dynamics occurs through chains of bifurcations where equilibria and cycles are first links (see Fig.(3.2(d, e)). Under stochastic excitation, the shape and size of attractor and saddle can change. They are respectively called the random attractor and the random saddle. The possible structural changes of the asymptotic behaviour of the system under parameter variation, called bi-
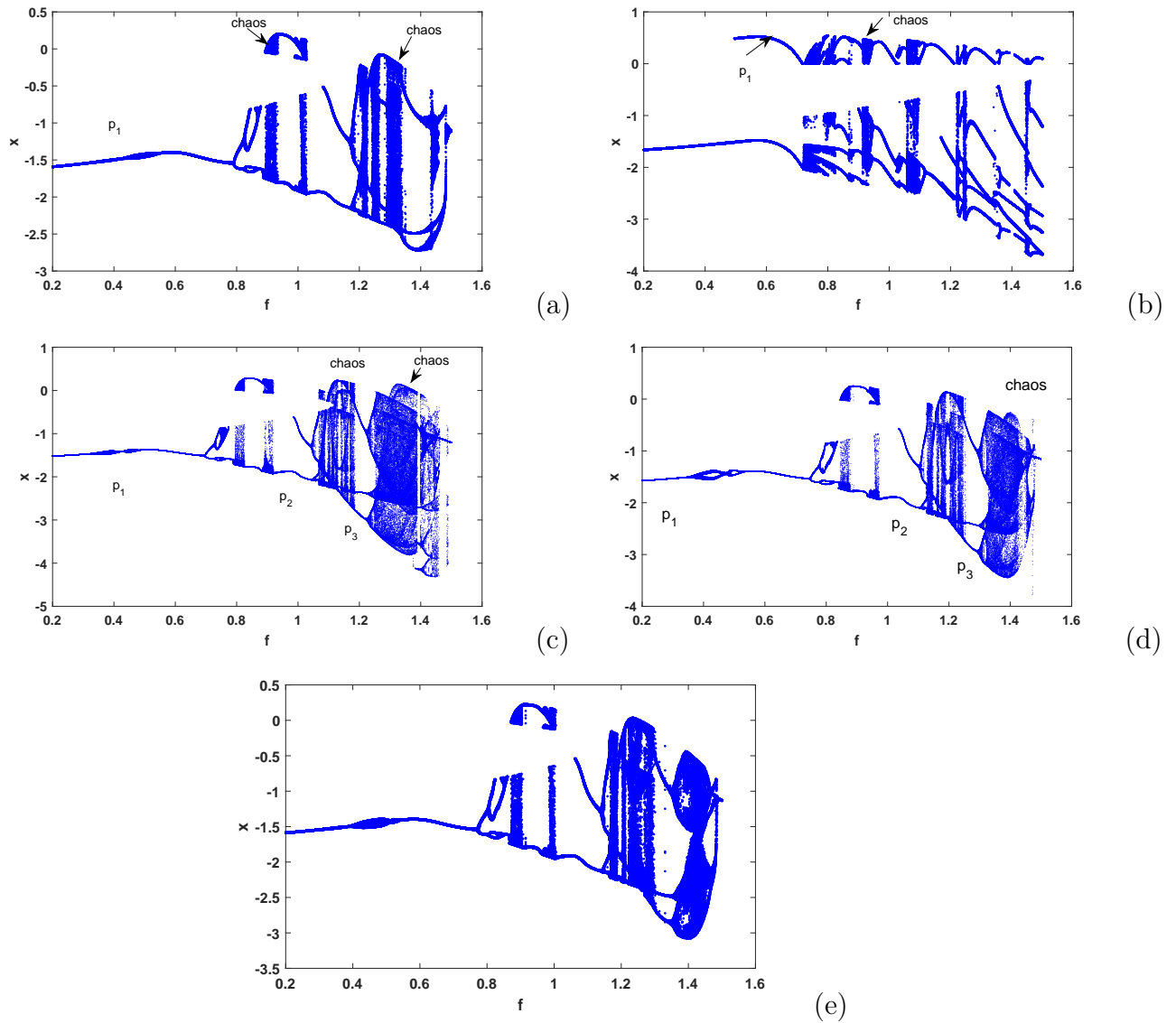
**Figure 3.2**: *Bifurcation diagrams for displacement $x = x_1$ versus f, $(x_0 = 1, y_0 = 0)$, $c = 0.048$, $x_{fk} = 0.25$; $x_{fs} = 1.0$: (a) $\alpha = 0.4$, $C_1 \neq 0$, $C_2 = C_3 = 0$,(b)$\alpha = 0.0$ ,$C_1 \neq 0$, $C_2 = C_3 = 0$. (c) $\alpha = 0.4$, $C_1 \neq 0$, $C_2 = 0.45$, $C_3 = 0.5$; (d) $\alpha = 0.4$, $C_1 \neq 0$, $C_2 = 0.015$, $C_3 = 0.25$; (e) $\alpha = 0.4$, $C_1 \neq 0$, $C_2 = 0.0$, $C_3 = 0.25$*

furcations. A slight modification in a parameter value can give rise to a radical change in the system behaviour. Therefore, through successive bifurcations where equilibriums and cycles are first links (see Fig.(3.2(d, e)) a transition from periodic to chaotic dynamics occurs. The shape and size of 'random attractor' and 'random saddle' can change under stochastic perturbation.

### 3.2.1 Hard bifurcation in SD oscillator

In many practical situations applications we need to estimate the probability of failure of a complex system. The need for such estimates come from the fact that in practice, while it is possible (and desirable) to minimize the risk, it is not possible to completely eliminate the risk. No matter how many precautions we take, there are always some very low probability events that potentially lead to a system's failure. All we do is to make sure that the resulting probability of failure does not exceed the desired small value $p_0$. For example, the probability of a catastrophic event is usually required to be at or below $p_0 = 10^{-9}$.

Fig.3.3(a, b) illustrates the influence of friction in the system. With the increasing of the noise intensity, Fig.3.3(a) shows a "hard" bifurcation. A hard bifurcation is defined as discontinuous change in the density function or support of a stationary measure of the system. The stationary measures provide the eventual distributions of typical trajectories. Their supports are the regions accessible to typical trajectories in the long run. In such systems, there can be more than one stationary measure and more radical changes can occur in response to parameter changes. In the theory of mechanical vibrations, mathematical models are helpful for the analysis of dynamic behavior of the structure being modeled [93]. In the opinion of Meunuer and Verga [94], due to lack of certain relationship between the shape variations of stationary probability density function and the random excitation, it is difficult to describe the true change of topological property of a stochastic system simply based on the shape change of stationary probability density function. For multiple cycles, noise induces a special type of P-bifurcations. As the noise intensity (or smoothness parameter) increases, peaks of the probability density function merge and multiplicity of cycle is appeared. While in Fig.3.3(b) ($\mu = 0$), the appearance of p-bifurcation diminishes with the increases of noise intensity. In [95] a loss of stability
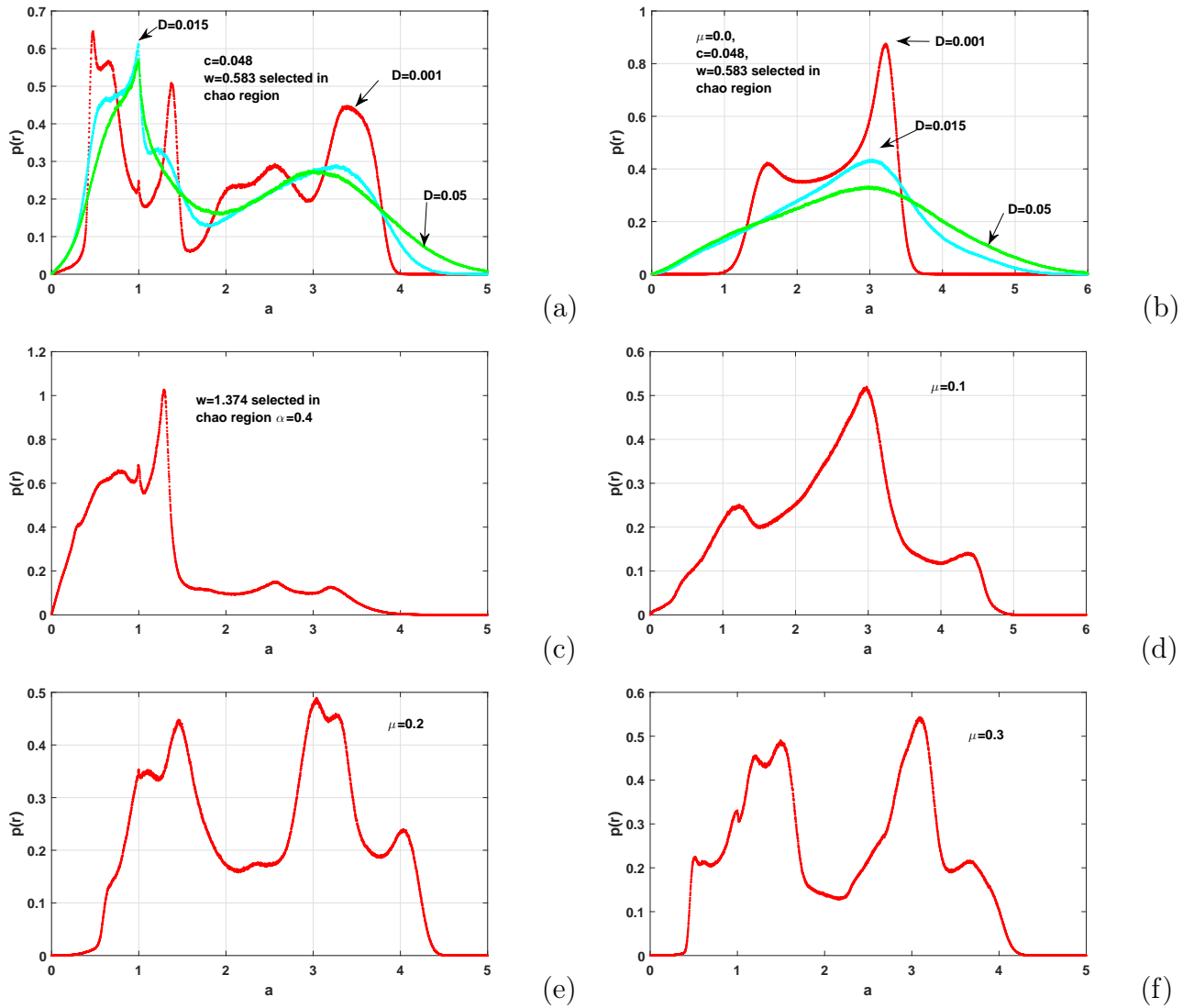
**Figure 3.3**: *from figure* 3(*a*): *Stationary amplitude distribution for:* $D = 0.001; c = 0.048. f_{01} = 0.85, C_1 \neq 0, C_2 = C_3 = 0$ *(a)* $\alpha = 0.4$, *(b)* $\alpha = 0.0$. *(c)* $\alpha = 0.4$ *(d)* $\mu = 0.10$ *(e)* $\mu = 0.2$; *(f)* $\mu = 0.3$;

of an invariant set is called hard if it involves a discontinuous change in Fig.3.3. The following changes is identified in the density functions:

1. the density function of a stationary measure might change discontinuously (including the possibility that a stationary measure ceases to exist), or

2. the discontinuous change of the support of the density function of a stationary measure. Fig.(3.3) also shows how adding a small amount of noise to a family of ordinary differential equations unfolding a bifurcation lead to a hard bifurcation of density functions. We also observe here that, as friction coefficients increase, peaks number increase, consequently appearing of p-bifurcation (see Fig.3.3(d, e, f) for $\mu = 0.1$, 0.2, 0.3). It is also an easy fact that the density function for the stationary measure varies continuously with any parameter of the system. In light of these facts, Zeeman proposed that a bifurcation in a stochastic system be defined as a change in character of the density function as a parameter is varied [96, 97]. He suggested left-right equivalence as the standard for change. Such bifurcations have come to be known as phenomenological, or P-bifurcations.

We observe that under parameter variation, stationary measures of SD oscillator can experience dramatic changes, such as a change in the number of stationary measures or a discontinuous change in one of their supports, see Fig.3.4. When increasing the damping coefficient. Fig.3.4(a) illustrates the increase in term of number of peaks and probability density function (PDF). The same observation is recognized in Fig.3.4(b), where the friction coefficients increase with the multiplicity of peaks number and height value of pdf. As an alternative choice, we think that a deep experimental analysis into the evolutionary behavior of the stochastic attractors may be helpful to understand the stochastic bifurcation in a nonlinear system with noise. In this dissertation, a stochastic attractor is taken as an invariant for a noisy steady-state response, and the sudden change of attribution (number, size, attraction) of a stochastic attractor and/or a stochastic saddle provides a topological change of a stochastic system to demonstrate the bifurcation behavior. Fig.3.4(c, d, e) shows the same observation of increase of peaks number with the increase of the smoothness parameter $\alpha = 0.0$, 0.3, 0.5. The deterministic system of the SD oscillator undergoes a pitchfork bifurcation when the smoothness parameter $\alpha$ increases up to certain value. The stochastic P-bifurcation and the deterministic pitchfork bifurcation in the SD oscillator are related. When $\alpha$ decreases to 0, the dynamics of the
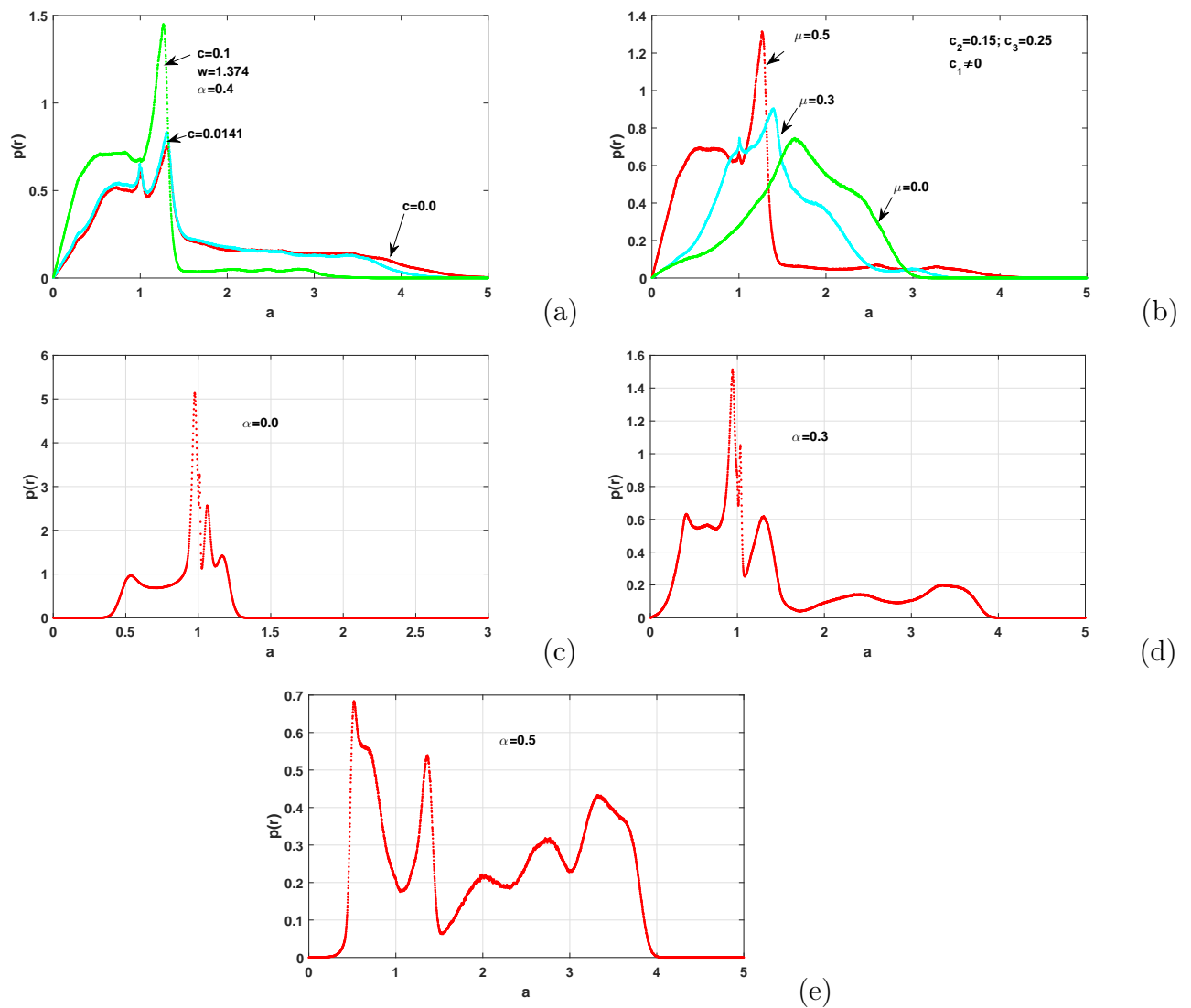
**Figure 3.4**:  $\alpha = 0.4; f_{01} = 0.85$, *(a) and vary values of damping $c = 0.0, 0.0141, 0.1$; $C_1 \neq 0$; $C_2 = C_3 = 0$ (b) $C_1 \neq 0$; $C_2 = 0.015$; $C_3 = 0.25$ and vary values of friction coefficient $\mu$; (c) $\alpha = 0.0$ (d) $\alpha = 0.3$; (e) $\alpha = 0.5$*

SD oscillator suddenly becomes discontinuous. In the deterministic system, the velocity flow goes through a jump when the system crosses from one well to another because of the loss of local hyperbolicity.

We can summarized this subsection saying that, the shape of stationary probability density does not depend on the bifurcation parameter. These results have been already observed by [98]. But, the stationary probability density function does change its shape from a mono-peak one into double-peak one at a critical parameter value [99]. Thus, one cannot help thinking about what has really happened for stochastic bifurcation, what is the topological property of a stochastic system, what kind of invariance is suitable for predicting stochastic bifurcation, and so on.

It is known that there is no single model that can describe a nonlinear system. Some mechanical elements can be represented with certain models, but their dynamic response will depend not only on the model, but also in the system's sensibility to the nonlinear terms. To illustrate the statistical characteristic of a random dynamical system, the stationary measure is an appropriate choice to describe the long term behaviour of solutions of differential equations with random perturbations. The Phenomenological (P)-bifurcation approach to stochastic bifurcation theory examines the qualitative changes of the stationary measures. There comes the idea that a stochastic attractor may be taken as invariance for the randomly perturbed steady-state response. The shape, size and stability of a stochastic attractor may be taken as its character. Whenever the character of an attractor changes radically, there occurs the stochastic bifurcation. P-bifurcation is deemed to occur when there is a change in the topology of the associated probabilistic structure of the state variables. However, the P-bifurcation has the advantage of allowing one to visualize the changes of the stationary density functions. Hence, for the P-bifurcation, we are only interested in the changes of the shape of the stationary density.

The slight variation of a parameter has created the "grazing-sliding bifurcations". The occurrence of 'catastrophic bifurcation' transition phenomenon is characterized by discontinuous jumps in the equations across a phase space limit. We were looking to the shape, size and stability of a "stochastic attractor" that may be taken as its character. Whenever the character of an attractor changes radically, there occurs the stochastic bifurcation. P-bifurcation is deemed to occur with a change in the structural behaviour

of the probabilistic structure of the state variables.

## 3.3 The dynamic behaviour of a spillway reinforced concrete (RC) building colliding with the abutment

The theory of structural pounding risk analysis may be considered as a branch of applied probability theory. The main issue of this theory is to define an event called "structural pounding" and to set up a "probability space" that contains that event. An event here is the appearance of the stochastic bifurcation for instance. This modeling part of structural pounding risk analysis is based on statistical information about the uncertainty of the relevant parameters or knowledge about the inherent stochastic nature of the applied earthquake loads. It is noted that out-of-phase vibrations may be induced when adjacent buildings are subjected to earthquake loading and pounding may occur if the separation distance is inadequate. This section considered stochastic bifurcation (p-bifurcation) as instability zone. This instability increases pounding effect with weak noise, hence high probability density function(PDF). Pounding between structures could produce large acceleration demands ($P_0$ big) on the floors which are directly involved in collisions [101]. Forces created by collisions, commonly proceed over a short period of time and the produced energy in pounding experience time is dissipated as heat due to molecular vibrations and internal friction of colliding bodies [100]. Concerning the phenomenon include impacts where contact forces suddenly and rapidly increase with an associated rapid change in velocity of the impacting object, when the study on the pounding of buildings in series or between several segments of a bridge is conducted, the structural response during the time when contact takes place is essential. This is due to the fact, that when the structural members rebound after collision they might come into contact with other members. Moreover it may also happen that at the time of contact between two given structural members other members may collide with each other. Not surprisingly, the pounding probability is small for the cases that the periods of adjacent buildings/ bridge are extremely closed and well separated [102]. During the whole time of impact, friction between the colliding members takes place and this effect is especially important in the case of rough surfaces. It has been shown that most of the energy which is

dissipated during impact is lost during the approach period of collision and a comparably small amount of energy is lost during the restitution period due to friction [103].

### 3.3.1 Probabilistic damage distribution

We recognized that for the longer bridge structures, it is often the seismic wave propagation effect that is considered to be a dominant factor leading to pounding of neighboring superstructure segments [104–106]. This effect, due to time lag and spatial variation of seismic wave, results in different seismic input acting on supports along the structure [107]. We also recognized that the seismic wave have an amplitude of excitation, for instance $P_0$. The damaging is function of the value of $P_0$. The behavior of a non-smooth system can change when white noise is added. For pure self- excitation the changing point underlies a normal distribution. However, if external excitation is considered, the white noise can cause a P-bifurcation for the distribution of the changing point coordinate [108]. P -bifurcations are instabilities that appear with weak noise and decreased when increasing noise.

For noise intensity $\xi(t) \neq 0$.

We introduce a smooth function which approximates the discontinuous drift and apply the Euler method with this input. The influence of the control gain $\alpha_0 = (\mu N)$ determines how quick the evolution of the sequence $\{x\}_n \geq 0$ switches around zero. In other words, a big $\alpha_0$ minimizes the influence of the random variable $\xi$. The results of this numerical investigation are shown in Figs.(3.5, 3.6). The chosen parameters are: $\alpha_0 = 0.005$; $k = 210.125$; $c = 2.47e + 6$; $\nu = 0.005$ [109].

For $\xi(t) = 0$.

In the numerical analysis, the spillway is modelled as a single-degree-of-freedom system as shown in Fig.2.3. The resulting system of second order equation is recast as a system of first order ordinary differential equations and solved using Matlab 'ode' solvers (such as ode45). We recognize that at some positions $x(t) = y_1(t) = \nu$ or if $x(t) = y_1(t) > \nu$ and $\dot{x}(t) = y_2(t) = 0$ the vector field $f(t, y)$ is non-smooth. We can observed two switching surfaces $g_1(y) = (y_1 - \nu)$ and $g_2(y) = y_2$. Moreover, the discontinuity limit (abutment area) $\Sigma$ separating the two areas is described as $\Sigma = \{x \in R^n : H(x) = 0\}$, where H is a smooth scalar function with non vanishing gradient $H_x(x) = \frac{\partial H(x)}{\partial x}$ on the discontinuity
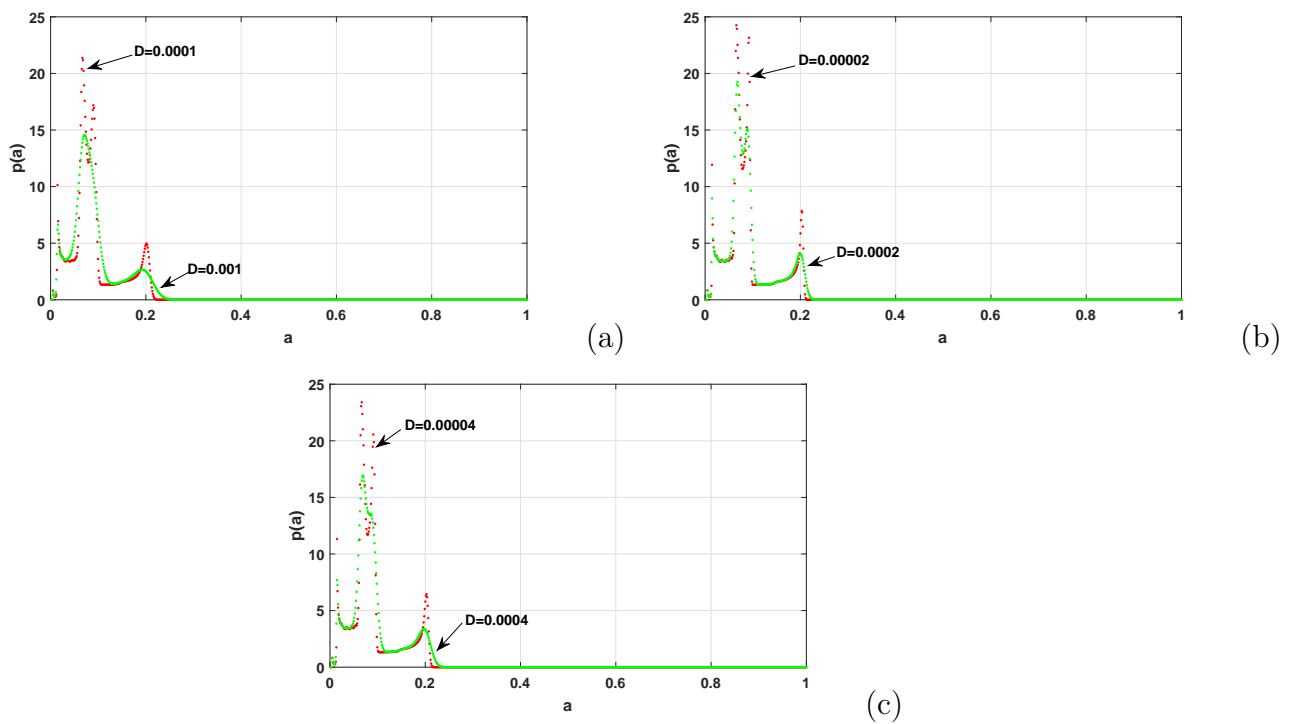
**Figure 3.5**: *Stationary amplitude distribution and varied values of the noise intensity D: $k = 210.125; c = 2.47e + 6; \nu = 0.005$: (a) $D = 0.0001, D = 0.001$ (b) $D = 0.00002, D = 0.0002$ (c)$D = 0.00004, D = 0.0004$ .*

separation $\Sigma$.

### 3.3.2 Pounding between a spillway and an abutment: Structural stability

Stability here leads the ultimate fate of the dynamics for perturbations of the initial conditions. Structural stability sometimes, deals with perturbation of the system itself, i.e. perturbations of the own system, including parameter variations. Knowing that the impact force term, $v(y, \dot{y})$ (an intermittent nonlinear discontinuous force), force between two masses, the notion of structural stability is broadened to also encompass a preservation in the event sequence, i.e. the order and number of interactions with discontinuity surfaces. This impact force $v(y, \dot{y})$ illustrated the same behavior as relations Eqs.(2.24,2.32) in the sense of discontinuities. The abutment is a transversal barrier i.e. $\Sigma = \{x \in R^n : H(x) = 0\}$, where H is a smooth scalar function with non vanishing gradient $H_x(x) = \frac{\partial H(x)}{\partial x}$ on the discontinuity separation $\Sigma$.

Two switching surfaces $g_1(t, y, y_0) = (y - 0.005)$ (spillway's area) and $g_2(t, y, y_0) = y_0$ (after the abutment) are defined. ($\nu = 0.005$ =Poisson's ratio of the soil). When defining the time impact-contact in between $t \in [0, 3]$, the response crosses the surface $g_1$ (area of the spillway) twelve times and the surface $g_2$ (region after the abutment) six times. Hence the data corresponding to 18 switching points (i.e. impact-contact) defined in the table (3.1). Numerical and experimental studies have shown that pounding introduces impact loads in addition to the forces caused by the ground acceleration itself. Due to pounding floor acceleration and inter-storey deflections are significantly amplified, which is upsetting the serviceability of the structures i.e., damaging the non structural sensitive in-house equipments. During collision of structures, there is a sudden break of momentum of the displacement at the pounding levels which results in large and quick short duration acceleration impulses in the opposite direction and causes a greater damage to the structures. When these impact loads and acceleration spikes from pounding are too high, then the structural system has to be modified by employing some of the impact mitigation measures (see chapter 1 subsection 1.1.2).

**Table 3.1**: *occurrence of discontinuities corresponding to contact-impact friction and displacement of structures during earthquake excitation*

| time (s) | displacement of the spillway ($g_1$) | abutment (transversal region) | region $g_2$ |
|---|---|---|---|
| 0.4006 | 0.0050 | 1 | 0.1664 |
| 0.4071 | 0.0055 | 2 | 0.0000 |
| 0.4172 | 0.0050 | 1 | $-0.0658$ |
| 0.8384 | 0.0050 | 1 | 0.2095 |
| 0.8446 | 0.0055 | 2 | 0.0000 |
| 0.8543 | 0.0050 | 1 | $-0.0820$ |
| 1.2818 | 0.0050 | 1 | 0.2079 |
| 1.2880 | 0.0055 | 2 | $-0.0000$ |
| 1.2977 | 0.0050 | 1 | $-0.0811$ |
| 1.7307 | 0.0050 | 1 | 0.2048 |
| 1.7368 | 0.0055 | 2 | 0.0000 |
| 1.7467 | 0.0050 | 1 | $-0.0799$ |
| 2.1798 | 0.0050 | 1 | 0.2047 |
| 2.1860 | 0.0055 | 2 | 0.0000 |
| 2.1958 | 0.0050 | 1 | $-0.0799$ |
| 2.6286 | 0.0050 | 1 | 0.2049 |
| 2.6348 | 0.0055 | 2 | 0.0000 |
| 2.6446 | 0.0050 | 1 | $-0.0799$ |

### 3.3.3    Analysis of pounding phenomenon under noise control

During an earthquake the ground motion is often defined by a time history of the ground acceleration. It can be obtained in three directions by instruments known as strong-motion accelerographs. When increasing the probability of pounding during an earthquake, it is verified that strong ground motion in the near-field area has different characteristics [110, 111]. A more advanced dynamic friction model has to be developed, or to be utilized for systems containing high variations of normal load, namely with impact-friction conditions.

We have defined two characteristics of noise intensity in Fig.(3.5, 3.6): very low noise intensity and weak noise. We observed a high probability density function (PDF) for $D = (0.0001, 0.00002, 0.00004)$, but the peak of this PDF reduces with the increasing of noise. The amplitude of propagation is reduced. Fig.(3.6)(a,b,c,d) shows the same observation of appearance of p-bifurcation at very low noise intensities with height PDF and p-bifurcation ceases to occur when noise intensity increases.

We reminder that pounding between structures could produce large acceleration demands ($p_0$ big) on the floors which are directly involved in collisions [101]. In Fig.(3.6)(e, f), we fixed $p_0$, the amplitude of external excitation and varying noise intensity. We observed large oscillation with large amplitude at weak noise intensity. Hence p-bifurcation occurs. The instability of the system is verified. The behavior of the system diminishes with the increase of noise. We can summarized these two Figures saying that during earthquake excitation, for the impact-friction events at very low noise intensity, p-bifurcation occurs and created instability that will increase pounding effects. The near-field buildings will being impacting and destruct. The disasters will be very pronounced if the amplitude of earthquake excitation $p_0$ of sine wave is big [112, 113]. The seismic perturbation decreases with the decreasing of $p_0$. In the same manner, when increasing noise intensity during impact-friction events, p- bifurcation occurs but at very low PDF, and the amplitude of oscillation is reduced, so that pounding effects is diminished for near-field buildings. We can note a relationship between impact-friction events saying that, small noise intensity means continuous friction, hence high PDF, but if the noise intensity is great, the impact event seems important with weak PDF. But successive jump effects can
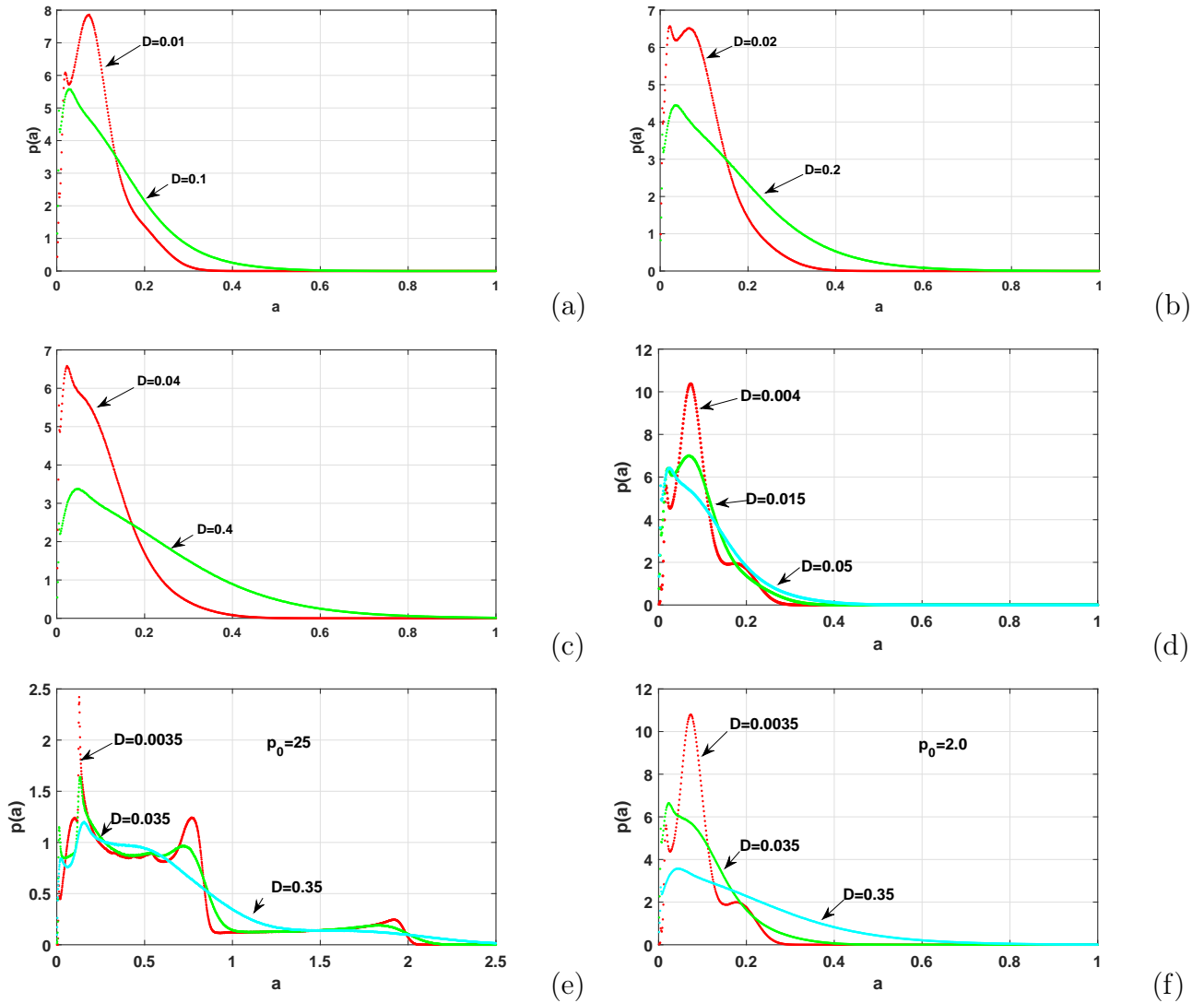
**Figure 3.6**: *Stationary amplitude distribution and varied values of the noise intensity D: $k = 210.125; c = 2.47e + 6; \nu = 0.005$: (a) $D = 0.01, D = 0.1$ (b) $D = 0.02, D = 0.2$ (c)$D = 0.04, D = 0.4$; (d)$D = 0.004, D = 0.015, D = 0.05$; (e) amplitude $p_0 = 25$; (f) amplitude $p_0 = 2.0$*

created continuous friction and impacting and the pounding force will influenced. These results have also been shown by [114–116].

Hence, Based on the survey and investigations conducted by *Jain et al.* [117], it was reported that there were mostly infill wall damages, column shear failures and possible collapse due to pounding in many of closely spaced buildings. Pounding in bridges have led to local crushing and spalling of pier bents, abutments, shear keys, bearing pads and restrainer, and also contributed to the collapse of decks. From the inspection report of *Agarwal et al.* [118] , it was reported that the Anand building and old Surajbari bridge were severely damaged and collapsed due to pounding action. For *P. Ndy Von et al.* [119], if $P_0$, the amplitude of external excitation, then varying noise intensity. We observed large oscillation with large amplitude at weak noise intensity. Hence p-bifurcation occurs. The instability of the system is verified. For the impact-friction events at very low noise intensity, p-bifurcation occurs and created instability that will increase pounding effects. The near-field buildings will being impacting and destruct. The disasters will be very pronounced if the amplitude of earthquake excitation $p_0$ of sine wave is big (see Fig.(3.6)(e).

### 3.3.4 The switching behavior of the whole structure during pounding phenomenon

The phenomenon of stick-slip is also very important during pounding effects at near-field buildings during the seismic wave propagation. Fig.(3.7) shows the dynamic of the transition of the wave. We reminder that $\nu$ is the Poisson's ratio of the soil. Talking about the switching surface $g_2$, the vector field is discontinuous only when $\dot{x}$ changes from positive to negative. This can appeared when the space position $x > \nu$. Sometimes, the function defining the vector field at the region $g_1(y) > 0$ is not defined when $g_1(y) < 0$ due to the two fractional incommensurable powers $\frac{1}{4}$ and $\frac{3}{2}$. As we have said above, f is the vector field and continuous function. Therefore $f_+(t_d, y_d) = f_-(t_d, y_d)$ at the switching points and the transversality (in the abutments) condition is satisfied unless the vector field is tangent to the switching surface (see Fig.(3.7)). The red horizontal lines that is drawn in Fig. (3.7)(b, e)) are the discontinuous regions corresponding to the abutments. Hence the gradient $\nabla g_1(y) \cdot f(t, y) = 1$ for all y and $\nabla g_2(y) = -210.125 y_1 - c(y_1 - \nu)^{\frac{3}{2}} - r(t)$
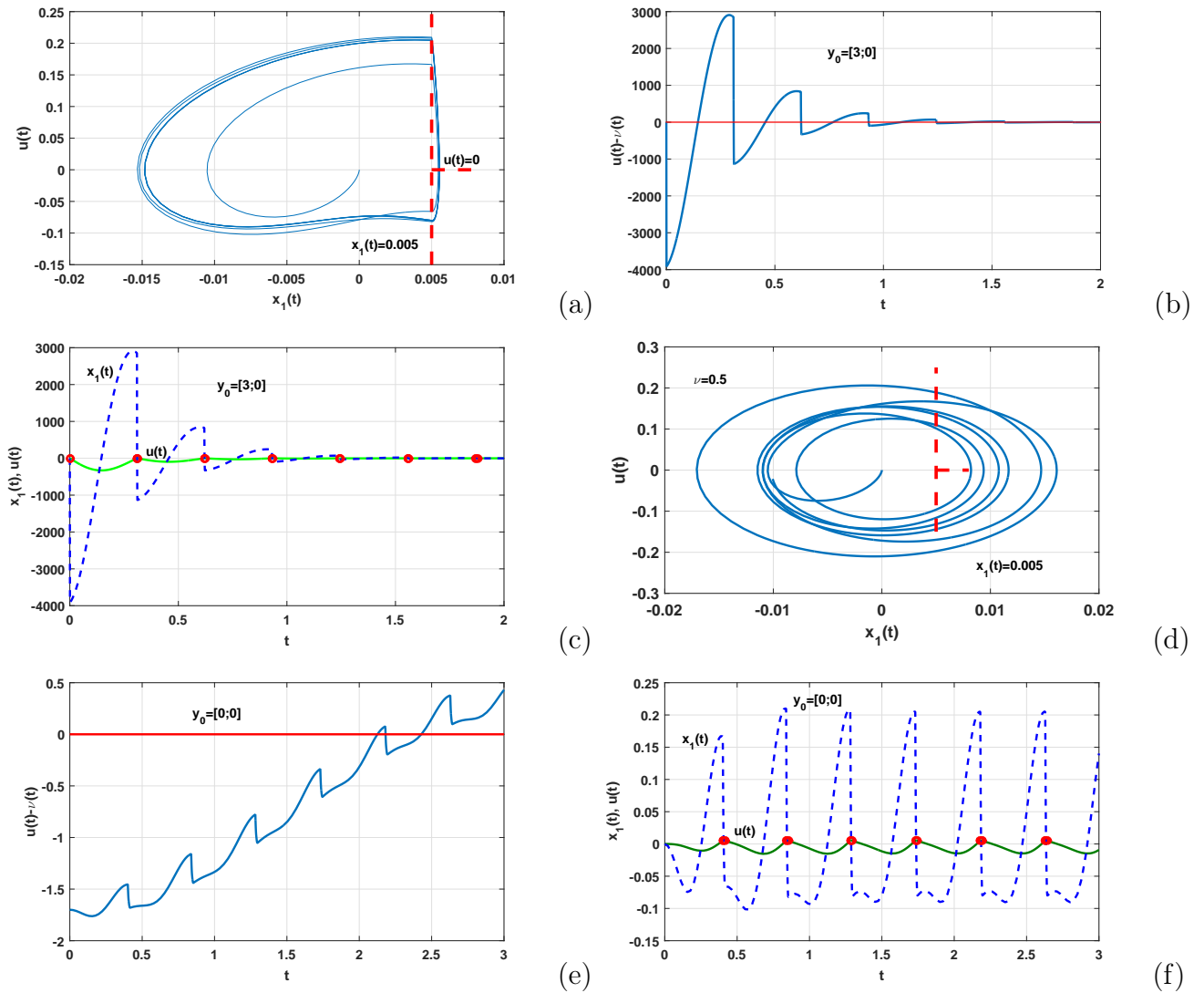
**Figure 3.7**: *Dynamics at the transition from stick to slip : the discontinuity points are indicated by means of small circles $k = 210.125; c = 2.47e + 6; \nu = 0.005$; (a) $y_0 = [3, 0]$: phase diagram,(b) $y_0 = [3, 0]$: solution against time (c) $y_0 = [3, 0]$: solution and derivative against time; (d) phase diagram $y_0 = [0, 0], \nu = 0.5$ (e) $y_0 = [0, 0]$: solution and derivative against time (f) $y_0 = [0, 0]$: solution and derivative against time;*

for switching points such that $y_2 = 0$. The discontinuity points corresponding to contact-impact areas between spillway and abutments are indicated by means of small red circles (see Fig.(3.7)(c,f)). It can be verified that, the transversality condition is satisfied. But this affirmation is not sure in some transitions points as: $y_2 = \dot{x} = 0$, $y_1 = x > \nu$ and $-210.125x(t) - c(x(t) - \nu)^{\frac{3}{2}} - e(t) = 0$ (see Fig.(3.7)(d, e)). Since $|e(t)| \leq 2$, and $|e(t)| \leq 25$, the switching points are transversal. The phase diagrams ($x_1$ versus $\dot{x}$) are founded in Fig. 3.7)(a, d).

In Fig. (3.7)(b, c, f)), the response, with the considered initial conditions, passes first through a transversal discontinuity (abutment), then it enters a sliding region for a short time until it exits it. After, it passes through two transversal discontinuities and enters into another sliding region. The red dashed lines denote the switching points (not continuous in the third derivative $x(t)'''$).

For reminder: The discontinuity points i.e. contact- impact regions (where the third derivative $\dddot{x}(t)$ is not continuous) are indicated by means of small circles. To recognize the sliding regions, see Fig. 3.7)(b, c, e, f). The function $(u(t) - \nu(t))$ is at the switching region. The sliding zones represent to the intervals at which the functions vanishes. (The dashed lines correspond to the switching surfaces in the phase diagrams plot 3.7(a, d)).

We can summarized Fig. 3.7 saying that for $t_2 \in [0, 3]$ the solution crosses the surface $g_1$ twelve times and the surface $g_2$ six times. In all the cases the discontinuity is transversal. We would like to mention that when considering the initial conditions, the response, passes first through a transversal discontinuity, then it gets in a sliding area for a small time until it exits it, then it continues through two transversal discontinuities and then it enters into another sliding region.

The response with $'-'$ in region $g_2$ means that the solution exits from the sliding region. The positive elements in that table mean that these discontinuities are transversal. (see table3.1).

### 3.3.5  Overview of the selected earthquakes

A further overview of the selected earthquakes is given in Fig. (3.8). It shows the magnitude and recorded peak acceleration in relation to the distance to the earthquake epicenters but also the peak acceleration versus the magnitude of the earthquakes. The

acceleration values are the absolute maximum values for each direction and the plotted values are on the one hand the peak ground acceleration (PGA) recorded in the basement of the spillway foundation. These values do not represent a total horizontal acceleration component but the highest value of both sensors recording in one direction and the highest value of the other direction sensor and it should be emphasized that both of those peak values of acceleration are not expected to occur at the exact same time. Although Fig.(3.8)(b) seems to indicate that the peak acceleration grows with longer distance to the epicenters, which is of course not the general case, it is important to see in Fig.(3.8)(a) that the earthquakes whose epicenters are the furthest away from the project were generally of greater magnitude than those with epicenters closer to the edifice. The intensity of pounding in neighboring structures due to earthquake is depended by many factors: the Peak Ground Acceleration (PGA) of the earthquake, the distances of separation between the buildings, soil configurations etc...
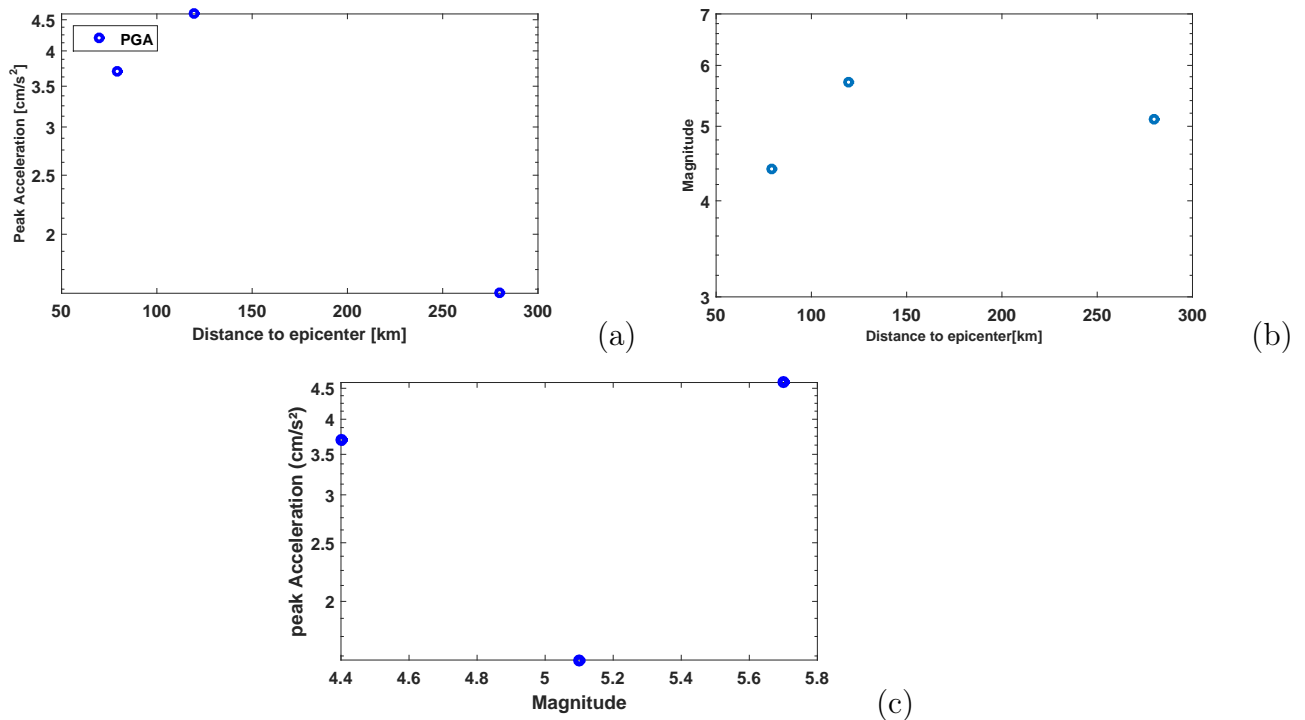


**Figure 3.8**: *Peak ground acceleration: (a) Earthquake magnitude in relation to distance to epicenters, (b)Peak acceleration in relation to distance to epicenters. The dots represents the peak ground acceleration (c) Peak acceleration in relation to earthquake magnitude. The dots represents the peak ground acceleration*

### 3.3.6   Ground Motion Characteristics

Earthquake ground motion at a certain site, is determined by the various types of seismic waves, their propagation paths and their corresponding arrival times at that site. Because of the different arrival times of seismic waves, the intensity of the ground motion varies with time [120]. Furthermore, due to discontinuities in soil conditions along the propagation path, seismic waves can be subject to reflection, refraction, diffraction and scattering [121]. Therefore, earthquake ground motion is a non-stationary process with time-variant frequency content. Moreover, local soil conditions can cause a change in the amplitude and frequency content of seismic motions. Ground motions measured on free soil surfaces are therefore likely to differ from those on the surface of outcropping bedrock [122]. This phenomenon is referred to as soil-amplification. Finally, due to soil-structure-interaction, the actual base motion of a structure may significantly differ from the corresponding free-field motion [122]. The size of earthquake ground motions can be expressed into intensity and magnitude as shown in Table2.2. The intensity of an earthquake denotes the severity at a particular location, based on qualitative observations of human perception (for instance: felt by persons at rest, felt inside buildings, felt by all, etc.) and building damage (cracks in external cladding, damage to masonry, etc.)

#### 3.3.6.1   Different intensity scales

Several intensity scales exist, such as the Modified Mercalli Intensity Scale (grades I to XII), the Medvedev-Sponheuer-Karnik Scale (twelve grades) and the Japanese Meteorological Agency Scale (eight grades, 0 to 7). The magnitude of an earthquake is a measure of the amount of energy release, based on quantitative measurements. An example of such a magnitude scale is the well-known Richter Scale. The Richter Magnitude is calculated as the (base 10) logarithm of the maximum amplitude (in millimeters) of the recorded seismogram on a Wood-Anderson seismograph, corrected for the epicentral distance. Detailed information on intensity and magnitude scales can be found in [123].

Ground motions can be expressed into three orthogonal components (two horizontal and one vertical component). These components usually have dominant frequencies in the range of 0.1 to 10 Hz [121, 122]. Vertical ground motions are often disregarded because

the majority of structures are designed to carry vertical loads and are less vulnerable to additional vertical loads, caused by earthquakes. Moreover, vertical components of ground motions are usually weaker than the horizontal ones, although vertical components become more significant for decreasing epicentral distance [121]. The two components of the horizontal ground motion are often not correlated and have their maximum values at different instants. The effect of the vector sum of the two components on the magnitude of the total horizontal motion, can therefore be disregarded. In addition, ground motions may cause torsional excitation of structures [122]. This is more likely to occur for structures with an asymmetric plan. Rotational excitation is often neglected when the structure's base dimensions are relatively small compared to the predominant wavelengths of the earthquake. It can then be assumed that the same ground motion acts simultaneously at all support points.

### 3.3.6.2 The influence of random character of earthquake ground motions

Due to the random character of earthquake ground motions, caused by the many influence factors, such as focal source mechanism, epicentral distance, focal depth and (variations in) geology along energy transmission paths, it is chosen to use recorded data of earthquakes in this research see Table2.2, instead of generating them artificially [124]. Because the measurement instruments (seismographs) can be regarded as mass-spring-damper systems, the measured data is corrected for the frequency dependency of these sensors. Furthermore, bandpass filtering is applied to remove noise contamination. It is assumed that this (corrected) measured motion is applied directly at all support points of the structures base, thus neglecting soil-amplification, soil-structure-interaction and rotational excitation. Moreover, in this thesis, both horizontal and vertical excitation will be taken into account. We can summarize this section saying that: To preserve structural integrity and prevent damage and injury to contents, numerous studies must be done to understand the stochastic effect of seismic wave. With a monitoring system installed and supplying full scale records of the structure response, considerable amount of data will be available for investigation to avoid disaster during seismic events. The required gap to avoid pounding is significantly determined by the table showing the impact-contact (displacement) between the spillway and the abutment see table (3.1). Under certain

conditions, the properties of the supporting soil must also be taken into consideration due to its influence on the impact- friction events. If pounding appears in a foundation of buildings it can be harmful. The impact forces that act during pounding can cause additional sliding of the concrete or steel of the building. With high noise intensity during the impact-friction effects, the pounding force is influenced. P-bifurcation occurs with small peak of PDF. But weak noise intensity created a large probability density function (PDF) (because of continuous sliding), hence a great value of pounding force. The impact in this case is not big (friction is greater than impacting). If noise intensity increases, (the impact is greater than friction), the pounding effects diminishes . In the case of successive jump-impact-friction, friction and impact events can be proportional. Hence friction increases the pounding effects. For the case of spillway and abutments, the calculation must take in view for different loading cases, it mainly includes calculation of sliding stability, overturning stability and stress under foundation. It is found that the relative displacements of the spillway can be obtained by calculating the impact-contact points of discontinuities of the system, which cannot be accessible without considering pounding phenomena.

## 3.4 Dynamic reliability assessment: structural dynamics

Structural dynamics is a branch of structural analysis which covers the behavior of structures subjected to dynamic loading, which include people, wind, waves, traffic, earthquakes, and blasts. When the dynamic excitation is earthquake motion, the probability density evolution method can be used to evaluate the seismic reliability of a nonlinear structure with random parameters. Suppose in this section buildings close to each other in fractured bedrock (earth), we reminder $\nu = 0.0$ in this case. At time $t = 21.0s$, Fig.2.10 shows the behaviour of buildings at different initial conditions. Fig.2.10(a, c, e), with $\dot{x}_0 = [0 \quad 0 \quad 0]^T$ and $x(0) = [0 \quad 0 \quad 0]^T$, no motion occurred. But when applying a sinusoidal excitation in Fig.2.10(b, d, f), we should observed the displacement of each building. Unfortunately, the physico-mechanical properties of engineering materials are always highly variable, uncertain or chaotic due to the complex in situ geological

conditions. Hence failure events are always present. Accurate determination of material properties may be the most challenging part of the evaluation process. Median values of material properties should be obtained.
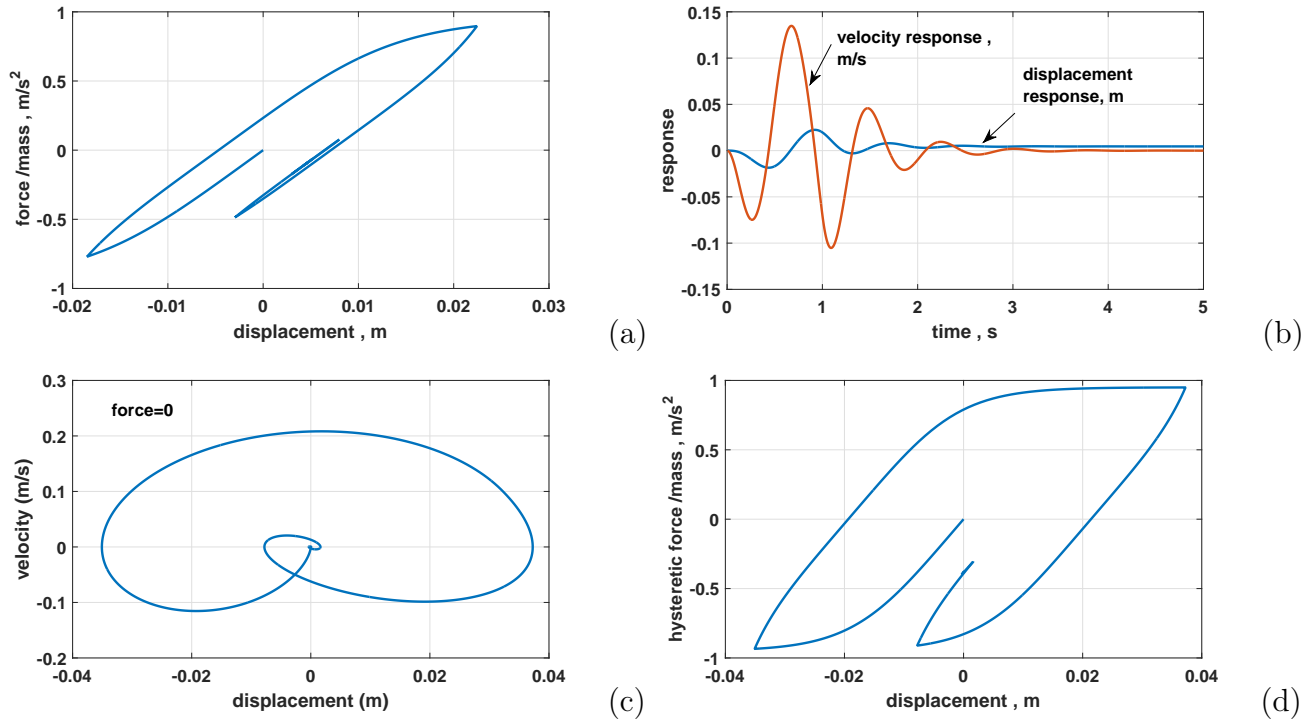
**Figure 3.9**: *The transient response of an elastic/inelastic system: (a) hysteretic force,(b) displacements (c) phase diagram y(2) versus y(1); (d) hysteretic diagram. ,*

In Fig.3.9, the large deflections of the storeys are merely due to large permanent rotations in the indicated yield hinge. Plastic deformation during excitation is allowed in special parts of the structure (for instance cantilever or the slab), often called plastic hinges, while the rest of the structure remains in its elastic range. These plastic hinges are designed for high ductility, in order to ensure global stability of the structure. Because the energy dissipation through plastic deformation is much larger than if the structure would remain elastic, the load-capacity of the structural members can be significantly reduced, resulting in a more economical design. Energy absorption in the inelastic range of response of structures and equipment to earthquake motions can be very significant. Fig.3.9(c) illustrates also the phase diagram when the force vanishes.

### 3.4.1 Inelastic behavior due to large deformation

The Bouc-Wen model has some advantages. It is a practically convenient representation of a force-displacement characteristic, which captures the essence of hysteretic behavior. Moreover, the model is in the form of a differential equation and is thus easy to incorporate in the equations of motion of the structure. Thus it is advised to provide adequate gap between two buildings greater than the sum of the expected bending of both the buildings at their top, so that they have enough space to vibrate.
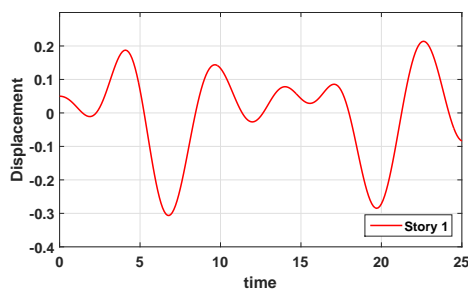
(a) *displacement of single story in horizontal plan: force = [-0.05\*sin(t); 0.1\*sin(t); 0.1\*cos(t)];*
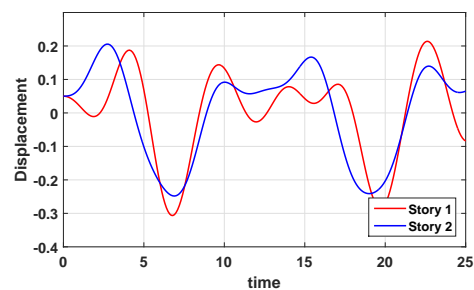
(b) *two storey -two bay in vertical plan: force = [-0.05\*sin(t); 0.1\*sin(t); 0.1\*cos(t)]*
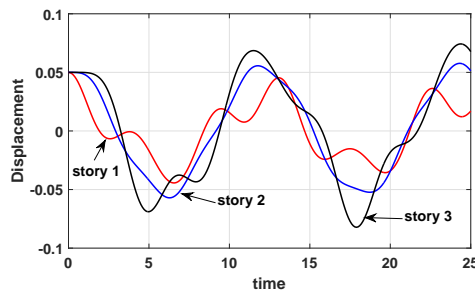
(c) *displacement of three storey -two bay in vertical plan: force = [0; 0; 0]*

**Figure 3.10**: *Displacements versus time: $u_0 = [0.05; 0.05; 0.05]$; $v_0 = [0.0; 0.0; 0.0]$*

Concerning Fig.3.9(d), the large hysteretic energy absorption can occur even for structural systems with relatively low ductility such as concrete shear walls or steel braced frames see Fig.1.9(c). Generally, an accurate determination of inelastic behavior necessitates dynamic nonlinear analysis [125] performed on a time-history time step integration basis. However, there are simplified methods to approximate nonlinear structural response

based on elastic response spectrum analysis through the use of either spectral reduction factors or inelastic energy absorption factors. Spectral reduction factors and inelastic energy absorption factors permit structural response to exceed yield stress levels a limited amount as a means to account for energy absorption in the inelastic range. Based on observations during past earthquakes and considerable dynamic test data, it is known that structures can undergo limited inelastic deformations without unacceptable damage when subjected to transient earthquake ground motion.

Fig.3.10 provides the motion of each story as drawn in Fig.2.10.



(a) *limited inelastic deformations*



(b) *solution and derivative against time*



(c) *Yielding displacement versus time*



(d) *phase diagram during pounding if the rock is fractured*
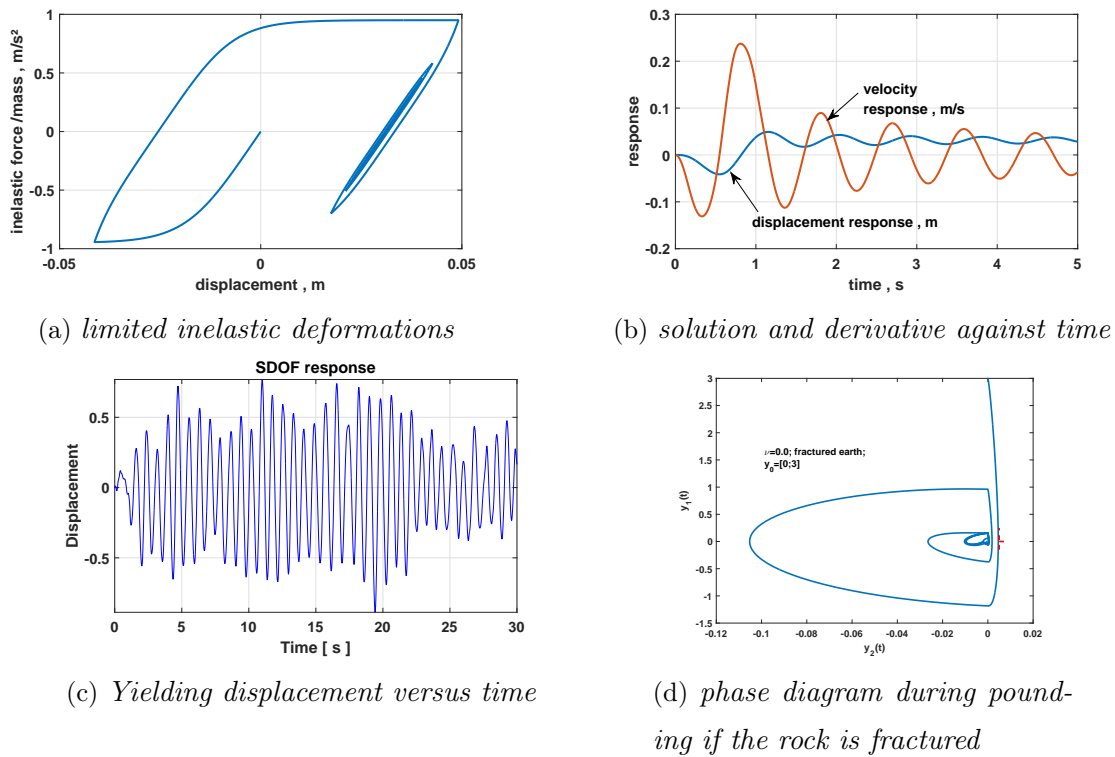
**Figure 3.11**: *limited inelastic deformations*

## 3.4.2 Cumulative distribution function (CDF) and failure modes

In Fig.3.11, the movement of the structure is observed. Fig.3.11(c) presents the case in earthquake excitation while the limit state of phase diagram of buildings constructed in fractured rock in the standard normal space is shown in Fig.3.11(d).

In this research, for reasons of simplicity, to appreciate the failure modes, it is assumed
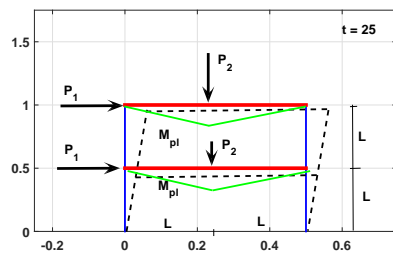
(a) *two-bay two-storey frame structure and failure modes*
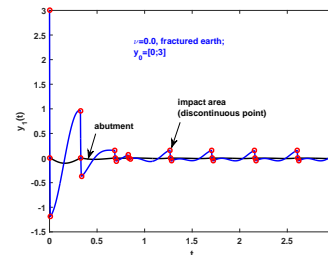


(b) *detection of impact area (pounding) or discontinuous points in the building if the bedrock is fractured*
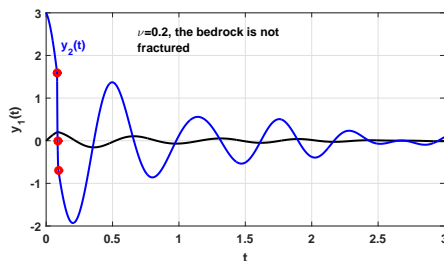


(c) *detection of impact area (pounding) or discontinuous points in the building if the bedrock is not fractured*
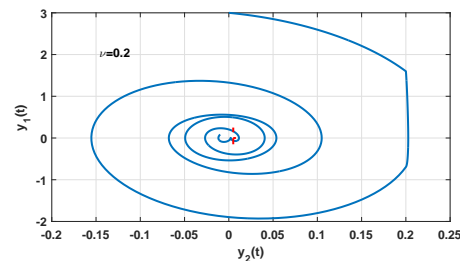


(d) *phase diagram in case of buildings pounding if the bedrock is not fractured*
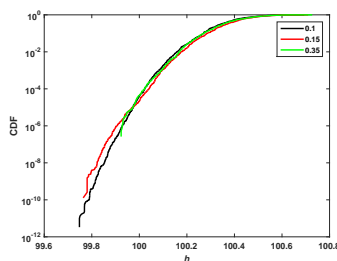


(e) *the deviation of a cantilever beam*
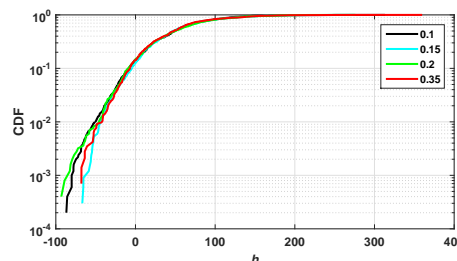


(f) *CDF plot for the inter-story*

**Figure 3.12**: *Cumulative distribution function and failure modes*

that the external excitation (earthquake) only acts in the lateral plane of the structure (Fig.3.12), leading to a $2 - D$ frame analysis. Hence, it suffices to model one portal. Two switching surfaces $g_1(t, y, y_0) = (y - \nu)$ and $g_2(t, y, y_0) = y_0$ are defined during pounding. Noticed that $\nu = 0.00 =$Poisson's ratio of the soil for fractured bedrock, but $\nu = 0.20$ if the earth is not fractured. The time impact-contact is taken between $t \in [0, 3]$, the

response crosses each surface of structures $g_1$ and $g_2$ twelve times respectively. Hence the data corresponding to 24 switching points (i.e. impact-contact events) in case of fractured bedrock Fig.3.12(b) but only 3 switching points of impact are observed when the bedrock is not fractured Fig.3.12(c), see also table (3.2). The table illustrated the impact-contact-displacement of the fractured earth is not shown here. Fig.3.12(d) shows the phase diagram when the rock is not fractured. The switching areas are the red dashed lines denote.

**Table 3.2**: *contact-impact friction and displacement of buildings during earthquake excitation for $\nu = 0.2$*

| time (s) | displacement of the first building ($g_1$) | abutment (transversal region) | region $g_2$ |
|---|---|---|---|
| 0.0823 | 0.2000 | 1 | 1.5992 |
| 0.0862 | 0.2027 | 2 | -0.0000 |
| 0.0922 | 0.2000 | 1 | $-0.6956$ |

For reminder: The discontinuity points i.e. contact- impact regions (where the third derivative $\dddot{y}(t)$ is not continuous) are indicated by means of small circles. The function $(y(t) - \nu(t))$ is at the switching region. The sliding zones represent to the intervals at which the functions vanishes. (The dashed lines correspond to the switching surfaces in the phase diagrams plot Fig.(3.11(d),3.12(d)). The response in region $g_2$ with the sign $'-'$ means that the solution exits from the sliding region. The positive elements in that table3.2 mean that these discontinuities are transversal.

Numerical studies have shown that pounding introduces impact loads in addition to the forces caused by the ground acceleration itself. A lot of impact areas are observed in case of structures constructed in fractured bedrock than those constructed where the soil is not fractured.

Recall that $P_{fss}$ the estimator of failure probability. We recognized that the estimate $p_f$

obtained through MCS is unbiased. The geometry of the failure domain not influenced its accuracy even the number of the random parameters involved. Instead, it only depends on $P_f$ and the number of samples N used in the simulation. $p_0$ is adopted as optimal choice of the conditional failure probability. The parameter $p_0$ governs how many intermediate failure domains $F_j$ are needed to reach the target failure domain F , which in turn affects the efficiency of Subset Simulation (SS). A very small value of the conditional failure probability means that fewer intermediate levels are needed to reach F but it results in a very large number of samples N needed at each level for accurate estimation of the small conditional probabilities. The CDF plots for $p_0 = 0.1, 0.15, ...$ are given in Fig.3.12(e, f), i.e. The CDF plot for the cantilever beam and the inter-story respectively. The estimated failure probabilities and the number of required samples are listed in illustrated tables. (SS) behaves differently by chosing different values of conditional catastrophes $p_0$. The CDF plot with $p_0 = 0.3, ...$ significantly jump all intermediated failure mode of the cantilever beam and the inter-story. The conditional catastrophes probability $p_0 = 0.1, 0.15, 0.20, ...$ are convenable for reliability analysis in case of very small values of $p_0$ less than 0.3.

Concludingly, after evaluation of static (gravitational) load and the ground motion characteristics, some structural applications are chosen. Subset Simulation (SS) is adapted for simulating rare events and estimating the corresponding small tail probabilities with intermediated failures. For typical engineering reliability problems, the failure probability $p_f$ is very small, $p_f << 1$. In other words, the system is usually assumed to be designed properly, so that its failure is a rare event. Defining the reliability of an element in a structure is completely dependent on the definition of failure. Different kinds of failure can be considered for an element. Each of these failure types can be assessed separately, and they can give different probabilities of failure or reliability indices. As a matter of fact, each failure can have its own specific limit state function (LSF) or performance function (sometimes also called the safety margin) which will consequently lead to a specific reliability index corresponding to that failure type. Hence, the CDF plot Fig.3.12(f) in the case of inter-story isn't adapted for all values of the conditional probability $p_0 > 0.3$. To come to the conclusion that, due to sudden applied loadings, undesired and unpredicted stresses are characteristics of Thom's theory. Given the design life of a structure, the probability for a specific live load to cause a failure depends on the magnitude of the

load structure it is designed to withstand (designed load).

## 3.5   Conclusion

The aim of this chapter was to present our results with some discussions. We have solve some main problems namely. To preserve structural integrity and prevent damage and injury to contents, numerous studies must be done to understand the stochastic effect of seismic wave. With a monitoring system installed and supplying full scale records of the structure response, considerable amount of data will be available for investigation to avoid disaster during seismic events. The required gap to avoid pounding is significantly important. Under certain conditions, the properties of the supporting soil must also be taken into consideration due to its influence on the impact- friction events. During collision, the forces produced act over a short period of time, due to random molecular vibrations and the internal friction of the colliding bodies, energy is dissipated as heat. If pounding appears in a foundation of buildings it can be harmful. The impact forces that act during pounding can cause additional sliding of the concrete or steel of the building. With high noise intensity during the impact-friction effects, the pounding force is influenced. P-bifurcation occurs with small peak of PDF. But weak noise intensity created a large probability density function (PDF) (because of continuous sliding), hence a great value of pounding force. During the resolution of these different issues, it appears many results summarized in concluding remarks.

# General Conclusion

⤳ **Main Results of the Thesis**

The scope of this thesis was based on investigating the phenomenon include impacts where contact forces suddenly and rapidly increase with an associated rapid change in velocity of the impacting object. Pursued in this work, was to model them with discrete jumps in the equations describing the dynamics. We discussed current dissertation in the dynamics of non-smooth systems, with an emphasis on stochastic bifurcation theory. We have also studied the effect of noises on this model and demonstrate a practical applicability of the SD oscillator. An introduction to the field of Non-smooth Structural Systems is given in Chapter 1. This chapter provides a briefly historical background of pounding phenomenon and the structural failure.

The second chapter was devoted to the methodological frame. We presented there the analytical and the numerical methods used within this dissertation. We shown how to construct the contact-impact friction in filippov' case and illustrated the points of discontinuity in the case of spillway-abutment as impacting points. As population of a country increase, land become the scarcest resource, because of the land cost wise utilization of the space becomes not a choice rather an obligation. Owners want to build their structure aligned with their property line ignoring adjacent structure that lead to pounding. In order to model highly non-linear pounding more-accurately, nonlinear viscoelastic model have been developed. In practice, adjacent structures tremble out of phase due to different dynamic characteristics. Moreover, in current design process, adjacent buildings with insufficient clear spacing are designed as a standardize structure by ignoring the pounding action during earthquake loading. This negligence causes failure of structures. This is because of huge amount of additional shear forces and bending moments developed in the columns due to repeated impulsive actions during tremor. The last chapter was concerned

by our principal findings followed by some comments.

The main results that have been obtained in this thesis can be summarized as follows:

⋄ P-bifurcation occurs and created instability that will increase pounding effects.

⋄ Because of the presence of both impact-friction events, p-bifurcations should be observed at weak noise intensities.

⋄ Some relationship between impact-friction events appears: small noise intensity occurs when the time of friction (continuous) is greater than the impacting events, hence high probability density function (PDF).

⋄ If the noise intensity increases, the impact events are great (small friction) with weak PDF. But successive jump effects can create noisy system and great impact.

⋄ The damaging (collapse) is function of the value of the amplitude of excitation.

⋄ Separation distance between neighbouring structures reduces pounding damage as pounding force is widely decreased for greater separation distance compared to low dimensional gap element.

The (SD) oscillator which is a strongly irrational nonlinear system (often concerned by engineering applications) is characterized with a coexistence of a stable limit cycle and a stable equilibrium state. We observed a large disparity between development and understanding of smooth and discontinuous (non-smooth) systems. There is a substantial departure in the dynamics from the standard one, at the discontinuous limit, in particular, the velocity flow suffers a jump in crossing from one well to another, caused by the loss of local hyperbolicity due to the collapse of the stable and unstable manifolds of the stationary state. Then, we have illustrated the phenomenon of pounding first with the abutment and then with adjacent buildings and investigate the failure events. A simulation-based approach is then employed to obtain accurate estimates of the pounding force statistics and the results of these simulations was used to evaluate the accuracy of the simplifying approach for pounding force assessment based on the proposed probabilistic model. We observed large oscillation with large amplitude at weak noise intensity. For the impact-friction events at very low noise intensity, p-bifurcation occurred and created instability that will increase pounding effects. The near-field buildings has being impacting and destructed. The disasters were pronounced if the amplitude of earthquake excitation was big. We have demonstrated that response of building is greatly affected in the direction

of pounding (longitudinal) while response in transverse direction is almost negligible. It is because the direction of pounding (longitudinal) is influenced by impact force but there is only friction force acting on transverse direction. Before design and construction of any structure it is necessary to step out and check the surrounding space of the structure to avoid future problem as in the Gouache's case in Cameroon.

⤳ **Open problems and future directions**

The work carried out in this dissertation and the results so far obtained are a source of encouragement for other studies. Other points of interest may be solved in the future.

◇ We expect that these theoretical findings will stimulate experimental works taking into account the stochastic contribution for eventual human life safety.

◇ The minimum pounding free distance could be calculated in our models taking into account the effects of delay.

◇ Elastic structures with impacts show much severe pounding response than inelastic structures, such systems arise in the analysis of bridges with seismic stoppers or the analysis of pounding of adjacent buildings. The sensitivity of the stochastic response and failure probability to the size of gaps can be explored.

# Bibliography

[1] Lin, J. H., and Weng, C. C., *Spectral Analysis on Pounding Probability of Adjacent Buildings*. Engineering Structures **23** (2001a)(7) 768-778.

[2] Lin, J. H., and Weng, C. C., *Probability Analysis of Seismic Pounding of Adjacent Buildings*. Earthquake Engineering and Structural Dynamics **30** (2001b)(10) 1539-1557.

[3] Selvaraj and S.P.Sharma, *Influnce of Construction Sequence on the Stresses in Tall Building Frames*, Regional Conference on Tall Building, Bangkok, (1974).

[4] Jankowski, R., Wilde, K. and Fujino, Y. *Pounding of superstructure segments in isolated elevated bridge during earthquakes*, Earthquake Engineering and Structural Dynamics, **27**, (1998) pp. 487-502.

[5] Maison, B.F. and Kasai, K. *Analysis for type of structural pounding*, Journal of Structural Engineering, **116**, (1990) pp. 957-977.

[6] Bertero VV and Collins R Cl., *Investigation of the Failures of the Olive View Stairtowers during the San Fernando Earthquake and Their Implications on Seismic Design*, Report no. EERC (1973), 73-26, Earthquake Engineering Research Center, University of California, Berkeley, CA.

[7] Moehle, J.P. and Mahin, S.A. *Observations on the behavior of reinforced concrete buildings during earthquakes, ACI SP-127, Earthquake-Resistant Concrete Structures: Inelastic Response and Design*, American Concrete Institute, Farmington Hills, Michigan, (1991), pp. 67-89.

[8] Penzien J, *Evaluation of building separation distance required to prevent pounding during strong earthquakes.* Earthquake Engineering and Structural Dynamics. **26**, (1997) pp. 849-858.

[9] Masroor, A. and Mosqueda, G., *Experimental simulation of base-isolated buildings pounding against moat wall and effects on superstructure response*, Earthquake Engineering and Structural Dynamics **41**, (2012a) 2093-2109 (DOI:10.1002/eqe.2177).

[10] Kim, E.-H., J. R. Johnson, E. Valeo, and C. K. Phillips, *Global modeling of ULF waves at Mercury*, Geophys. Res. Lett., **42**, (2015a), 5147-5154, doi:10.1002/2015GL064531.

[11] Bi Y, Sunada H, Yonezawa Y, Danjo K, Otsuka A, Iida K, *Hiroshi Oyaizu, Satoshi Matsumoto1 and Makoto M. Watanabe, Preparation and evaluation of a compressed tablet rapidly disintegrating in the oral cavity*, **44(11)** (1996) 2121-7.

[12] Taflanidis, A.A, *Optimal probabilistic design of seismic-dampers for protection of isolated bridges against near-fault seismic excitations.* Engineering Structures, **33(12)**(2011) 3496-3508.

[13] Han, G., Santner, T. J., Notz, W. I., and Bartel, D. L., *Prediction for computer experiments having quantitative and qualitative input variables.* Technometrics, **51(3)**(2009) 278-288.

[14] Darragh, R.B., Huang, M. J., and Shakal, A. F., (1994), *Earthquake Engineering Aspects of Strong Motion Data from Recent California Earthquakes*, Proc. 5th U.S. Nat. Conf. Earthqu. Eng. Chicago, IL, **July 10-14, v. III**, (99-108), (Earthqu. Eng. Res. Inst., Oakland, CA).

[15] Alexandros A. Taflanidis Gaofeng Jia, *A simulation-based framework for risk assessment and probabilistic sensitivity analysis of base-isolated structures*, Earthquake Engineering and Structural Dynamics *40(14)* (2011) 1629-1651.

[16] Nagarajaiah, S., Sahasrabudhe, S., and Iyer, R. *Seismic response of sliding isolated bridges with MR dampers.* Proc., American Control Conference (2000).

[17] Manuel Pellissetti et al. *Statistical analysis of impact forces and permanent deformations of fuel assembly spacer grids in the context of seismic fragility*, Conference: 24th International Conference on Structural Mechanics in Reactor Technology, (2017).

[18] Zhu Weiqiu, Cai Guoqiang, *Nonlinear stochastic dynamics: a survey of recent developments.* Acta Mechanica Sinica (English Series), **18(6)**, December (2002), The Chinese Society of Theoretical and Applied Mechanics, Chinese Journal of Mechanics Press, Beijing, China, Allerton Press, INC., New York, U.S.A.

[19] Zhilin Qu, Gang Hub, Alan Garfinkel, James N. Weiss. *Nonlinear and stochastic dynamics in the heart.* Physics Reports **543** (2014) 61-162.

[20] P. Ndy Von Kluge, G. Djuidjé Kenmoé, T. C. Kofané, *Application to nonlinear mechanical systems with dry friction: hard bifurcation in SD oscillator.* SN Applied Sciences **1** (2019) 1140 | https://doi.org/10.1007/s42452-019-0987-1.

[21] Filippov AF (1988) *Differential equations with discontinuous right-hand sides.* Kluwer Academic Publication, Dortrecht (Russian 1985).

[22] Rong H, Meng G, Wang X, Xu W, Fang T *Response statistic of strongly non-linear oscillator to combined deterministic and random excitation.* Int J Non Linear Mech 39(6)(2004) 871-878.

[23] Leine RI, Nijmeijer H *Dynamics and bifurcations of nonsmooth mechanical systems*, vol **18** (2013) Springer, Berlin.

[24] Santhosh B, Narayanan S, Padmanabhan C *Numericanalytic solutions of the smooth and discontinuous oscillator.* Int J Mech Sci **84** (2014) 102-119.

[25] Fajfar P. *A nonlinear analysis method for performance-based seismic design*, Earthquake Spectra **16(3)** (2000) 573-592.

[26] Ford, C.R. *Earthquakes and building constructions,* whitcombe and Tombs, Auckland (1926).

[27] Rosenblueth, E, Meli, R. *The 1985 earthquake: causes and effects in mexico city, Concrete* International Magazine, American Concrete Institute (ACI), **8** (1986) 23-34.

[28] Anagnostopoulos, S.A. *Building pounding re-examined: how serious a problem is it?* Eleventh World Conference on Earthquake Engineering, Acapulco, Mexico, p. 2108 (1996).

[29] Tsai H.C. *Dynamic analysis of base-isolated shear beams bumping against stops.* Earthquake Engineering and Structural Dynamics; **26**(1997) 515-528.

[30] Westermo, B.D. *The dynamics of inter-structural connection to prevent pounding*", Earthquake Engineering and Structural Dynamics, **18** (1989) pp. 687-699.

[31] Anagnostopoulos, S.A. *Building pounding re-examined: how serious a problem is it?* Eleventh World Conference on Earthquake Engineering, Acapulco, Mexico, p. 2108 (1996).

[32] Jankowski, R., Wilde, K. and Fujino, Y. *Reduction of pounding effects in elevated bridges during earthquakes*, Earthquake Engineering and Structural Dynamics, **29**(2000), pp. 195-212

[33] Sheikh, M.N., Xiong, J. and Li, W.H. *Reduction of seismic pounding effects of base-isolated RC highway bridges using MR damper*, Structural Engineering and Mechanics, **41(6)** (2012), pp. 791-803 .

[34] Van Mier, J.G.M., Pruijssers, A.F., Reinhardt, H.W. and Monnier, T. *Load-time response of colliding concrete bodies*, Journal of Structural Engineering, ASCE, **117**(1991), pp. 354-374.

[35] Papadrakakis, M. and Mouzakis, H.P. *Earthquake simulator testing of pounding between adjacent buildings*, Earthquake Engineering and Structural Dynamics, **24** (1995), pp. 811-834.

[36] Chau, K.T., Wei, X.X., Guo, X. and Shen, C.Y. *Experimental and theoretical simulations of seismic poundings between two adjacent structures*, Earthquake Engineering and Structural Dynamics, **32** (2003), pp. 537-554.

[37] Jankowski, R. *Experimental study on earthquake-induced pounding between structural elements made of different building materials*, Earthquake Engineering and Structural Dynamics, **39**(2010) pp. 343-354 .

[38] Park YJ, Ang AHS. *Mechanistic seismic damage model for reinforced concrete.* Structural Division Journal ASCE **111(4)**(1985)722-739.

[39] Getachew Kifle, *Assessment of adjacent RC buildings in Addis Ababa against pounding* (2013).

[40] Jing H-S, Young M. *Impact interactions between two vibration systems under random excitation.* Earthquake Engineering and Structural Dynamics **20**(1991) 667-681.

[41] D. E. Stewart and J. C. Trinkle, *An implicit time-stepping scheme for rigid body dynamics with inelastic collisions and Coulomb friction,* Internat. J. Numer. Methods Engrg., **39** (1996), pp. 2673-2691.

[42] Ivanov, A. P. *Analytical methods in the theory of vibro-impact systems*, Journal of Applied Mathematics and Mechanics, **57, (2)**, (1993) pp. 221-236.

[43] Deepti Adhikari, Ashmita Gautam, *Structural Failure Analysis of Earthquake Affected Buildings in Gorkha (Nepal)* earthquake (2015) in Kathmandu Valley. Journal of Advanced College of Engineering and Management, Vol.**4**, (2018).

[44] A.K. Chopra: *Dynamics of Structures: Theory and Applications to Earthquake Engineering* (Prentice Hall, USA (1995).

[45] Anagnostopoulos SA, Spiliopoulos KV. *An investigation of earthquake induced pounding between adjacent buildings.* Earthquake Engineering and Structural Dynamics **21**(1992) 289-302.

[46] Azevedo J, Bento R. *Design criteria for buildings subjected to pounding.* Eleventh World Conference on Earthquake Engineering, Acapulco, Mexico, (23-28) **(1063)** June (1996).

[47] Papadrakakis M, Mouzakis H, Plevris N, Bitzarakis S. *A Lagrange multiplier solution method for pounding of buildings during earthquakes.* Earthquake Engineering and Structural Dynamics **20** (1991) 981-998.

[48] Jankowski R, Wilde K, Fujino Y. *Pounding of superstructure segments in isolated elevated bridge during earthquakes.* Earthquake Engineering and Structural Dynamics **27**(1998) 487-502.

[49] Zhu P, Abe M, Fujino Y. *Modelling three-dimensional non-linear seismic performance of elevated bridges with emphasis on pounding of girders.* Earthquake Engineering and Structural Dynamics **31** (2002)1891-1913.

[50] Ruangrassamee A, Kawashima K. *Relative displacement response spectra with pounding eect.* Earthquake Engineering and Structural Dynamics **30** (2001) 1511-1538.

[51] Goldsmith W. *Impact: The Theory and Physical Behaviour of Colliding Solids*, 1st edn, Edward Arnold: London, U.K., (1960).

[52] van Mier JGM, Pruijssers AF, Reinhardt HW, Monnier T. *Load-time response of colliding concrete bodies.* Journal of Structural Engineering (ASCE) **117** (1991) 354-374.

[53] Goland M, Wickersham PD, Dengler MA. *Propagation of elastic impact in beams in bending.* Journal of Applied Mechanics **22** (1955) (1-7).

[54] Kasai K, Maison BF. *Building pounding damage during the (1989) Loma Prieta earthquake.* Engineering Structures **19** (1997) 195-207.

[55] Komodromos P, Polycarpou PC, Papaloizou L, Phocas MC. *Response of seismically isolated buildings considering poundings*, Earthquake Engineering and Structural Dynamics, **36**(2007) 1605-22.

[56] Pant R, Wijeyewickrema AC. *Seismic pounding between reinforced concrete buildings: A study using recently proposed contact element models*, Proceeding of the 14th European Conference on Earthquake Engineering, Republic of Macedonia, (2010).

[57] Davis RO. *Pounding of buildings modeled by an impact oscillator*, Earthquake Engineering and Structural Dynamics, **21**(1992) 253-74).

[58] Chau KT, Wei XX, Guo X, Shen CY. *Experimental and theoretical simulations of seismic poundings between two adjacent structures*, Earthquake Engineering and Structural Dynamics, 32(2003) 537-54.

[59] Jankowski R. *Pounding force response spectrum under earthquake excitation*, Engineering Structures, **28**(2006) 1149-61.

[60] Muthukumar S, DesRoches RA. *Hertz contact model with nonlinear damping for pounding simulation*, Earthquake Engineering and Structural Dynamics, **35**(2006) 811-28.

[61] Jankowski R, Wilde K, Fujino Y. *Reduction of pounding eects in elevated bridges during earthquakes*. Earthquake Engineering and Structural Dynamics **29** (2000) 195-212.

[62] Xing S, Halling MW, Meng Q. *Structural pounding detection by using wavelet scalogram*, Advances in Acoustics and Vibration, Article ID 805141, Doi:10.1155/2012/805141, (2012), 10 p.

[63] Barros RC, Khatami SM. *An estimation of damping ratio for the numerical study of impact forces between two adjacent concrete buildings subjected to pounding*, Proceedings of 15th International Conference on Experimental Mechanics, Porto, Portugal, Paper Ref. 4051, 22-27th July, (2012).

[64] J.C Breton. *Cours Processus Gaussiens*. Universite de la Rochelle, $M_2$(2006).

[65] A. F. Filippov. *Differential Equations with Discontinuous Righthand Sides*. Kluwer Academic Publ. Dortrecht; (1988) (Russian 1985).

[66] James H. Dieterich, *time-dependent friction in rock*, journal of geophysical research vol.**77 (20)**, july 10 , (1972).

[67] J. R. Rice, A. L. Ruina, *Stability of Steady Frictional Slipping*, Journal of Applied Mechanics, vol. **50**,(1983), pp. 343-349.

[68] James R. Rice, Nadia Lapusta, K. Ranjith, *Rate and state dependent friction and the stability of sliding between elastically deformable solids*, Journal of the Mechanics and Physics of Solids **49** (2001); 1865-1898.

[69] B. P. Ndemanou, J. Metsebo, B.R. Nana Nbendjo et P. Woafo, *Dynamique et contrôle magnéto-rhéologique des vibrations du faisceau en porte-à-faux de Timoshenko sous les charges sismiques.* Nonlinear Dyn **78** ( 2014 ); 163-171.

[70] B.P. Ndemanou, B.R. Nana Nbendjo et U. Dorka. *Extinction des modes de vibration sur deux bâtiments interconnectés soumis à des charges sismiques à l'aide d'un dispositif magnéto-rhéologique.* Mécanique Recherche Communications **78**, (2016) 6-12.

[71] Paz, M. *Structural Dynamics: Theory and Computation.* Chapman and Hall, New York, fourth edition, (1997).

[72] Chopra, A. *Dynamics of Structures: Theory and Application to Earthquake Engineering.* Prentice-Hall, Upper Saddle River, second edition. (2001).

[73] Jean-Pierre Magnan, *Description, identification et classification des sols.* Doc. C (208).

[74] Chau KT, Wei XX. *Pounding of structures modelled as non-linear impacts of two oscillators.* Earthquake Engineering and Structural Dynamics **30**(2001); 633-651.

[75] Jeng-Hsiang Lin, *Evaluation of seismic pounding risk of buildings in Taiwan*, Journal of the Chinese Institute of Engineers Volume **28**, (2005); Issue 5 .

[76] Robert Jankowski, *Non-linear viscoelastic modelling of earthquake-induced structural pounding*, Earthquake Engng Struct. Dyn. **34** (2005); 595-611.

[77] Chopra, A. *Dynamics of Structures: Theory and Application to Earthquake Engineering.* Prentice-Hall, Upper Saddle River, second edition, (2001).

[78] Zhu P, Abe M, Fujino Y. *Modelling three-dimensional non-linear seismic performance of elevated bridges with emphasis on pounding of girders.* Earthquake Engineering and Structural Dynamics **31** (2002); 1891-1913.

[79] Annual Geophysics, (4, B, 6, 11) August (1986), pp.(679-702).

[80] Cornell , *Engineering seismic risk analysis* Bulletin of the Seismological Society of America, **58 (5)**, (1968); 1583-1606.

[81] Trifunac, M. D., and A. G. Brady, *On the correlation of seismic intensity with peaks of recorded ground motion*, Bull. Seismol. Soc. Am. **65** (1975a), 139-162.

[82] Ayad S.Adi and B.S.Karkare, *Empirical Formulation for Prediction of Flexural Strength of Reinforced Concrete Composite Beams*, Journal of Advances in Civil Engineering, Vol. **3(1)**(2017). (1-8), https://dx.doi.org/10.18831/djcivil.org/2017011001.

[83] P. Ndy Von Kluge., G. Djuidjé Kenmoé, T. C. Kofané. *Colliding solids interactions of earthquake-induced nonlinear structural pounding under stochastic excitation.* Soil Dynamics and Earthquake Engineering. https://doi.org/10.1016/j.soildyn.2020.106065.

[84] J. R. Dormand and P. J. Prince. (1980). *A family of embedded Runge-Kutta formulae.* J. Comput. Appl. Math. **(6)( 1)** (1980), (19-26).

[85] M. Calvo, J. I. Montijano, and L. Randez. A fifth-order interpolant for the Dormand and Prince Runge-Kutta method. J. Comput. Appl. Math. **29(1)** (1990), 91-100.

[86] Petri T. Piiroinen and Yuri A. Kuznetsov. 2008. *An event-driven method to simulate Filippov systems with accurate computing of sliding motions.* ACM Trans. Math. Software **(34)(3)** (2008), Art. 13, 24.

[87] Cash, J.R. and Karp, A.H., *A Variable Order Runge-Kutta Method for Initial Value Problems with Rapidly Varying Right-Hand Sides*, ACM Transactions on Mathematical Software, vol **16 (3 )**, (1990) 201-222. http://www.duke.edu/ hpgavin/cee541/Cash-90.pdf

[88] Robert C, Casella G. *Monte Carlo Statistical Methods.* New York: Springer; (1999).

[89] Au SK. *On the Solution of First Excursion Problems by Simulation with Applications to Probabilistic Seismic Performance Assessment.* PhD Thesis in Civil Engineering

(2001), Division of Engineering and Applied Science, California Institute of Technology, California, USA.

[90] Au SK, Beck JL. *Estimation of small failure probabilities in high dimensions by Subset Simulation.* Probabilistic Eng Mech **16(4)** (2001) 263Ű77.

[91] Thompson, J. M. T. and Hunt, G. W., *A General Theory of Elastic Stability*, Wiley, London, (1973).

[92] Thompson, J. M. T. and Hunt, G. W., *Elastic Instability Phenomena*, Wiley, Chichester, (1984).

[93] Kerschen, G., Worden, K., Vakakis, A. and Golinvala, J. *Past, present and future of nonlinear system identification in structural dynamics*, Mechanical Systems and Signal Processing ; **20** (2006) , pp 505-592.

[94] C. Meunier, A.D. Verga, *Noise and bifurcation*, J. Stat. Phys.,**50 (2)** (1988) 345-375.

[95] V.I. Arnold, V.S. Afrajmovich, Yu.S. Il'yashenko, L.P. Shil'nikov, *Bifurcation theory and catastrophe theory*, Springer Verlag; 1999.

[96] E.C. Zeeman, *Stability of dynamical systems*, Nonlinearity **1 (1)**(1988), 115-155.

[97] E.C. Zeeman, *On the classification of dynamical systems*, Bull. London Math. Soc., **20 (6)** (1988), 545-557).

[98] Baxendale, P. *Asymptotic behavior of stochastic flows of diffeomorphisms*, in Stochastic Processes and Their Applications, eds. Ito, K. and Hida, T., Lecture Notes in Mathematics, Vol., **1203** (1986) (Springer, Berlin, NY), pp. 1-19.

[99] Crauel, H., Flandoli, F. *Additive noise destroys a pitchfork bifurcation*, J. Dyn. Diff. Eqs.,**10** (1998) 259-274.

[100] Muthukumar, S. and DesRoches, R. *A Hertz contact model with non-linear damping for pounding simulation*, Earthquake Engineering and Structural Dynamics, **35**, (2006) 811-828.

[101] Cole, G.L., Dhakal, R.P., Carr, A.J. and Bull, D.K. *Building pounding state of the art: identifying structures vulnerable to pounding damage*, NZSEE Conference (2010).

[102] Jeng-Hsiang Lin and Cheng-Chiang Weng, *A study on seismic pounding probability of buildings in Taipei metropolitan area*, Journal of the Chinese Institute of Engineers, **25(2)**, (2002) 123-135, DOI:10.1080/02533839.2002.9670687.

[103] Goldsmith W. Impact: *The Theory and Physical Behaviour of Colliding Solids*, 1st edn, Edward Arnold: London, U.K., (1960).

[104] Jankowski R, Wilde K, Fujino Y. *Pounding of superstructure segments in isolated elevated bridge during earthquakes.* Earthquake Engineering and Structural Dynamics **27** (1998); 487-502.

[105] Zanardo G, Hao H, Modena C. *Seismic response of multi-span simply supported bridges to a spatially varying earthquake ground motion.* Earthquake Engineering and Structural Dynamics **31**(2002); 1325-1345.

[106] Jeng V, Kasai K. *Spectral relative motion of two structures due to seismic travel waves.* Journal of Structural Engineering (ASCE) **122** (1996); 1128-1135.

[107] Jankowski R, Wilde K. *A simple method of conditional random field simulation of ground motions for long structures.* Engineering Structures **22** (2000); 552-561.

[108] Nicole Gaus and Carsten Proppe, *Bifurcation analysis of a stochastic non-smooth friction model.* PAMM ů Proc. Appl. Math. Mech. **9**, (2009) 281-282 / DOI 10.1002/pamm.200910114.

[109] Robert Jankowski, *Non-linear viscoelastic modelling of earthquake-induced structural pounding*, Earthquake Engng Struct. Dyn. **34**(2005); 595-611.

[110] Maison, B.F., Kasai, K., *Dynamics of pounding when two buildings collide*, Earthquake Engineering and Structural Dynamics, **21** (1992); 771-786.

[111] Anagnostopoulos, S.A., Spiliopoulos, K.V., *An investigation of earthquake induced pounding between adjacent buildings*, Earthquake Engineering and Structural Dynamics, **21** (1992); 289-302.

[112] Hao, H., Zhang, S.R., *Spatial ground motion effect on relative displacement of adjacent building structures*, Earthquake Engineering and Structural Dynamics, **28** 1999; 333-349.

[113] Jankowski, R., Wilde, K., *A simple method of conditional random field simulation of ground motions for long structures*, Engineering Structures, **22** 2000; 552-561.

[114] Lin, J. H., Weng, C. C., *Probability Analysis of Seismic Pounding of Adjacent Buildings*, Earthquake Engineering and Structural Dynamics, Vol. **30 (10)**, (2001b;) 1539-1557.

[115] Jeng-Hsiang Lin, Cheng-Chiang Weng, *A study on seismic pounding probability of buildings in Taipei metropolitan area*, Journal of the Chinese Institute of Engineers, **25(2)**, (2002); 123-135, DOI:10.1080/02533839.2002.9670687.

[116] Lin, J. H., Weng, C. C., *Seismic Pounding Risk Analysis of Adjacent Buildings*, Proceedings, Conference on Computer Applications in Civil and Hydraulic Engineering, Vol. **2**, (2000); pp. 2049-2058.

[117] Jain, S. K., Lettis, W. R. , Murty, C.V.R. and Bardet, J. P. (2002), *Bhuj, India earthquake of January 26, 2001 reconnaissance report,* Public No-2-01, Earthquake Engineering Research Institute (EERI), Oakland, CA.

[118] Agarwal, P., Thakkar, S. K. and Dubey, R. N. (2012),*Behavior of building, bridges, dams and ports during Bhuj earthquake of January 26, 2001,* ISET Golden Jubilee Symposium, October.

[119] P. Ndy Von Kluge., G. Djuidjé Kenmoé, T. C. Kofané. *Colliding solids interactions of earthquake-induced nonlinear structural pounding under stochastic excitation.* Soil Dynamics and Earthquake Engineering. https://doi.org/10.1016/j.soildyn.2020.106065.

[120] Wang and Zhou, *Modelling Urban Population Densities in Beijing 1982-90: Suburbanisation and its Causes*, Sage journal; First Published Feb **1**, (1999); pp. 223-237.

[121] C. J. Burgoyne, 2001, *Recommendation for design and construction of concrete structures using continuous fiber reinforcing materials*, Technology and Engineering, JSCE 1997 , p.98-101 9. JSCE - E 533-1995

[122] R.W. Clough and J. Penzien, *Dynamics of Structures, 2nd edn, McGraw-Hill Book Co., NY,* (1993).

[123] Tedesco et al., *Structural Dynamics*, Structural Engineering and Geomechanics, Vol. II 1999

[124] Solomon P.PEER, *support/peer provided services underlying processes, benefits and critical ingredients.* Psychiatr Rehabil J. (2004) **27(4)** 392-401.

[125] Vaughan et al., *Recent Rapid Regional Climate Warming on the Antarctic Peninsula.* Climatic Change **60**, (2003), 243-274. Kluwer Academic Publishers. Printed in the Netherlands, DOI: 10.1023/A:1026021217991

# List of publications in international refereed journals

**P. Ndy Von Kluge, G. Djuidjé Kenmoé and T.C. Kofané**, *Application to nonlinear mechanical systems with dry friction: hard bifurcation in SD oscillator.* SN Applied Sciences **1** (2019) 1140.

**P. Ndy Von Kluge, G. Djuidjé Kenmoé and T.C. Kofané**, *Colliding solids interactions of earthquake-induced nonlinear structural pounding under stochastic excitation.* Soil Dynamics and Earthquake Engineering **132** (2020) 106065.

# Application to nonlinear mechanical systems with dry friction: hard bifurcation in SD oscillator

P. Ndy Von Kluge[1] · G. Djuidjé Kenmoé[1] · T. C. Kofané[1]

## Abstract

The stochastic model approach of a nonlinear non-smooth dynamical system with the probable occurrence of stochastic P-bifurcations is devoted. The response probability density functions (PDF) for the stationary measure of a smooth and discontinuous oscillator under moving loads belt frictions is constructed. The appearance of abrupt changes and unpredictable events illustrate the complexity of the system. The stationary measure varies continuously with system's parameters and describes various kinds of catastrophic events. In light of these facts, the behaviour of the "stochastic attractors" is examined through the stationary solution of the PDF. According to Zeeman, in the phenomenological approach in the presence of noise, "a change in character of the density function as a parameter is varied is known as p- bifurcation". Numerous new events unique to non-smooth systems are observed under slight variation of system's parameters. Discontinuous bifurcations are defined as the "hard bifurcations" that were the subject of Catastrophe theory. Peaks numbers increase as coefficient of friction μ (or smoothness parameter $a$) increases. Numerical simulations are presented that provide insights into the dynamics of these oscillators.

**Keywords** Hard bifurcation · Stochastic attractor · Stochastic bifurcation · Self-excited SD oscillator

## 1 Introduction

Discrete and instantaneous transition are always observed in physical systems. Very often in engineering and biology, vibrations are influenced by physical discontinuities. The stick–slip phenomenon occurs.

Systems with friction as the state variables representing the system dynamics are confined to both subspaces at different instants of time belongs to the category of "discontinuous systems". It should be noted that, because of discontinuous vector fields, we will focus on Filippov systems. Therefore, stick–slip phenomena are important examples of this last one. Some bifurcations referred as non-smooth bifurcations or C-bifurcations may occur.

Under the effects of periodic impulse and random force; the nonlinear system has some propensities to oscillate.

Complex behaviours occur in the system's response including the transitions among the multiple motion patterns [1], chaotic phenomena [2] and bifurcation Phenomenon, such as phenomenological [3]. Under the action of fast vibration friction properties change. There is the source of "self-sustained Oscillations" under certain conditions. A lot of researches have been done in this field [4]. They are illustrated by a common phenomenon: switching behaviour upon appearance of intermittent events.

Systems with dry friction under necessary conditions show the catastrophic case ("grazing-sliding bifurcation").

Non-smooth systems are receiving a great curiosity because of their ubiquity in applications of biological

---

Published online: 03 September 2019

and engineering nature. From interaction with the environment, discontinuities occur naturally. Little attention has been paid on bifurcation behaviours of the nonlinear friction system characterized by geometric nonlinearities. Mechanical systems are subject to background vibrations and other sources of noise [5]: The possible structural changes of the asymptotic behaviour of the system under parameter variation. The stick–slip phenomenon and the related intermittent motion are the motivation of our studies, being the key driver of our non- smooth stochastic model.

For studying noise phenomena in nonlinear dynamical systems coupled to a fluctuating environment one of the main statistical characteristics of these systems is the probability density of the solution. These have attracted a growing interest also from a theoretical point of view (see for instance [6, 7]). A whole new area of research is opened, surely not completely known when adding noise to the non-smooth dynamic system. The interplay of dry friction and random forces in terms of so-called P-bifurcations has been reported in [8]. Phenomenological bifurcations are defined here as changes in the distribution laws i.e. "the qualitative changes of the stationary probability distribution of amplitude"; alternatively, it is a sudden change in character of a "stochastic attractor" when the bifurcation parameter of the system passes through a critical value. Under certain circumstances the Collision between the "stochastic attractor" with a "stochastic saddle" created the loss of the stability of the system. It can happen that a slight variation in a parameter can have significant impact on the solution. By "hard bifurcation", we are talking about the abrupt and unpredicted change in the probability density function (PDF), the presence of discontinuities on the support of a stationary measure or PDF of the system.

In 1973, Thompson and Hunt proposed a simple shallow "arch model" to study the buckling behaviour under a static load [9]. Cao et al. [10–12] proposed in 2006 the "smooth and discontinuous" (SD) oscillator where the nonlinearity is irrational. The geometrical nonlinearity caused by large deformation was illustrated. Complex motions and coexisting attractors are also devoted. An applied force moves an object and created the sliding process, otherwise the object sticks. Remove this constraint, the system becomes two dimensional. Consequently, another friction force must be added to separate permanent sliding motions from jumping effects.

Friction constitutes an important area of many other disciplines rich in interesting examples and applications such as seismology and tectonic fault dynamics under geometrical nonlinearities by considering the large scale displacement of the system [13, 14] or climate and weather changes with possible stick slip motion [15], Reliability and braking power [16, 17] are some illustrations.

Recent studies have successively explained novel behaviour that may occur in such systems [18, 19]. But, little is known when adding random parameters to "discontinuous systems" in spite of some new publications [20, 21].

To avoid the lack of detailed of the statistical characteristic of a random dynamical system, an appropriate choice is to describe the stationary measure. Because of the long term behaviour of solutions with an emphasis of probability densities when talking about the stationary and dynamical behaviour of the system.

In real systems moreover, parameter uncertainty, background vibrations and other sources of noise are ubiquitous.

The dynamic of systems with dry friction subjected to random forces have abrupt changes occurrence when a stable equilibrium is lost. A Gaussian white noise is sufficed to describe the influence of random perturbations.

Terminology from "catastrophe" returned to singularities, discontinuous bifurcations. What types of long-term dynamical behaviour are possible talking about SD oscillator? The "hard bifurcations" were the subject of "Tom's Catastrophe Theory", this proved to be basic to nonlinear friction system with geometric nonlinearity in mechanical engineering. Thus, one cannot help thinking about unexpected events that cannot be predicted for appearance of p-bifurcations or how does the structure of the steady state solution set change as the parameters are varied? How to predict (in the presence of noise) qualitative changes in system's behaviour (stochastic perturbations) occurring at these equilibrium points?

The paper is organized into the following sections. Section 2 contains the model studied. Section 3 presents the dry-friction oscillator as a Filippov system. Section 4, is devoted to theoretical discussion and physical phenomena analyse. The conclusion is made in Sect. 5.

## 2 System description and modelling assumptions for stochastically perturbed sliding motion

Consider a non-deformable moving belt, moving with a constant velocity $V_1$, the block of mass $m_1$ moving in the lying flat surface and connected to a damping capacity C (or damping function $\Phi(x_1(t); \mu)$) and a fixed backing by an inclined linear spring of stiffness coefficient K, which is capable of opposing both tension and compression (see Fig. 1a). The block can either ride on the belt, with zero relative velocity with respect to it, or slip on it because friction is added as a constraint on a rough surface between the mass and the belt. We then suppose large displacements of the mass same as large deformations in continuum mechanics so that the

**(a)**



**(b)**
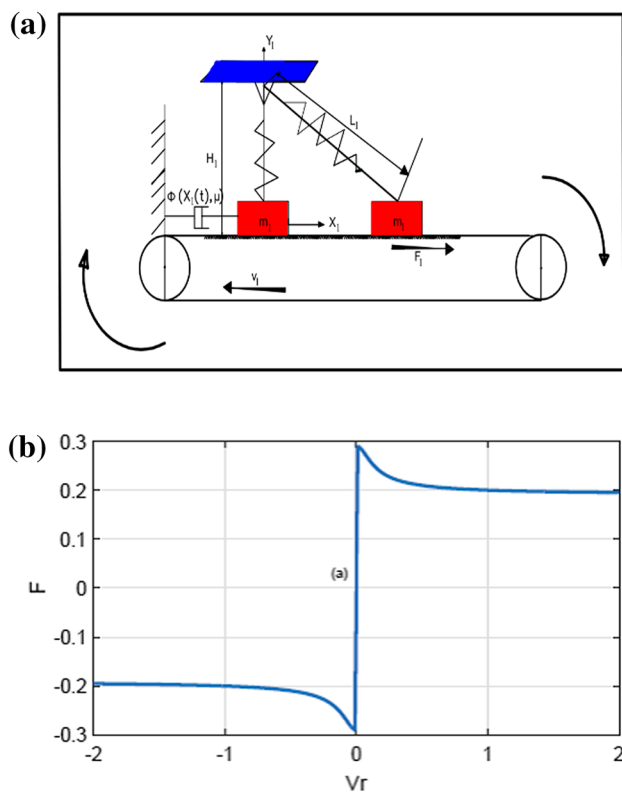


**Fig. 1** The mechanical model: **a** the "self-excited SD oscillator", **b** Coulomb friction Eq. 2 with $G_s = \mu\left(\left(g_1 - \alpha\left(1 - \frac{1}{\sqrt{x^2(t)+\alpha^2}}\right)\right) + C_1|x| + C_2|\dot{x}|\right)$ sgn $(\dot{x})$; $\psi\alpha = 0.1$; $g_1 = 2.0$; $\mu = 0.1$; $v_0 = 0.0$

system is strongly nonlinear. (Refs. therein). $X_1$ is displacement from the rest state. If there is also damping, restoring and external forces, the following equation is studied

$$m_1 \frac{d^2X_1(t)}{dt^2} + C\frac{dX_1(t)}{dt} + KX_1(t)\left(1 - \frac{L}{\sqrt{X_1^2(t) + L_1^2}}\right) + F_\mu$$

$$= F_e \cos(wt) + \xi(t) \tag{1}$$

$L_1$ and $H_1$ are respectively the spring's length and the distance between fixed point and belt, $F_\mu$ due to contact friction force. $\xi(t)$ is the normalized source of Gaussian white noise:

$$\langle \xi(t)\xi(t') = 2D\delta(t - t')\rangle,$$

$\langle \xi(t) = 0\rangle$ and

D—the noise intensity. The dry friction [22] force $F_\mu = G_s$ is due to the surfaces in contact and can be defined during the slip mode. The extended friction law is [23]:

$$F_\mu = -\mu\left(C_0 + C_1|x_1| + C_2|\dot{x}_1|\right) \text{sgn}(\dot{x}_1) \tag{2}$$

So that $x_1$ and $\dot{x}_1$ are respectively the sliding displacement, and correspondent velocity, $C_0$ is the vertical component of

the spring force, coefficients $C_1$ and $C_2$ are respectively the friction interface amplitude, with the correspondent velocity. $\mu$ stands to friction coefficient (equivalent to the static friction coefficient in general). Suppose the weight, $F_N = C_0$ is in the sense of the weight in the contact area assuming that the direction of $C_0$ always points down ($F_N > 0$) only if $Mg > KH_1$, i.e., the weight of the system. Hence:

$$F_\mu = Mg - KH_1\left(1 - \frac{L}{\sqrt{X_1^2(t) + H_1^2}}\right);$$

$$\mu = \begin{cases} \mu_k, & \frac{dx}{dt} = v_0 \\ \mu_s, & \frac{dx}{dt} \neq v_0 \end{cases} \tag{3}$$

$\mu$ is depending on $v_r = \dot{x} - v_0$, i.e., the vertical component of the spring force. The friction force $F_\mu = G_s$ modelled as Stribeck friction between objects in contact is described as

$$G_s = \mu\left(F_N + C_1|x_1| + C_2|\dot{x}_1|\right) \text{sgn}(\dot{x}_1);$$

and is determined by the material characteristics of the block and the belt. If the moving load acceleration is equal to zero, i.e. $\ddot{x}_1 = 0$ when the load sticks, with the belt velocity $\dot{x}_1 = v_1$, thus the value of the friction force

$$\left(G = -KX_1(t)\left(1 - \frac{L}{\sqrt{X_1^2(t) + H_1^2}}\right)C_1|x_1| + C_2|\dot{x}_1|\right),$$

is confined to the interval $(-G_{max} < G < G_{max})$. Knowing that

$$Gmax = \mu\left(Mg - KH_1\left(1 - \frac{1}{\sqrt{X_1^2(t) + H_1^2}}\right)C_1|x_1| + C_2|\dot{x}_1|\right),$$

is the total static friction force derived from the product of the friction coefficient with the normal force. Hence the Stribeck friction force $F_\mu$ of the system is illustrated in Fig. 1b. We have described the intermittent behaviour (or the set-valued extension) of the system in the differential inclusion of Filippov type as:

$$sgn(x_1) = \begin{cases} 1 & \text{if } x_1 > 0 \\ 0 \in [-1, 1] & \text{if } x_1 = 0 \\ -1 & \text{if } x_1 < 0 \end{cases} \tag{4}$$

The equation of motion Eq. (1) can be normalized using the non-dimensional procedure as follows: $x = \frac{X_1}{L_1}$; $w_0^2 = \frac{K}{m_1}$; $c = \Phi(x_1(t), \mu) = \frac{C}{m_{1w0}}$; $\tau = w_0 t$; $\alpha = \frac{H_1}{L_1}$; $v_0 = \frac{V_1}{L_{1w0}}$; $g_1 = \frac{g}{L_1 w_0^2}$. Then, substituting these variables into Eq. (1) we have:

$$\ddot{x} + c\dot{x} + x\left(1 - \frac{1}{\sqrt{x^2 + \alpha^2}}\right)$$
$$- \mu\big(C_0 + C_1|x| + C_2|\dot{x}|\big)\,\text{sgn}(\dot{x}) = a_m \cos(wt) + \xi(t),$$

$$(5)$$

where

$$C_0 = \left(g_1 - \alpha\left(1 - \frac{1}{\sqrt{x^2(t) + \alpha^2}}\right)\right);$$

and (·) represents the non-dimensional ratio of time $\tau$. Knowing that $c = \Phi(x_1(t); \mu)$. The slip and stick modes characterized the motion of the mass.

(F$\mu$): depends of the velocity $\dot{x}$, and displacement from the rest state x. The smoothness parameter $\alpha$. When $\alpha > 0$, the system is continuous and for $\alpha = 0$, the system nonlinearity is discontinuous. The dynamics of the SD oscillator has been investigated random domains.

The discontinuous case equation of motion of the (SD) Oscillator is given by:

$$\ddot{x} + c\dot{x} + (x - z\,sgn(x)) - d\,sgn(\dot{x}) = a_m \cos(wt) + \xi(t),$$

$$(6)$$

where $d = - \mu\big(C_0 + C_1|x| + C_2|\dot{x}|\big)$. At least one coefficient will be null in practical case. (One between $z$ and $d$ will be zero). Thus, for intermittent mode, "sgn(x)" and "sgn($\dot{x} - v_0$)", one could have the excited SD oscillator ($z = d = 0$), the dry friction models ($z = 0$; $d = 1$). Filippov [24] representation for the discontinuous SD oscillator is given by:

("The dynamical planar Filippov" system).

A solution of Eq. (7) should be continuously differentiable. If $c = \Phi(x(t); \mu)$, this equation describes many physical systems collectively called "SD oscillators".

## 3 System with friction

The stick–slip process occurs by pulling the system i.e. because of the variation of the position.

### 3.1 Generic "Filippov system" analysis

Consider $x \in R^n$, and $f^{(i)} : R^n \to R^n$, $i = 1, 2$, are sufficiently smooth. Let us suppose that the vector field is discontinuous along $\Sigma$,

$$x = \begin{cases} L + (x), & \text{for } x \in S_1 \\ L - (x), & \text{for } x \in S_2 \end{cases} \quad (8)$$

is defined in Fig. 2 (smooth vector fields L+, L−).

In order to better analyse the non-smooth dynamics, define the intervals as: $\Sigma = \{x \in R^n, H(x) = 0\}$, where H is a scalar indicator function

$$H_x(x) = \frac{\partial H(x)}{\partial x}$$

on the a hyper-surface $\Sigma$, (an unique surface of discontinuity: Mathematically, it is the "switching manifold"; physically it corresponds to zero velocity), then the system domain will be divided into three sub-spaces as:

$$F_1(x,\ \mu) = \begin{cases} \dot{x} = x_2, & x_2 - v_0 < 0 \\[2mm] \dot{x}_2 = -cx_2(t) - x_1(t)\left(1 - \dfrac{1}{\sqrt{x_1^2 + \alpha^2}}\right) \\[4mm] \quad - \mu\left(g_1 - \alpha\left(1 - \dfrac{1}{\sqrt{x_1^2 + \alpha^2}}\right) + c_1|x_1| + c_2|x_2|\right) & x_2 - v_0 < 0 \\[4mm] \quad + f_0 \cos(x_3) + \xi(t), \end{cases}$$

$$F_2(x,\ \mu) = \begin{cases} \dot{x} = x_2, & x_2 - v_0 > 0 \\[2mm] \dot{x}_2 = -cx_2(t) - x_1(t)\left(1 - \dfrac{1}{\sqrt{x_1^2 + \alpha^2}}\right) \\[4mm] \quad + \mu\left(g_1 - \alpha\left(1 - \dfrac{1}{\sqrt{x_1^2 + \alpha^2}}\right) + c_1|x_1| + c_2|x_2|\right) & x_2 - v_0 > 0 \\[4mm] \quad + f_0 \cos(x_3) + \xi(t), \end{cases}$$

$$(7)$$

**(a)**



**(b)**



**(c)**
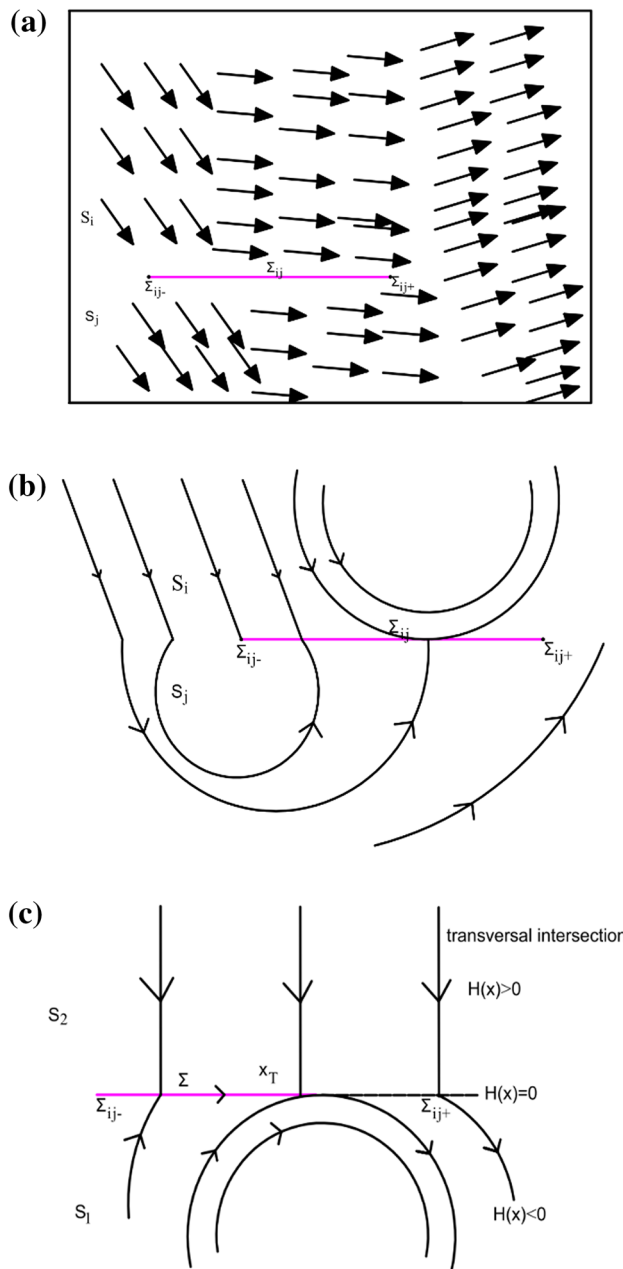


**Fig. 2** Filippov representation: **a** two vector fields $F_i$ and $F_j$ and an open $\Sigma_{ij}$ (up), of the corresponding trajectories (down, **b**). **c** Filippov' piecewise smooth system

$$S_1 = \{x \in R^n,\ H(x) < 0\};$$
$$S_2 = \{x \in R^n,\ H(x) > 0\}; \tag{9}$$
$$\Sigma = \{x \in R^n,\ H(x) = 0\},$$

The subspaces $S_{1;2}$ and *attracting* sliding occur in a region on $\Sigma$ obtained with the well-known convexification [25], we can construct the desired general solutions of (8).

Let $\beta_{ij}(x) = \langle H_x(x), L^{(+)} \rangle \langle H_x(x), L^{(-)} \rangle$, be a transversal intersection, $\Sigma$ in which $\langle .,. \rangle$ is the inner product in $R^n$. The crossing set $\Sigma_c \subset \Sigma$ is defined as $\Sigma_c = \{x \in \Sigma: \beta_{ij}(x) > 0\}$ i.e. the total of all points $x \in \Sigma$, the orbit of system (8) at these points crosses the separation area $\Sigma$ i.e., the orbit reaching x from $S_i$ concatenates with the orbit entering $S_j$, $i \neq j$, from x. the complement to $\Sigma_c$ in $\Sigma$: $\Sigma_s = \{x \in \Sigma: \beta_{ij}(x) \leq 0\}$, where at these points $x \in \Sigma_s$, the orbit of system (8) which reaches x does not leave $\Sigma$ and will therefore have to move along $\Sigma$. Since the vector field $H_x(x)$ determines the system flow along the barrier of separation, we have $H_\Sigma^T(x) = 0$, (In the sliding domain, T is a tangent point at the boundary. Both vectors H (i)(T) are non-vanishing values, but one of them is tangent to $H_\Sigma^T(x) = (0, 1)$: equilibria of the boundary, and singular sliding points) (See Fig. 2).

### 3.2 Numerical solution of "differential equations with switching conditions" in the case of Filippov

In the piecewise smooth system (8), L(x) is not well defined when x is on the discontinuity surface $\Sigma$. A way to define the vector field on $\Sigma$ is to consider the Filippov approach that is the set valued extension G(x) below:

$$\dot{x} \in G(x) = \begin{cases} L_+(x, \mu), & x \in S_1; \\ \overline{co}\{L + (x, \mu), L - (x, \mu)\}, & x \in \Sigma; \\ L_-(x, \mu), & x \in S_1 \end{cases} \tag{10}$$

where $(L_+(x); L_-(x))$ are given by the smooth functions, and $\overline{co}\{A\}$; is a vector field along the barrier of discontinuity, ("the closure of the convex hull"). It denotes the smallest closed convex set containing A.

$$\overline{co}\{L_+, L_-\} = \{L_G : x \in R^n \to R^n :$$
$$L_G = (1 - \alpha)L_+ + \alpha L_-,\ \alpha \in [0,\ 1]\};$$

then the system vector field can be described by a "differential inclusion" (systems with multi valued right-hand sides).

### 3.3 The convex approach of non-smooth dynamics

Talking about the nonlinear system with discontinuous right-hand side

$$\dot{x} = L(x) = \begin{cases} L + (x), & \text{for } v(x) > 0 \\ L - (x), & \text{for } v(x) < 0 \end{cases} \tag{11}$$

When x is on hyper-surface $\Sigma$ then $v(x) = 0$. In order to study the dynamics in the neighbourhood of the equilibrium set, the endpoints are studied separate from the other points of the equilibrium set [26, 27]. Mechanical systems with

set-valued friction, equilibrium sets will occur, generically when a system switches between two systems (suppose the intermittent behaviour of the friction force $G \equiv I$), then we form their convex combination as

$$\dot{x} = \begin{cases} L(x, \lambda) = \frac{l_+(x)+l_-(x)}{2} + \lambda \frac{l_+(x)-l_-(x)}{2} \\ \text{sgn}(v) & \text{(if } v \neq 0); \\ [-1; +1] & \text{(if } v = 0); \end{cases} \quad (12)$$

Thus $L(x; +1) \equiv L_+(x)$ and $L(x; -1) \equiv L-(x)$. The standard approach then seeks so-called sliding modes which satisfy "$\dot{x} = 0$ on $v = 0$".

## 4 Results and discussion

It is evident that a deep analysing of the role of non-smooth sliding process of our model is of crucial importance in the nature and many engineering cases. Friction processes upon geometrical nonlinearity with large deformations open new windows to observe "Tom's catastrophic Theory" in SD oscillator. We have computed Eq. (7) numerically to illustrate the theoretical predictions using fourth-order Runge–Kutta algorithm. In all the calculations we assume that: $c = 0.048$, $x_{fk} = 0.25$; $x_{fs} = 1.0$; $f_0 = 0.85$; $\alpha = 0.4$; $C_0 \neq 0$; $C_1 = C_2 = 0$; $\mu = 0.5$. Stick–slip effects in friction oscillators are very complicated. The asymptotic convergence (or divergence) properties of the trajectories of non-smooth systems are observed. Furthermore, we introduced a smooth function which approximates the discontinuous drift (see "Appendix").

The system exhibits different shapes of periodic windows follow by a sudden occurrence of chaotic responses certainly due from jumps that are characteristics of "grazing-sliding bifurcations".

Figure 3 shows the influence of friction coefficient in the dynamic of the system. We have observed the time histories and phase plane plots of the solution when varying friction Coefficients $\mu = 0.0$; $0.1$; $0.3$. The stick slips friction and limit cycle oscillation (LCO) are really identified in Fig. 3b, c. But, Fig. 3d, e, shows a segment of trajectory crosses the sliding region, enter into the slipping area and joins back the sliding surface. The stick and slip phases are consecutives. Thus, to verify directly the dynamical features of the motion patterns transition we focus at the statistic occurrence of sticking and sliding times, i.e., the distribution of time intervals the load spends in states $v = 0$ (sticking events) and $v \neq 0$ (the statistics of the sliding events). The transition value from stick to slip is reached at $G_s = \mu F_N$. The slip event finishes for $\dot{x}_2 = v_0$. Besides, we can count the same number of sticks and slips because the system response ends during a slip mode (Fig. 3d, e).

A random sequence alternating stick and slip events occur. When a stick starts, suppose the mass' position is known, and that the base speed is constant in time, the number of time intervals, or the instants at which stick consecutively slip occur can be estimated.

We consider the bifurcations under changes in the driving force and frequency.

From Fig. 4, both periodic and chaotic responses are presented. We observed an abrupt transition from the periodic to chaotic response and, afterwards, from the chaotic to the periodic effect. The presence of "grazing sliding bifurcations" may cause a sudden jump to chaos. It is also found that sliding dramatically change the characteristics of the frequency–response curve. From the smooth to discontinuous regime, periodic windows and chaotic responses are found. The possible structural changes of the asymptotic behaviour of the system under parameter variation, called bifurcations. A slight modification in a parameter value can give rise to a radical change in the system behaviour. When noiseless nonlinear dynamical system exhibits chaos phenomenon, the chaotic attractor is structurally unstable. Whereby, the periodic motions are found and occupy open sets in the parameter space (see Fig. 4c, d, e).

A special chaotic orbit exits for a fixed set of parameters that fills a finite area. It is follow by a series of islands dominated by different chains of fixed points. Therefore, through successive bifurcations where equilibriums and cycles are first links (see Fig. 4d, e) a transition from periodic to chaotic dynamics occurs. The shape and size of "random attractor" and "random saddle" can change under stochastic perturbation.

Figure 5a, b illustrates the influence of friction in the system. With the increasing of noise intensity, Fig. 5a shows a "hard bifurcation" i.e., Tom's catastrophic (due to "grazing-sliding bifurcations") that occur as parameters vary. Abrupt change involves a discontinuity of the steady state at the bifurcation point. The stationary measures provide the possible distributions of traditional trajectories. Their fixed backings are the perspective areas to typical trajectories in the long run. As usual in this case, there can be a lot of possibilities of stationary measure and more radical changes can occur in response to parameter varies. "Tom's Catastrophe" theory sufficed to be the basic to the study of qualitative dynamics. In some disciplines, mathematical models are efficient for the examination of dynamic behaviour of the system being modelled [28]. According to [29], because of the absence of little relationship between the shape variations of stationary probability density function and the random excitation, it is not easy to describe the true change of topological property of a stochastic system simply based on the shape change of stationary
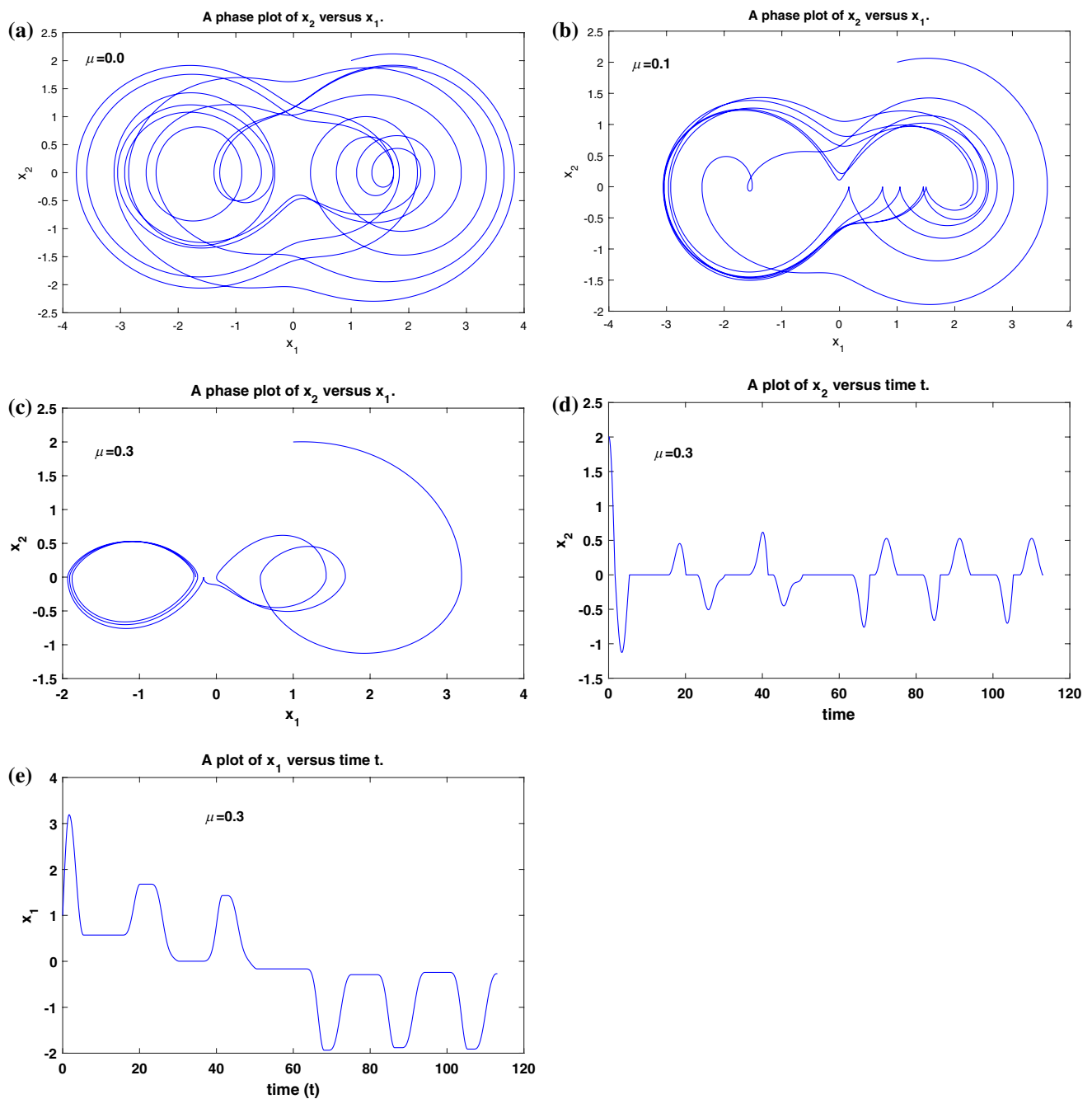
**Fig. 3** Sliding Filippov method: $c = 0.048$; $\alpha = 0.4$; $g_1 = 2.0$; $f_0 = 0.85$; $w = \frac{1}{3}$: **a** phase plane plot $\mu = 0.0$ no friction, **b** phase plane plot with friction, **c** limit cycle occurred in phase plane plot as friction increases, **d**–**e** dynamics at the transition from stick to slip

PDF. For multiple cycles, noise induces a special type of P-bifurcations.

As the noise intensity (or smoothness parameter) increases, peaks of the probability density function merge and multiplicity of cycle is appeared. While in Fig. 5b ($\mu = 0$), the appearance of p-bifurcation diminishes with the increases of noise intensity. In [30], an adjective "hard" is due to a loss of stability of an "invariant set". This

phenomenon is verified if the stability involves a discontinuous change; see Fig. 5a, c, e, f. The following changes can be identified in the PDF:

(1) Sliding bifurcations introduce "discontinuous transitions" between different motions. Hence, signatures of the stick–slip transition become dynamically possible above such a critical value.
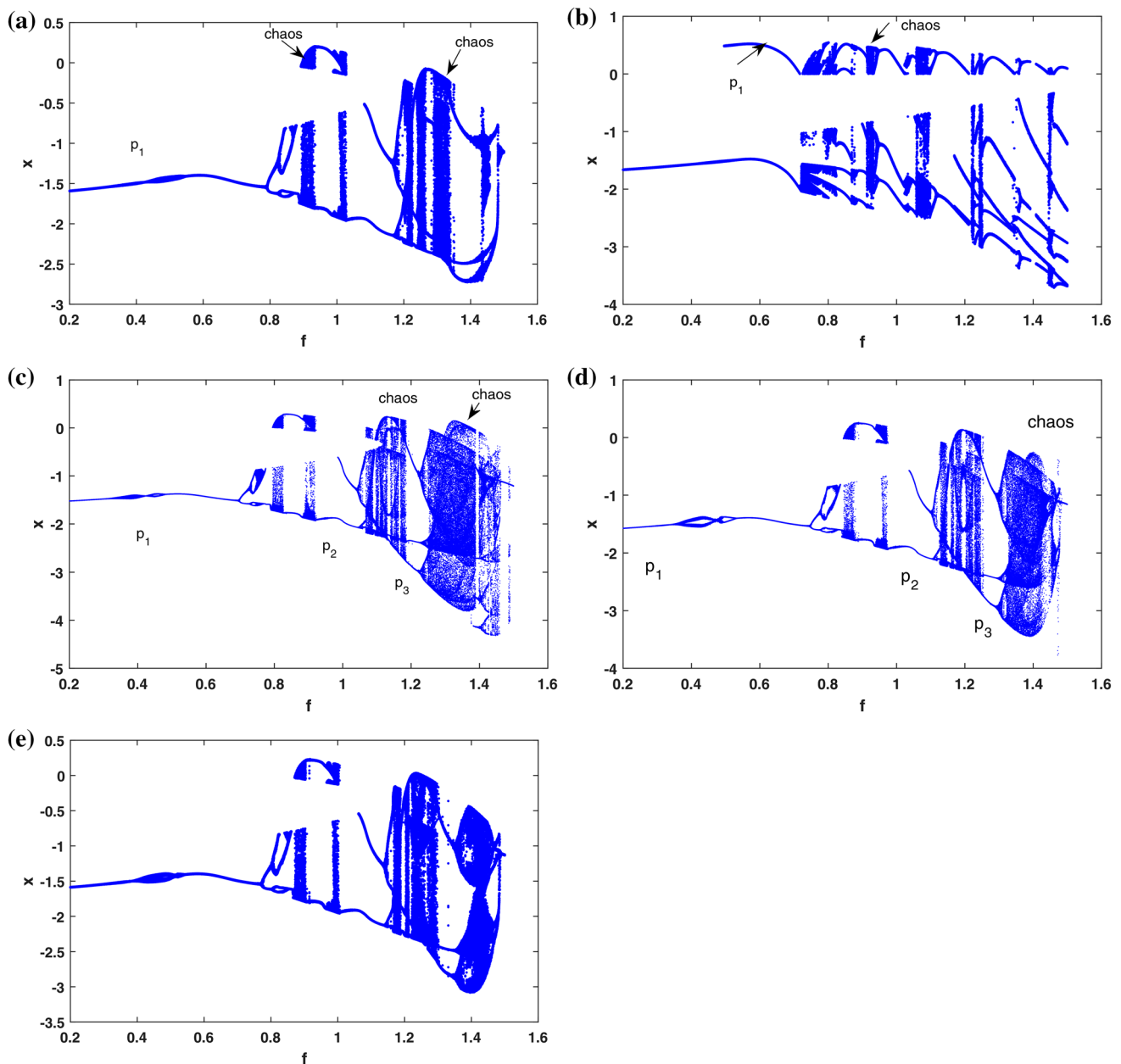
**Fig. 4** Bifurcation diagrams for displacement x versus f, ($x_0 = 1$; $y_0 = 0$), $c = 0.048$, $x_{fk} = 0.25$; $x_{fs} = 1.0$: **a** $\alpha = 0.4$, $C_1 \neq 0$, $C_2 = C_3 = 0$, **b** $\alpha = 0.0$, $C_1 \neq 0$, $C_2 = C_3 = 0$. **c** $\alpha = 0.4$, $C_1 \neq 0$, $C_2 = 0.45$, $C_3 = 0.5$; **d** $\boldsymbol{\alpha = 0.4}$, $C_1 \neq 0$, $C_2 = 0.015$, $C_3 = 0.25$; **e** $\boldsymbol{\alpha = 0.4}$, $C_1 \neq 0$, $C_2 = 0.0$, $C_3 = 0.25$

(2)  We are interested in possible changes equilibrium (maxima, minima) provides the asymptotic behaviour for large values of PDF.

(3)  Observation of jump effects due to the phenomenon of "grazing-sliding bifurcation".

(4)  "Catastrophic (or abrupt) transitions" occur characterized by discontinuous changes in system properties.

Hence, knowing that a system is functioning in one of its asymptotic regimes, is it possible that a slight variation of A parameter triggers a transient toward an abrupt different asymptotic regime? In this case, we say that a "catastrophic transition" occurs.

Figure 5 Shows that with a slight variation of noise to a family of non-smooth system unfolding a bifurcation can lead to a "hard bifurcation" of stationary density functions. We also observe here that, as friction coefficients increase, peaks number, consequently appearing of p-bifurcation (see Fig. 5d–f for μ = 0.1; 0.2; 0.3). Any parameter can change the behaviour of the system. That's why, Zeeman
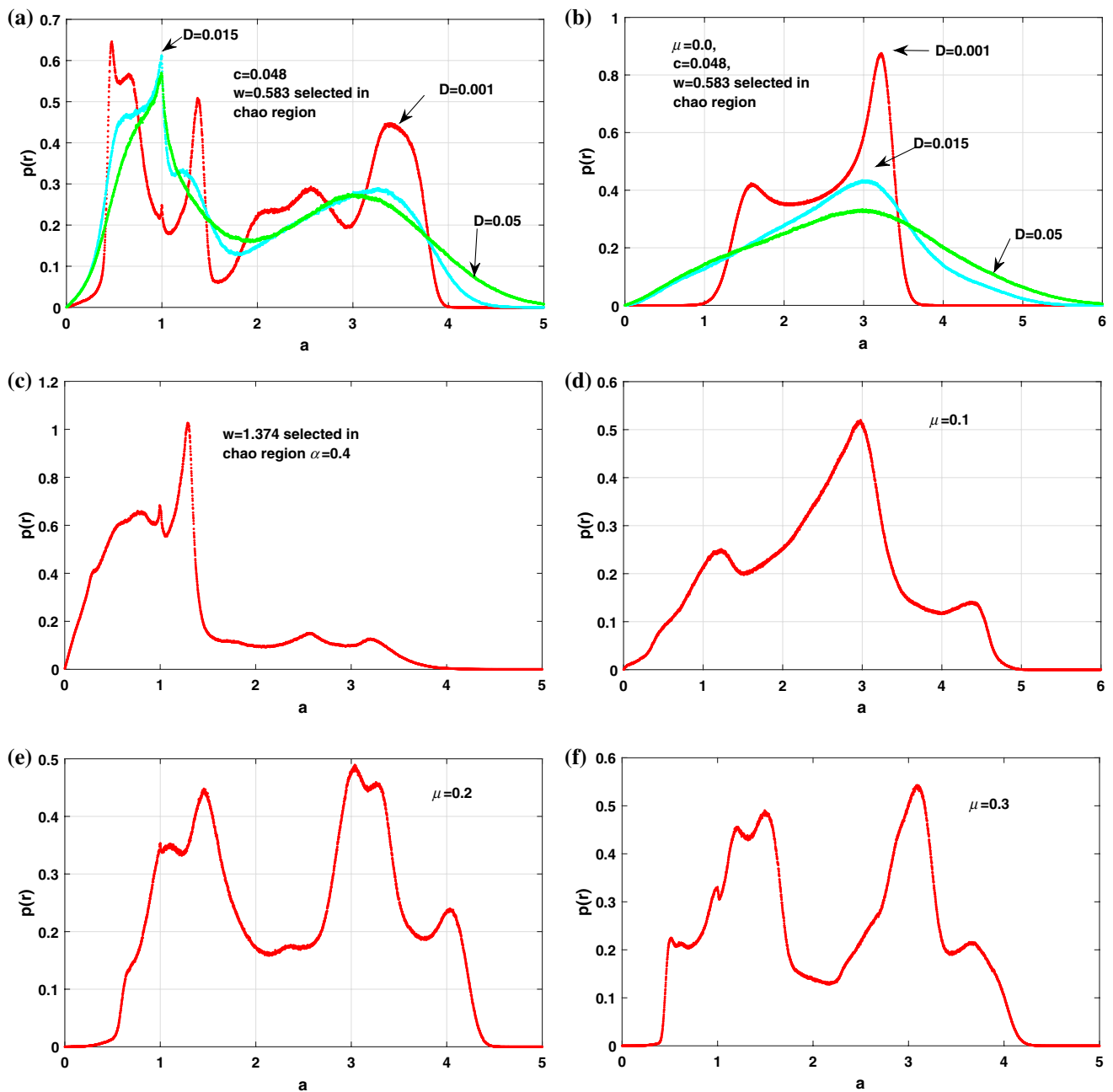
**Fig. 5** From Fig. 3a: stationary amplitude distribution for: $D = 0.001$; $c = 0.048$, $f_{01} = 0.85$, $C_1 \neq 0$, $C_2 = C_3 = 0$, **a** $\alpha = 0{:}4$, **b** $\alpha = 0.0$, **c** $\alpha = 0.4$, **d** $\mu = 0.10$, **e** $\mu = 0.2$, **f** $\mu = 0.3$

defined a bifurcation in a stochastic system as a "change in character of the density function as a parameter is varied" [31, 32]. Hence the phenomenological, or P-bifurcations.

Under parameter change, stationary measures of SD oscillator can illustrate abrupt changes. We observed a change in the number of stationary measures or a discontinuous change in one of their supports (see Fig. 6).

When increasing the damping coefficient c, Fig. 6a illustrates the increase in term of number of peaks and probability density function (PDF) as above. The same

observation is recognized in Fig. 6b, where the friction coefficients increase with the multiplicity of peaks number and height value of PDF. Another point of view is to cover a deep experimental analysis into the evolutionary behaviour of the "stochastic attractors" in SD oscillator. This may be importantly to understand the stochastic bifurcation in a nonlinear system with noise. In this paper, a "stochastic attractor" is chosen as an invariant for a noisy steady-state response, and the abrupt change of attribution (number, size, attraction) of a stochastic attractor and/or
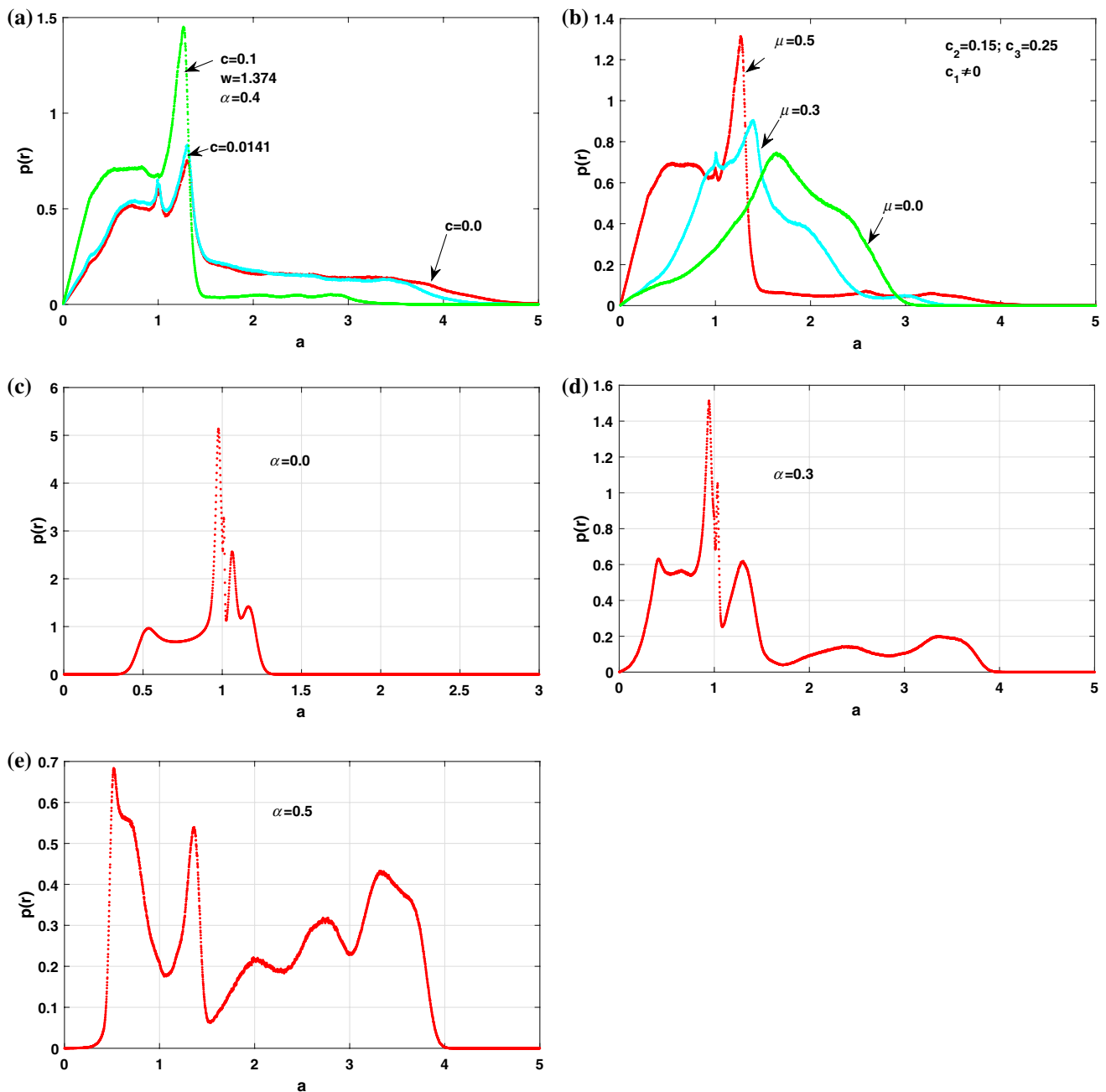
**Fig. 6** $\alpha = 0.4$; $f_{01} = 0:85$ (**a**) and vary values of damping $c = 0.0$; 0.0141; 0.1, $C_1 \neq 0$, $C_2 = C_3 = 0$ (**b**) $C_1 \neq 0$, $C_2 = 0.015$; $C_3 = 0.25$ and vary values of friction coefficient $\mu$; **c** $\alpha = 0.0$, **d** $\alpha = 0.3$; **e** $\alpha = 0.5$

a "stochastic saddle" provides a structural change of a stochastic system to demonstrate the bifurcation behaviour.

Figure 6c–e show the same observation of increasing of peaks number with the increase of the smoothness parameter $\alpha = 0.0$; 0.3; 0.5. The noiseless system of the SD oscillator undergoes a "pitchfork bifurcation" when the smoothness parameter $\alpha$ increases up to certain value. The stochastic P-bifurcation and the deterministic pitchfork bifurcation in the SD oscillator are related. Suppose $\alpha$ is tending to 0, the behaviour of the SD oscillator suddenly

becomes discontinuous. The speed flow goes through a jump when the system crosses from one side to another in the deterministic system.

This study shows the uncertainties associated with the possible future occurrence of abrupt events, called "catastrophic events". A non-linear approach to detect dynamical transitions and infer the causality behind events (Sliding bifurcation). These Figures try to detect and interpret the existence of multiple equilibriums and can sometimes fail in complex models. Moreover, we highlight promising

phenomena to detect abrupt effects and to obtain information about the mechanisms behind them.

We can summarize this subsection saying that, the shape of stationary PDF does not depend on the bifurcation parameter [33]. But, the stationary PDF does change its shape at a critical parameter value [34].

## 5 Conclusions

For "discontinuous systems" in Filippov case, the term bifurcation exists in literature with different definitions. They can be inconsistent with one another. The non-uniqueness of solutions is observed. A measure differential inclusion is able to describe discontinuities in the state. We recognize that dry friction is a nonlinearity which is abundant in nature. It presence can induced "self-sustained vibration". The sudden change in a slight variation of any parameter of the system is seems catastrophe, due to loss of stability of the system. This phenomenon occurs in non-smooth systems illustrated in a piecewise-smooth model of a SD oscillator Eq. (7). The slight variation of a parameter has created the "grazing-sliding bifurcations". The occurrence of "catastrophic bifurcation" transition phenomenon is characterized by discontinuous jumps in the equations across a phase space limit.

We were looking to the shape, size and stability of a "stochastic attractor" that may be taken as its character. Whenever the character of an attractor changes radically, there occurs the stochastic bifurcation. P-bifurcation is deemed to occur with a change in the structural behaviour of the probabilistic structure of the state variables.

## 6 Appendix

Due to the lack of continuity, we have construct a function $f_N(x)$ which has point wise convergence to the sign-function as $N \to \infty$.

$$F_N(x) = \begin{cases} 1, & \text{for } x > \frac{1}{N}; \\ \frac{-N^3 x^3}{2} + \frac{3Nx}{2} & \text{for } \frac{-1}{N} \leq x \leq \frac{1}{N}; \\ -1, & \text{for } x < \frac{1}{N} \end{cases}$$

We used $f_N(x)$ in order to avoid the discontinuous challenges by the sign function.

## Compliance with ethical standards

**Conflict of interest** The authors declare that they have no conflict of interest.

## References

1. Rong H, Meng G, Wang X, Xu W, Fang T (2004) Response statistic of strongly non-linear oscillator to combined deterministic and random excitation. Int J Non Linear Mech 39(6):871–878
2. Rajendiran S, Lakshmi P (2016) Simulation of PID and fuzzy logic controller for integrated seat suspension of a quarter car with driver model for different road profiles. J Mech Sci Technol 30(10):4565–4570
3. Huang Z, Zhu W, Suzuki Y (2000) Stochastic averaging of strongly non-linear oscillators under combined harmonic and white-noise excitations. J Sound Vib 238(2):233–256
4. Hinrichs N (1997) Reibungsschwingungen mit Selbst- und Fremderregung. VDIVerl., Duesseldorf
5. Horsthemke W, Lefever R (1984) Noise-induced transitions. Springer, Berlin
6. Tateno T (2002) Noise-induced effects on period-doubling bifurcation for integrate and fire oscillators. Phys Rev E (3) 65(2):021901
7. Arnold L (1998) Random dynamical systems. Springer, Berlin
8. Gulyayev V, Andrusenko E, Glazunov S (2019) Computer simulation of dragging with rotation of a drill string in 3D inclined tortuous bore hole. SN Appl Sci 1:126. https://doi.org/10.1007/s42452-018-0121-9
9. Li ZX, Cao QJ, Léger A (2016) Complex dynamics of an archetypal self-excited SD oscillator driven by moving belt friction. Chin Phys B 25:010502-1–010502-9
10. Cao QJ, Wiercigroch M, Pavlovskaia EE, Grebogi C, Thompson JMT (2006) Archetypal oscillator for smooth and discontinuous dynamics. Phys Rev E 74:046218-1–046218-5
11. Cao QJ, Wiercigroch M, Pavlovskaia EE, Grebogi C, Thompson JMT (2008) The limit case response of the archetypal oscillator for smooth and discontinuous dynamics. Int J Nonlinear Mech 43:462–473
12. Cao QJ, Wiercigroch M, Pavlovskaia EE, Thompson JMT, Grebogi C (2008) Piecewise linear approach to an archetypal oscillator for smooth and discontinuous dynamics. Philos Trans R Soc A 366:635–652
13. Burridge R, Knopoff L (1967) Model and theoretical seismicity. Bull Seismol Soc Am 57:341–371
14. Carlson JM, Langer JS (1989) Mechanical model of an earthquake fault. Phys Rev A 40:6470–6484
15. Sergienko OV, Macayeal DR, Bindschadler RA (2009) Stick–slip behaviour of ice streams: modelling investigations. Ann Glaciol 50:87–94
16. Li B (2007) Analysis of non-smooth dynamics of brake system with dry-friction. MS thesis, Tianjin University, Tianjin. **(in Chinese)**
17. Rui-Lan T, Qi-Liang W, Zhong-Jia L, Xin-Wei Y (2012) Dynamic analysis of the smooth-and-discontinuous oscillator under constant excitation. Chin Phys Lett 29(8):084706
18. Cao Qingjie, Léger Alain, Wiercigroch Marian (2017) A smooth and discontinuous oscillator theory, methodology and applications. Springer, Berlin
19. von Kluge PN, Djuidjé Kenmoé G, Kofané TC (2015) Dry friction with various frictions laws: from wave modulated orbit to stick–slip modulated. Mod Mech Eng 5:28–40
20. Simpson DJW, Kuske R (2014) Stochastic perturbations of periodic orbits with sliding. arXiv: 1404.6845v1 [math.DS]
21. Jeffrey MR, Simpson DJW (2013) Non-Filippov dynamics arising from the smoothing of nonsmooth systems, and its robustness to noise. arXiv: 1310.8328v1 [math:DS]
22. Anderson J, Ferri A (1990) Behavior of a single-degree-of-freedom-system with a generalized friction law. J Sound Vib 140(2):287–304

23. Danca MF, Lung N (2013) Parameter switching in a generalized Duffing system: finding the stable attractors. Appl Math Comput 223:101–114
24. Filippov AF (1988) Differential equations with discontinuous right-hand sides. Kluwer Academic Publication, Dortrecht **(Russian 1985)**
25. Utkin VI (1992) Sliding modes in control and optimization, vol 116. Springer, Berlin
26. Leine RI, Nijmeijer H (2013) Dynamics and bifurcations of non-smooth mechanical systems, vol 18. Springer, Berlin
27. Santhosh B, Narayanan S, Padmanabhan C (2014) Numeric-analytic solutions of the smooth and discontinuous oscillator. Int J Mech Sci 84:102–119
28. Kerschen G, Worden K, Vakakis A, Golinvala J (2006) Past, present and future of nonlinear system identification in structural dynamics. Mech Syst Signal Process 20:505–592
29. Meunier C, Verga AD (1988) Noise and bifurcation. J Stat Phys 50(2):345–375
30. Arnold VI, Afrajmovich VS, Yu S, Il'yashenko Y, Shil'nikov LP (1999) Bifurcation theory and catastrophe theory. Springer, Berlin
31. Zeeman EC (1988) Stability of dynamical systems. Nonlinearity 1(1):115–155
32. Zeeman EC (1988) On the classification of dynamical systems. Bull Lond Math Soc 20(6):545–557
33. Baxendale P (1986) Asymptotic behavior of stochastic flows of diffeomorphisms. In: Ito K, Hida T (eds) Stochastic processes and their applications. Lecture notes in mathematics, vol 1203. Springer, Berlin, pp 1–19
34. Crauel H, Flandoli F (1998) Additive noise destroys a pitchfork bifurcation. J Dyn Diff Equ 10:259–274

# Colliding solids interactions of earthquake-induced nonlinear structural pounding under stochastic excitation

P. Ndy Von Kluge [a,*], G. Djuidjé Kenmoé [a,b], T.C. Kofané [a,b]

[a] *Department of Physics, Mechanics Laboratory, Faculty of Sciences, The University of Yaoundé I, P.O. Box 812, Yaoundé, Cameroon*
[b] *The African Center of Excellence in Information and Communication Technologies (CETIC), Yaoundé, Cameroon*

| A R T I C L E   I N F O | A B S T R A C T |
|---|---|
| *Keywords:*<br>Structural pounding<br>Contact-impact events<br>Earthquakes<br>Coefficient of restitution | A simplified analysis model of structural pounding, used in the study of the effects of earthquakes subjected to Gaussian white noise of relatively high intensity, filtered through a Kanai-Tajimi filter is proposed in this investigation. The required distance to avoid pounding is important in structural engineering. As a consequence of frictional contact phenomena, energy is dissipated and the state of a system can change slowly and rapidly, depending on the nature of the contact, continuous or impact condition. Buildings without enough separation often create structural pounding under seismic events. Other effects associated with friction in mechanical systems are the vibration and noise propagation of the system components, nonlinear systems behavior and wear. In this paper, we prove that because of the inherent stochastic nature of the applied earthquake loads or the uncertainty arising from randomness (non-smooth behavior), stochastic p-bifurcations occur at law noise intensities and disappear when increasing noise intensities. Because of the presence of both impact-friction events, p-bifurcations should be observed at weak noise intensities. P-bifurcation occurs and created instability that will increase pounding effects. Some relationship between impact-friction events appears: small noise intensity occurs when the time of friction (continuous) is greater than the impacting events, hence high probability density function (PDF). But if the noise intensity increases, the impact events are great (small friction) with weak PDF. But successive jump effects can create noisy system and great impact. The models stochastic processes of stationary probability density function (PDF) of the earthquake ground motion are set up. The demonstrative application examples which include friction in systems involving contact-impact events are illustrated in Central Africa, a part of Congo Stable Block. |

## 1. Introduction

This study focuses on the dynamic behaviour of a spillway reinforced concrete building colliding with the abutment and how it responds to earthquake induced excitation. The efficient analysis of nonlinear systems subject to evolutionary excitations [1] has always been in the general area of structural dynamics, an interesting and challenging branch. Nonlinearities in the structure are to be considered when the structure enters into inelastic range during devastating earthquakes. For dynamic inelastic analysis, researchers tend to adopt simplified non-linear static procedures instead of rigorous non-linear dynamic analysis when evaluating seismic demands. This is due to the problems related to its complexities and suitability for practical design applications.

Talking about non-smooth dynamical systems, the main instances in

mechanics are multibody systems with Signorini's unilateral contact, the Coulomb-like friction [2] and impacts, or ideal plasticity, fracture or damage in continuum mechanics. Under the action of earthquakes most of the investigations emphasized the deterministic aspect of the problem. The earthquakes are stochastic events, hazardous phenomenon due to insufficient clear spacing often called pounding effects and noise due to internal friction of colliding bodies could include either architectural or severe structural damage in both spillway structures and bridges, dam during strong ground motion vibrations.

Despite an extensive previous research [3–5], there are still many open questions; based on the statistical information about the uncertainty of some relevant parameters or knowledge about the inherent stochastic nature of the applied earthquake loads, pounding may cause both architectural as well as structural damages and, in some cases, it may lead to collapse of the whole structure. To predict the behavior of a

real system with a possibility of different disturbances existence need carefully understanding under certain type of excitations. Within the earthquake energy input, a rational estimation of the maximum impact force would help us to control the extent of damages in different structures, stick-slip friction.

Due to the random character [6,7] of earthquake ground motions, caused by the many influence factors, such as focal source mechanism, epicentral distance, focal depth and (variations in) geology along energy transmission paths, it is chosen to use in this research, Gaussian white noise excitation. Because the measurement instruments (seismographs) can be regarded as Spring-mass damper system. Furthermore, noise contamination occurs. The statistical characteristics of the stochastic model represent the key features of ground motions (i.e., ground motion intensity, duration, and frequency content) that are important for determination of structural response and estimation of damage induced from earthquakes. The problem of predicting appropriate ground motions for future seismic events is currently receiving a great deal of attention in the engineering community [8–10]. Engineers use seismic ground motions for a variety of reasons, including seismic hazard assessment and estimation of nonlinear structural response history.

During the whole time of impact, friction between the colliding members takes place and this effect is especially important in the case of rough surfaces considering Dimitrakopoulos [11] proposed a novel non-smooth rigid body approach to analyze the seismic response of pounding skew bridges which involve obliquely frictional multiple contact phenomena.

The use of non-smooth system theory to predict and understand the kinematics of colliding rigid bodies in the presence of impacts and friction is a useful commodity in engineering in particular and research of such systems in general. Usually non-smooth dynamical systems are represented as differential inclusions, complementarity systems, evolution variational inequalities, each of these classes itself being split into several subclasses. Under certain type of excitations, the dynamic response of a system depends on the nature of the induced excitation. (Characteristics of ground excitations having various peak ground accelerations, together with the dynamic properties of structures, are potentially the most important factors affecting the seismic response behaviour). Response analysis of building structures under random dynamic forces, such as earthquake, wind, and blast loads and others natural hazard phenomena are responsible to induce excitation. In this paper, the external earthquake excitation is used.

In the case of earthquake loading the ground excitation of the structure is determined not only by the geological properties along the path of wave propagation from the source to the structural site and the properties of the local site, but also by the stiffness ratio between the structural footing (pier) and the supporting ground. The embedment of the footing and the interface between piers and subsoil can also alter the characteristics of the incoming waves and consequently the ground excitation of the system.

It has been shown that most of the energy which is dissipated during impact is lost during the approach period of collision and a comparably small amount of energy is lost during the restitution period due to friction [12].

In this research, for reasons of simplicity, it is assumed that the external excitation (earthquake) interacts with rough noisy system.

The paper is organized as follows. In section 2, we discuss the analytical contact force models proposed in the literature are briefly recalled. Section 3. The practical study of seismic vulnerability in the southern plateau area of Cameroon. Section 4. Presents the numerical results and discussion. Conclusions are drawn in section 5.

## 2. Analytical contact models proposed in the literature and problem formulation

### 2.1. General formulation

James H. Dieterich et al. [13], described the phenomenon to model the friction between the crustal plates of Earth. J. R. Rice et al. [14], have analyzed a special friction model in the stability of tectonic sliding. The model has also been used in connection with control, see James R. Rice et al., [15]. Due to discontinuities in soil conditions along the propagation earthquake excitation, there are both evident randomness and strong nonlinearity owing to the evaluation norms of seismic intensity but also the site soil classification. A realistic analysis and design of structural systems subjected to such earthquake excitations must account for the uncertainty arising from randomness, impact and friction.

Let us consider an n-degree-of-freedom nonlinear structural system governed by eq. 1

$$m_1 \frac{d^2 q(t)}{dt^2} + c_1 \frac{dq(t)}{dt} + k_1\, q(t) = f(t) \qquad (1)$$

In which $m_1$ is the mass matrix or consistent $c_1$, is a viscous damping matrix (which is normally selected to approximate energy dissipation in the real structure) and $k_1$ is the static stiffness matrix for the system of structural elements. Forces $f(t) = p_j(t)$ acting on each point mass $m_j$ has a resisting force $f_s$, and the damping force $f_d$ acting against them. Newton's second law of motion gives for each mass: $(p_j - f_{sj} - f_{dj} = m_j \ddot{u}(j)$ or $m_j \ddot{u}(j) + f_{sj} + f_{dj} = p_j(t))$. Where $m_j \ddot{u}$ is the inertia force and the damping force $f_d$ is related to the velocity $\dot{u}$ across the linear viscous damper.i.e. $(f_d = c_1 \dot{u}; f_s = k_1 u, k_1$ is the lateral stiffness of the system).

The column $q(t) = u(t)$ represents the degrees of freedom of the system. The first and second derivative of the column $q(t)$, with respect to time t, are $\dot{q}(t)$ and $\ddot{q}(t)$, respectively. The column $f(t)$ denotes the external excitation of the system with intermittent characteristics due to friction. The mass is able to move or vibrate in one direction, perpendicular to the column. As the vibration of the structure diminishes in amplitude as the excitation finishes, rather than continuing to oscillate.

It is considered to have certain amount of damping, $c_1$ [16,17], see Table 1.

The dependency on time (t), will be omitted in this paper. while earthquakes are recurrent and aperiodic on a continuum time scale, the stick-slip of spring-block oscillations has mostly been periodic on a short time scale (see Fig. 1). In this research, the excitation exists of gravity; earthquake ground motion and noise due to friction. The relatively complex phenomenon of friction has a discontinuous behaviour caused by the fact that the friction force always opposes the relative velocity between two contacting surfaces which are subjected to friction. Then, friction may be a function of the relative velocity during sliding. Furthermore, dynamic effects, such as pre-sliding and varying breakaway level, may be present.

### 2.2. Non-linear viscoelastic model: numerical modeling of colliding structures to estimate the induced pounding forces

The proposed model is a nonlinear spring following the Hertz law of contact [18]. An other complex phenomenon involving plastic deformations at contact points is structural pounding. It causes local cracking or crushing, fracturing due to impact, friction, etc. Forces created by collisions are applied and removed during a short interval of time initiating stress waves which travel away from the region of

**Table 1**
Damping ratios of the fixed-base eigen frequencies of the dynamic model.

| mode no. | 1 | 2 | 3 | 4 | 5 | 6 and higher |
|---|---|---|---|---|---|---|
| Eigen frequency [Hz] | 0.46 | 1.27 | 1.98 | 2.98 | 4.10 | 4.25 and higher |
| damping ratio [−] | 0.03 | 0.04 | 0.05 | 0.06 | 0.08 | 0.10 |
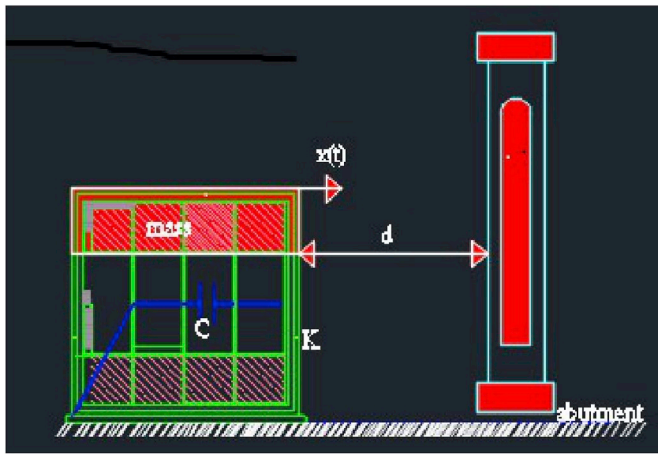
**Fig. 1.** Model of a spillway which interacts with an abutment.

contact. The process of energy transfer during impact is highly complicated which makes this type of problem difficult in the mathematical analysis. In general, to calculate impact force during contact we use the formula:

$$F_{im}(t) = k_{st}\,\delta^n(t) + c_{im}\dot{\delta}(t) \tag{2}$$

such that $k_{st}$ represents the stiffness of impact, $\delta$ represents the relative displacement, $\dot{\delta}$ represents the relative velocity, and $c_{im}$ denotes the damping coefficient. For $n = 1$, we are talking about linear systems, but in this paper, $n = 1.5$ because of nonlinear systems. We should obtain $k_{st}$ by iteration of experimental and numerical simulation of the peak pounding force. And then $c_{im} = 2\zeta_{im}\sqrt{k_{st}\sqrt{\delta(t)}}\,m_e$ for nonlinear systems. Where $m_e = \frac{m_1\,m_2}{m_1\,+m_2}$; $m_i$ (i=1, 2): masses of colliding structures. The deformation $\delta(t)$ is expressed as $\delta(t) = x(t) - d$ where $d$ is the initial separation gap between the spillway and the abutment and $x(t)$ is the displacement of the spillway.

### 2.3. The law of the conservation of momentum and Newton's collision rule govern each collision between two masses

Let us consider for example the collision between $m_1$ and $m_2$. Suppose $v_i$ and $v_i^+$ to be the velocity just before and just after the impact between the masses, respectively. Therefore, Newton's collision rule implies that

$$v_1^+ - v_2^+ = -\varepsilon(v_1 - v_2) \tag{3}$$

where $\varepsilon$ is the coefficient of restitution. It can be obtained from that eq. (4).

$$\varepsilon = \frac{v_2^+ - v_1^+}{(v_1 - v_2)} \tag{4}$$

The case of a fully elastic collision is $\varepsilon = 1$. Hence $\varepsilon = 0$ represents a fully plastic one. The rule of conservation of momentum determines the velocities just after the collision:

$$m_1\left(v_1^+ - v_1\right) = m_2\left(v_2 - v_2^+\right) \tag{5}$$

A collision between $m_1$ and $m_2$ happens when $x_1 \geq x_2$ and $v_1 > v_2$. In this case, the post-collisions velocities are

$$v_1^+ = v_1\frac{m_1 - \varepsilon\, m_2}{m_1 + m_2} + v_2\frac{1 + \varepsilon}{m_1 + m_2} \tag{6}$$

and

$$v_2^+ = v_1\frac{m_1(1 + \varepsilon)}{m_1 + m_2} + v_2\frac{m_2 - \varepsilon\, m_1}{m_1 + m_2} \tag{7}$$

The state variables of the system are represented by the position and velocity of each mass. Friction between the colliding bodies takes place during the whole time of impact. For the reasons of simplicity, in the model, during the restitution period the minor energy loss is neglected. The pounding force during impact, F(t), for that type of impact element is expressed as

$$F(t) = \begin{cases} \zeta_1\delta^{\frac{3}{2}}(t) + c_1(t)\dot{\delta}(t), & \text{if} \quad \dot{\delta}(t) > 0 \text{ (approach period)}; \\ \zeta_1\delta^{\frac{3}{2}}(t) & \text{if} \quad \dot{\delta}(t) \leq 0 \text{ (restitution period)} \end{cases} \tag{8}$$

where $\zeta_1$ is the impact stiffness parameter, $c_1(t)$ is the impact elements damping. The equation of motion is written as in eq. (1) above including the impact force term, and the friction force term.

We recognize that the equation of motion for a single degree of freedom (SDOF) system under seismic action is generally expressed as:

$$m\ddot{u} + c\dot{u} + ku = -m\ddot{u}_g \tag{9}$$

$\ddot{u}_g$ denotes the ground acceleration: horizontal motion of bedrock. The bedrock acceleration is related to the earth surface motion through the above differential equation.

u: vector of all translational and rotational degrees-of-freedom relative to earth surface. We can divide eq. (9) by the mass, m, it results

$$\ddot{u} + 2\varsigma w_n\dot{u} + w_n^2 u = -\ddot{u}_g \tag{10}$$

which demonstrates that the response of a system due to an earthquake induced ground acceleration only depends on the natural frequency, $w_n$, of the system and its critical damping ratio, $\varsigma$. The dynamic effects of the sublayer deposit are specified by a Kanai-Tajimi filter with the parameters $\varsigma$ and $w_n$. $\{\ddot{u}_g (t), t \in [0,\infty]\}$ is modelled as a modulated Wiener process

$$\ddot{u}_g dt = \beta(t)dB(t) \tag{11}$$

$\beta(t)$ is a deterministic intensity function.

$\{B(t),\ t \in [0, \infty]\}$ is a unit Wiener process, which is a Gaussian process with the incremental properties.

$$E\left[dB(t)\right] = 0, \qquad E\left[dB(t_1)dB(t_2)\right] = \begin{cases} 0, & t_1 \neq t_2; \\ dt, & t_1 = t_2. \end{cases} \tag{12}$$

Appearance of the resonant effect is in an amplification of ground motions, which can be as large as a factor ten relative to the rock sites [19] at different frequencies between 0.3 to 15 Hz.

Let us consider a simplified model of structural pounding as illustrated in Fig. 1, used in the study of the effects of earthquakes [20] defined by the second order equation

$$2\ddot{x} + 4.1\dot{x} + 210.125x + v(x,\ \dot{x}) + F_f - e(t) = \xi(t) \tag{13}$$

Parameters of interest in earthquake analysis, are relative displacement and velocity, and total acceleration, which is simply the sum of relative plus ground accelerations: $\ddot{x}_T (t) = \ddot{x}_g(t) + \ddot{x} (t)$.

Knowing that Newton's second law of motion gives for each mass: $(m_j\ddot{u} (j) + f_{sj} + f_{dj} = m_j\,\ddot{x}_g(t))$. Where $m_j\,\ddot{u}$ is the inertia force and the damping force $f_d$ is related to the velocity $\dot{u}$ across the linear viscous damper i.e. $(f_d = c_1\dot{u}; f_s = k_1u, k_1$ is the lateral stiffness of the system). (See eqs. (9) and (10)). A system consists of a mass $m_1 = 2$ kg (for instance), a frame (or spillway's spans) that provides stiffness to the system for example $k_1 = 210.125$, and a viscous damper that dissipates vibrational energy of the system $c_1 = 4.10$. Each structural member contributes to the inertia (mass), elasticity (stiffness of flexibility), and energy dissipation (damping) properties. These properties can be considered as separate components (mass component, stiffness

component, viscous component) [21]. For an inelastic system, $v(x, \dot{x})$, is incorporated in the equation. When using Newton's second law (see eq. (1)), we deduced eq. (13) including the impact force term, and the friction force term. Moreover, in eq. (13), $v(x,\dot{x})$ represents the pounding force which is equal to zero if $x(t) < d$ (d is an initial separation gap). It is illustrated by eqs. (2) and (8) when $x(t) > d$, where deformation $\delta(t)$ is expressed as $\delta(t) = x(t) - d$. We denote $c_1 = 4.10$ the damping, $k_1 = 210.125$ the stiffness coefficients. $t \in [0,3]$ the displacement time history of the spillway, with $e(t) = 2sin(14t)$ where the external force is acting on the system with a certain frequency, $w = 14$ Hz, and the maximum amplitude of the force is $p_0 = 2$. $v(x,\dot{x})$ is given by the knowledge of peak impact force during collisions and frictions.

The friction can be expressed as:

$$F_f = -\mu N \text{sgn}\left(\dot{x}_1\right).$$

where $\mu$ is the coefficient of sliding friction, N is the weight of elements in friction

$$\left(N = \sum_{i=1}^{n}\left(m_i g\right)\right).$$

$\xi(t)$ is the normalized source of Gaussian white noise:

$$\langle \xi(t)\xi(t^{'})\rangle = 2D\delta(t - t^{'}),$$

$\langle \xi(t)\rangle = 0$ and $D -$ the noise intensity.

The equation of motion is written including the impact force term, $v(x\dot{x})$, force between two masses

$$v(x, \dot{x}) = \begin{cases} 0 & \text{if } x < \nu; \\ c(x - \nu)^{\frac{3}{2}} + 1.98\sqrt{2c}\,(x-\nu)^{\frac{1}{4}}\dot{x} & \text{if } x > \nu, \ \dot{x} > 0 \\ c(x - \nu)^{\frac{3}{2}} & \text{if } x > \nu, \ \dot{x} < 0; \\ c = 2.47e\,10^6 & \nu = 0.005 \end{cases} \quad (14)$$

$\nu$ is the Poisson's ratio of the soil. Recall that the deformation $\delta(t)$ is expressed as $\delta(t) = x(t) - d$ where $d$ is the initial separation gap between the spillway and the abutment. Moreover eq. (14) denotes the pounding force as eqs. (2) and (8) [22]. It is a discontinuous nonlinear contact-impact term with friction. This impact force between the spillway and the abutment will be our concerned in the numerical simulation.

As is the case for most forced vibration problems, the diffusion vector e(t) is independent of the state vector x. Then the associated *Itô* and Stratonovich differential equations of the problem are equivalent.

## 3. The practical study of seismic vulnerability in the southern plateau area of Cameroon

The ground generally descends from north towards south at an elevation varied between 400 m and 700 m above the Atlantic Ocean level. No seismic study has been carried out since the following analysis. The southern plateau area of Cameroon is a part of Congo Stable Block. Tectonic features in the region mainly comprise folds and faults striking in a generally $NE - SW$ direction. A major fault (Ntem Fault) runs in $NE -SW$ direction at some 500 m downstream of the proposed dam site. It controls the flow of Ntem river, making the Ntem course bended from northwest to southwest and forming a waterfall of 35 height near the faulted zone, then linearly traced to the "Gorge Du Ntem" about 40 km. Several faults are encountered at Ntem Fault that generally strike $NE30 \sim 40$, dip northwesterly at an angle of $50 \sim 60$, each of limited fractured zone. They are filled with breccia and cataclasite and are well cemented with fair behavior. It might be formed at Mesozoic era to Eogene period. Given the terrain feature and earthquake history, Ntem Fault is

considered to be passive.

Since seismic network was built in Cameroon in 1984, there have been in our knowledge only six unfelt events that were recorded. Earthquake data of the area bounded by latitude $(N - 4.33)$ degrees to $(S - 0.33)$ degrees and longitude $(E-8.25)$ degrees to $(E-12.25)$ degrees was searched by international seismological center (ISC) in United Kingdom by the request of JICA study team, which indicate no earthquake that may affected to the project site was found out from the ISC historical events in the period of 1904–1990 and ISC comprehensive catalogue in the period of $1964 - 1988$. According to Seismicity of West Africa [23], Ambrasey and Adams studied seismic data near some important projects area. As shown in Table 2 and Fig. 5 illustrated, only three events are depicted in the report which might be affected to these projects site.

Where (*) M, Magnitude(assumed); r, Distance from the epicenter of earthquake to the site in kilometer, so that I, Intensity by modified Mercalli Scale theoretically calculated for the site

$$I = 8.0 + 1.5\,M - 2.5lnr \quad (15)$$

(by Cornell [24]).

Hence Ah, Acceleration in $cm/sec^2$ theoretically calculated

$$Log\,(Ah) = 0.014 + 0.30\,I \quad (16)$$

(by Trifunac and Brady [25]).

The analysis for an earthquake coefficient based on the relation between intensity felt at the site as above listed and frequency of occurrence (Nc) in the period for 100 years and 250 years by ISC method, Japan Meteorological Agency (JMA) method and Munich Reinsurance (M.R.) company. The results of the analysis are calculated and summarized as shown in Table 3.

From the above calculated, the earthquake coefficient ($k = gal/980$) is resulted as $k = 0.0006$ say; $k = 0.01$ for the return period of 100 years and $k = 0.03$ for 250 years respectively. The value of $k = 0.01$ is the proposed earthquake coefficient for the Nachtigal Amont Hydropower project locating some 350 km northeast of Memve'ele project site.

As defined in American Regulation No. $ER1110-2-1806$, Operating Basic Earthquake (OBE) is an earthquake that can reasonably be expected to occur within the service life of the project, that is with 50-percent probability of exceedance during the service life. (This corresponds to a return period of 144 years for a project with a service life of 100 years). For conservative design, OBE is currently recommended to be 0.03$g$ (corresponding to a return period of 250 years as calculated in 1993) and MCE to be double of OBE, i.e. 0.06$g$ for Memve'ele hydroelectric project.

To sum up, Memve'ele hydroelectric power development project is tectonically and seismologically located on a stable block. Therefore, full-scale validation (monitoring) of structural response through recorded wind and earthquake excitation is important. The non-smooth properties can be exploited to design new mechanical devices. As suggested in this work it opens up the possibility of, for example, fast limit switches and energy transfer mechanisms.

## 4. The numerical results and discussion

### 4.1. Numerical solution of the case study

For piecewise-smooth systems it is important to record the

**Table 2**
Historical earthquakes near the project area.

| Date | Epicenter | M(*) | r; DIS(*) | I; INT(*) | Ah; ACC* |
| --- | --- | --- | --- | --- | --- |
| 1903 *June* 10 | 3N10.0E | 4.4 | 79.4 | 3.7 | 13.0 |
| 1911 *March* 26 | 3.1N11E | 5.7 | 119.3 | 4.6 | 24.8 |
| 1913 *October* 9 | 3.8N12.3E | 5.1 | 280.0 | 1.6 | 3.1 |

**Table 3**
Calculation of earthquake coefficient.

| Return Period | ISC method(i) | JMA method(ii) | M.R.(i) |
|---|---|---|---|
| 100 *years* | 2.5(= 5.8gal) | I − II(2.5gal) | … |
| 250 *years* | 4.0(= 16.4gal) | III(= 14gal) | 5 or blow ( < 32.7gal) |

Where (i) $log(Ah) = 0.014 + 0.30I$ (I: Intensity in ISC scale) (ii) $a(gal) = 0.45 * 10^{S/2}$ (S: Intensity in JMA scale).

transitions through the discontinuity surfaces, i.e. at impacts or switches between different vector fields of the system. Such transitions are called events and are triggered by zero crossings of scalar valued event functions. Matlab solvers (such as ode45) contains built in routines for detecting zero crossings of event functions have therefore been used here.

The structural model defined by eq. (13) is the basis of the numerical analysis.

We present the expression as a first order system (non-smooth, non-stiff differential systems $y'(t) = f(t, y(t)), y(0) = y_0 \in R^m, t \in [t_0, t_f]$) with two components:

$$\begin{cases} y_1(t) = x(t) \\ y_2(t) = \dot{x}(t) \end{cases} \tag{17}$$

Then

$$\dot{y} = \begin{pmatrix} \dot{y}_1 \\ \dot{y}_2 \end{pmatrix} = \left\{ \begin{pmatrix} y_2 \\ -4.1\, y_2 - 210.125\, y_1 - u(y_1, y_2) - e(t) \end{pmatrix} = f(t, y) \tag{18} \right.$$

For noise intensity $\xi(t) \neq 0$.

The numerical scheme used to find the probability density function (PDF) is based on the Euler version algorithm. We introduce a smooth function which approximates the discontinuous drift (see appendix) and apply the Euler method with this input. The influence of the control gains $\alpha_0 = (\mu N)$ determines how quick the evolution of the sequence $\{x\}$ $n \geq 0$ switches around zero. In other words, a big $\alpha_0$ minimizes the influence of the random variable $\xi$. The results of this numerical investigation are shown in Figs. (2, 3).

The chosen parameters are: $\alpha_0 = 0.005; k = 210.125; c = 2.47e\,10^6; \nu = 0.005$ [20].

For $\xi(t) = 0$

In the numerical analysis, the spillway is modelled as a single-degree-of-freedom system as shown in Fig. 1.

The resulting system of second order equation is recast as a system of first order ordinary differential equations and solved using Matlab ode solvers (such as ode45). We recognize that at some positions $x(t) = y_1(t) = \nu$ or if $x(t) = y_1(t) > \nu$ and $\dot{x}(t) = y_2(t) = 0$ the vector field $f(t, y)$ is non-smooth. We can observe two switching surfaces $g_1(y) = (y_1 - \nu)$ and $g_2(y) = y_2$. Moreover, the discontinuity limit (abutment area) $\Sigma$ separating the two areas is described as $\Sigma = \{x \in R^n: H(x) = 0\}$, where H is a smooth scalar function with non-vanishing gradient: $H_x(x) = \frac{\partial H(x)}{\partial x}$ on the

discontinuity separation $\Sigma$ (See appendix A).

### 4.2. Pounding between a spillway and an abutment: structural stability

Stability here leads the ultimate fate of the dynamics for perturbations of the initial conditions. Structural stability sometimes, deals with perturbation of the system itself, i.e. perturbations of the own system, including parameter variations. Knowing that the impact force term, $v(y,\dot{y})$ (an intermittent nonlinear discontinuous force), force between two masses, the notion of structural stability is broadened to also encompass a preservation in the event sequence, i.e. the order and number of interactions with discontinuity surfaces. This impact force $v(y, \dot{y})$ illustrated the same behavior as relations eqs. (2) and (8) in the sense of discontinuities. The abutment is a transversal barrier i.e. $\Sigma = \{x \in R^n: H(x) = 0\}$, where H is a smooth scalar function with non-vanishing gradient $H_x(x) = \frac{\partial H(x)}{\partial x}$ on the discontinuity separation $\Sigma$.

Two switching surfaces $g_1(t, y, y_0) = (y - 0.005)$ (spillway's area) and $g_2(t, y, y_0) = y_0$ (after the abutment) are defined. ($\nu = 0.005 =$ Poisson's ratio of the soil). When defining the time impact-contact in between $t \in [0,3]$, the response crosses the surface $g_1$ (area of the spillway) twelve times and the surface $g_2$ (region after the abutment) six times. Hence the data corresponding to 18 switching points (i.e. impact-contact) defined in table (4).

### 5. Discussion

During an earthquake the ground motion is often defined by a time history of the ground acceleration. It can be obtained in three directions by instruments known as strong-motion accelerographs. When increasing the probability of pounding during an earthquake, it is verified that strong ground motion in the near-field area has different characteristics [26,27]. A more advanced dynamic friction model has to be developed, or to be utilized for systems containing high variations of normal load, namely with impact-friction conditions. We have defined two characteristics of noise intensity in Figures (2, 3): very low noise intensity and weak noise. We observed a high probability density function (PDF) for $D = (0.0001; 0.00002; 0.00004)$, but the peak of this PDF reduces with the increasing of noise. The amplitude of propagation is reduced. Fig. (3) (a, b, c, d) shows the same observation of appearance of p-bifurcation at very low noise intensities with height PDF and p-bifurcation ceases to occur when noise intensity increases [28–30].

In Fig. (3) (e, f), we fixed $p_0$, the amplitude of external excitation and varying noise intensity. We observed large oscillation with large amplitude at weak noise intensity. Hence p-bifurcation occurs. The instability of the system is verified. The behavior of the system diminishes with the increase of noise. We can summarize these two Figures saying that during earthquake excitation, for the impact-friction events at very low noise intensity, p-bifurcation occurs and created instability that will increase pounding effects. The near-field buildings will be impacting and destruct. The disasters will be very pronounced if the amplitude of earthquake excitation $p_0$ of sine wave is big [31,32].
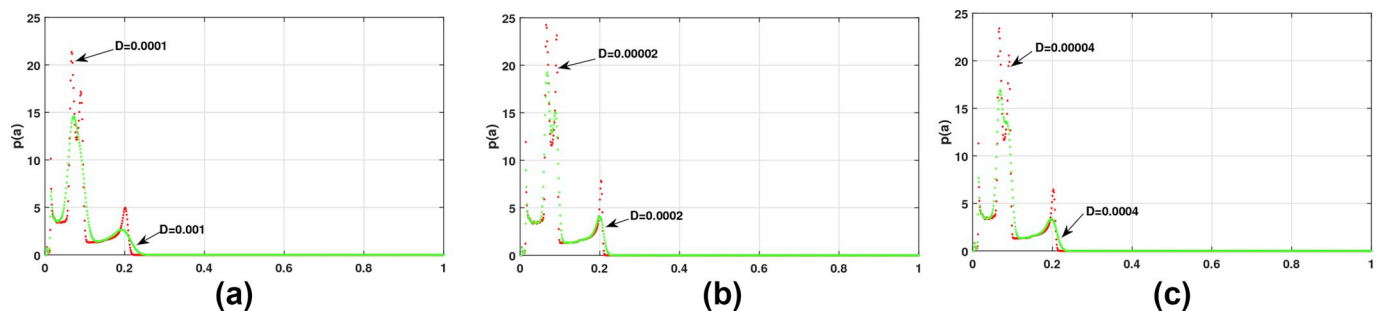


**Fig. 2.** Stationary amplitude distribution and varied values of the noise intensity D: $k = 210.125; c = 2.47e+6; \nu = 0.005$: (a) $D = 0.0001, D = 0.001$ (b) $D = 0.00002, D = 0.0002$ (c) $D = 0.00004, D = 0.0004$.
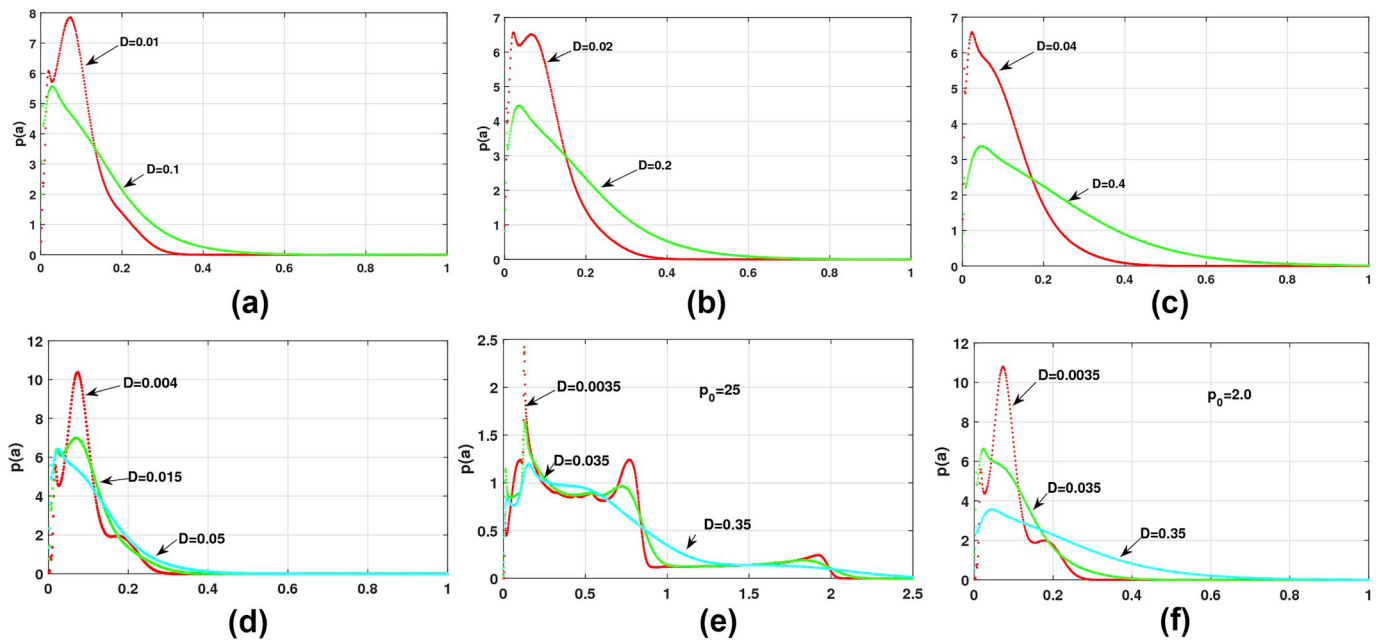
**Fig. 3.** Stationary amplitude distribution and varied values of the noise intensity D: $k = 210.125$; $c = 2.47e+6$; $\nu = 0.005$: (a) $D = 0.01$, $D = 0.1$ (b) $D = 0.02$, $D = 0.2$ (c) $D = 0.04$, $D = 0.4$; (d) $D = 0.004$, $D = 0.015$, $D = 0.05$; (e) amplitude $p_0 = 25$; (f) amplitude $p_0 = 2.0$.

The seismic perturbation decreases with the decreasing of $p_0$. In the same manner, when increasing noise intensity during impact-friction events, p-bifurcation occurs but at very low PDF, and the amplitude of oscillation is reduced, so that pounding effects is diminished for near-field buildings. We can note a relationship between impact-friction events saying that, small noise intensity means continuous friction, hence high PDF, but if the noise intensity is great, the impact event seems important with weak PDF. But successive jump effects can create continuous friction and impacting and the pounding force will influence [33–35].

The phenomenon of stick-slip is also very important during pounding effects at near-field buildings during the seismic wave propagation.

Fig. (4) shows the dynamic of the transition of the wave. We reminder that $\nu$ is the Poisson's ratio of the soil.

Talking about the switching surface $g_2$, the vector field is discontinuous only when $\dot{x}$ changes from positive to negative. This can appear when the space position $x > \nu$. Sometimes, the function defining the vector field at the region $g_1(y) > 0$ is not defined when $g_1(y) < 0$ due to the two fractional incommensurable powers $\frac{1}{4}$ and $\frac{3}{2}$ As we have said in appendix A, f the vector field continuous function. Therefore, $f_+(t_d, y_d) = f_-(t_d, y_d)$ at the switching points and the transversality (in the abutments) condition is satisfied unless the vector field is tangent to the switching surface (see Fig. (4)). The red horizontal lines that is drawn in fig. (4) (b, e)) are the discontinuous regions corresponding to the
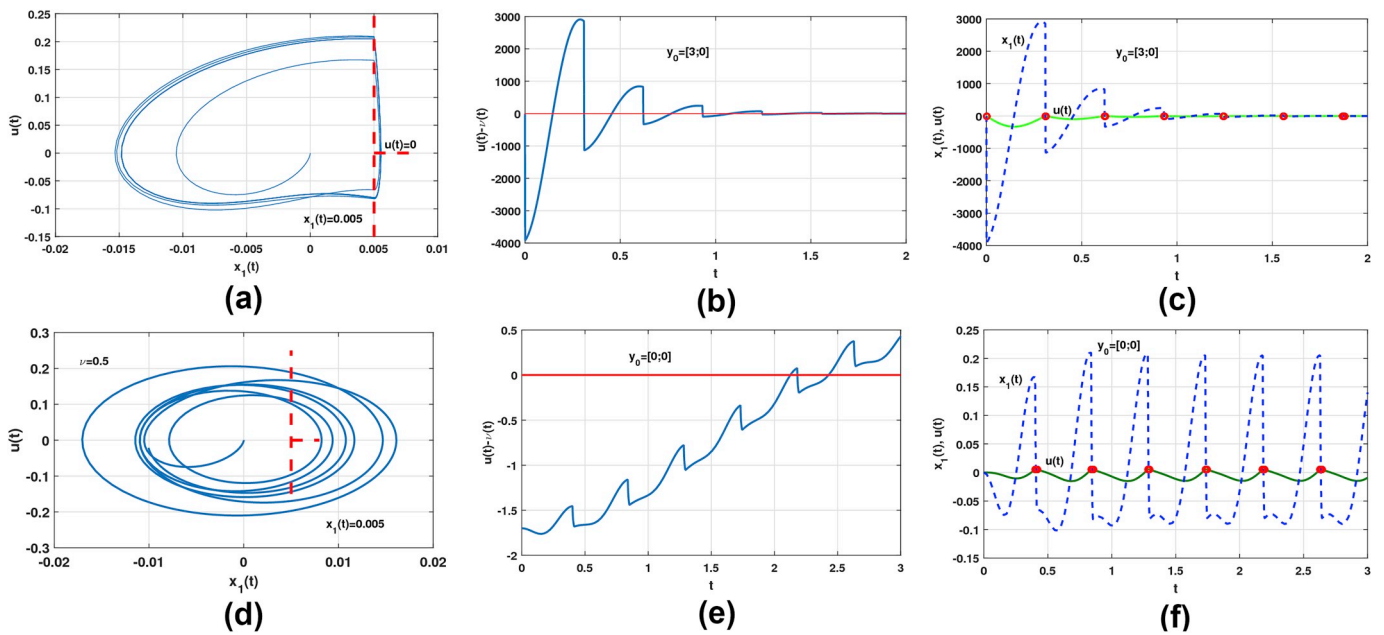


**Fig. 4.** Dynamics at the transition from stick to slip: the discontinuity points are indicated by means of small circles $k = 210.125$; $c = 2.47e+6$; $\nu = 0.005$; (a) $y_0 = [3,0]$: phase diagram, (b) $y_0 = [3,0]$: solution against time (c) $y_0 = [3,0]$: solution and derivative against time; (d) phase diagram $y_0 = [0,0]$, $\nu = 0.5$ (e) $y_0 = [0,0]$: solution and derivative against time (f) $y_0 = [0,0]$: solution and derivative against time.

**Table 4**

Occurrence of discontinuities corresponding to contact-impact friction and displacement of structures during earthquake excitation.

| time (s) | displacement of the spillway ($g_1$) | abutment (transversal region) | region $g_2$ |
|---|---|---|---|
| 0.4006 | 0.0050 | 1 | 0.1664 |
| 0.4071 | 0.0055 | 2 | 0.0000 |
| 0.4172 | 0.0050 | 1 | −0.0658 |
| 0.8384 | 0.0050 | 1 | 0.2095 |
| 0.8446 | 0.0055 | 2 | 0.0000 |
| 0.8543 | 0.0050 | 1 | −0.0820 |
| 1.2818 | 0.0050 | 1 | 0.2079 |
| 1.2880 | 0.0055 | 2 | −0.0000 |
| 1.2977 | 0.0050 | 1 | −0.0811 |
| 1.7307 | 0.0050 | 1 | 0.2048 |
| 1.7368 | 0.0055 | 2 | 0.0000 |
| 1.7467 | 0.0050 | 1 | −0.0799 |
| 2.1798 | 0.0050 | 1 | 0.2047 |
| 2.1860 | 0.0055 | 2 | 0.0000 |
| 2.1958 | 0.0050 | 1 | −0.0799 |
| 2.6286 | 0.0050 | 1 | 0.2049 |
| 2.6348 | 0.0055 | 2 | 0.0000 |
| 2.6446 | 0.0050 | 1 | −0.0799 |

abutments. Hence the gradient $\nabla g_1(y) \cdot f(t, y) = 1$ for all y and $\nabla g_2(y) = -210.125\, y_1 - c(y_1 - \nu)^{\frac{3}{2}} - r(t)$ for switching points such that $y_2 = 0$. The discontinuity points corresponding to contact-impact areas between spillway and abutments are indicated by means of small red circles (see Fig. (4) (c, f)).

It can be verified that, the transversality condition is satisfied. But this affirmation is not sure in some transitions points as: $y_2 = \dot{x} = 0, y_1 = x > \nu$ and $-210.125\, x(t) - c(x(t) - \nu)^{\frac{3}{2}} - e(t) = 0$ (see Fig. (4) (d, e)) Since $|e(t)| \leq 2$, and $|e(t)| \leq 25$ the switching points are transversal. The phase diagrams ($x_1$ versus $\dot{x}$) are founded in Fig. 4)(a, d).

In Fig. (4) (b, c, f), the response, with the considered initial conditions, passes first through a transversal discontinuity (abutment), then it enters a sliding region for a short time until it exits it. After, it passes through two transversal discontinuities and enters into another sliding region.

The red dashed lines denote the switching points (not continuous in the third derivative $x(t)'''$).

For reminder: The discontinuity points i.e. contact-impact regions (where the third derivative $\ddot{x}(t)$ is not continuous) are indicated by means of small circles. To recognize the sliding regions, see Fig. 4) (b, c, e, f). The function $(u(t) - \nu(t))$ is at the switching region. The sliding zones represent to the intervals at which the functions vanish. (the dashed lines correspond to the switching surfaces in the phase diagrams plot 4(a, d))

We can summarize Fig. 4 saying that for $t_2 \in [0,3]$ the solution crosses the surface $g_1$ twelve times and the surface $g_2$ six times. In all the cases the discontinuity is transversal. We would like to mention that when considering the initial conditions, the response, passes first

through a transversal discontinuity, then it gets in a sliding area for a small time until it exits it, then it continues through two transversal discontinuities and then it enters into another sliding region. The response with $'-'$ in region $g_2$ means that the solution exits from the sliding region. The positive elements in that table mean that these discontinuities are transversal (see Table 4).

- A further overview of the selected earthquakes is given in Figure (5)

Figure (5) shows the magnitude and recorded peak acceleration in relation to the distance to the earthquake epicenters but also the peak acceleration versus the magnitude of the earthquakes. The acceleration values are the absolute maximum values for each direction and the plotted values are on the one hand the peak ground acceleration (PGA) recorded in the basement of the spillway foundation. These values do not represent a total horizontal acceleration component but the highest value of both sensors recording in one direction and the highest value of the other direction sensor and it should be emphasized that both of those peak values of acceleration are not expected to occur at the exact same time. Although Fig.(5)(b) seems to indicate that the peak acceleration grows with longer distance to the epicenters, which is of course not the general case, it is important to see in Fig.(5)(a) that the earthquakes whose epicenters are the furthest away from the project were generally of greater magnitude than those with epicenters closer to the edifice. The intensity of pounding in neighboring structures due to earthquake is depended by many factors: The Peak Ground Acceleration (PGA) of the earthquake, the distances of separation between the buildings, soil configurations …

## 6. Conclusion

To preserve structural integrity and prevent damage and injury to contents, numerous studies must be done to understand the stochastic effect of seismic wave. With a monitoring system installed and supplying full scale records of the structure response, considerable amount of data will be available for investigation to avoid disaster during seismic events. The required gap to avoid pounding is significantly determined by the table showing the impact-contact (displacement) between the spillway and the abutment. Under certain conditions, the properties of the supporting soil must also be taken into consideration due to its influence on the impact-friction events. During collision, the forces produced act over a short period of time, due to random molecular vibrations and the internal friction of the colliding bodies, energy is dissipated as heat. If pounding appears in a foundation of buildings it can be harmful. The impact forces that act during pounding can cause additional sliding of the concrete or steel of the building. With high noise intensity during the impact-friction effects, the pounding force is influenced. P-bifurcation occurs with small peak of PDF. But weak noise intensity created a large probability density function (PDF) (because of continuous sliding), hence a great value of pounding force. The impact



**Fig. 5.** Peak ground acceleration: (a) Earthquake magnitude in relation to distance to epicenters, (b) Peak acceleration in relation to distance to epicenters. The dots represent the peak ground acceleration (c) Peak acceleration in relation to earthquake magnitude. The dots represent the peak ground acceleration.

in this case is not big (friction is greater than impacting). If noise intensity increases, (the impact is greater than friction), the pounding effects diminishes. In the case of successive jump-impact friction, friction and impact events can be proportional. Hence friction increases the pounding effects. For the case of spillway and abutments, the calculation must take in view for different loading cases, it mainly includes calculation of sliding stability, overturning stability and stress under foundation. It is found that the relative displacements of the spillway can be obtained by calculating the impact contact points of discontinuities of the system, which cannot be accessible without considering pounding phenomena.

## Declaration of competing interest

The authors declare that they have no conflict of interest.

## Appendix A

In the discontinuous differential system, f (x) is not well defined when the position x is on the discontinuity surface $\Sigma$. A way to define the vector field on $\Sigma$ is to consider the Filippov approach, that is the set valued extension F(x) below

$$\dot{x}\varepsilon\, F(x) = \begin{cases} f_+(x,\ \mu), & x \in S_1 \\ \overline{co}\{f_+(x,\ \mu), f_-(x,\ \mu)\}, & x \in \sum \\ f_-(x,\ \mu), & x \in S_2 \end{cases} \tag{19}$$

where $(f_+(x),\ f-(x))$ are given by the smooth functions, and $\overline{co}\{A\}$, is a vector field along the separation boundary. It represents the smallest closed convex set containing A.

$\overline{co}\{f_+, f_-\} = \{f_F\colon x \in R^n \to R^n\colon f_F = (1-\alpha)f_+ + \alpha f_-,\ \alpha \in [0,1]\}$, then the system vector field can be described by a differential inclusion (systems with multi valued right-hand sides).

## Appendix B

Approximation of Sign-Function: Due to the lack of continuity, we have construct a function $f_N(x)$ which has pointwise convergence to the sign-function as N → ∞.

$$f_N(x) = \begin{cases} 1, & for \qquad x > \dfrac{1}{N}; \\ \dfrac{-N^3 x^3}{2} + \dfrac{3\,N\,x}{2}\colon & for \qquad \left(-\dfrac{1}{N} \le x \le \dfrac{1}{N}\right) \\ -1, & for \qquad x < \dfrac{1}{N} \end{cases}$$

We used $f_N(x)$ in order to avoid the discontinuous challenges by the sign function.

## Appendix A.  Supplementary data

Supplementary data to this article can be found online at https://doi.org/10.1016/j.soildyn.2020.106065.

## References

[1] Rosenblueth E, Meli R. The 1985 earthquake: causes and effects in Mexico City. Concr Int 1986;8:23–34.
[2] Von Kluge Ndy P, Djuidjé Kenmoé G, Kofané TC. Dry friction with various frictions laws: from wave modulated orbit to stick−slip modulated. Mod Mech Eng 2015;5:28–40.
[3] Jing H-S, Young M. Impact interactions between two vibration systems under random excitation. Earthq Eng Struct Dynam 1991;20:667–81.
[4] Pantelides CP, Ma X. Linear and nonlinear pounding of structural systems. Comput Struct 1998;66:79–92.
[5] Chau KT, Wei XX. Pounding of structures modelled as non-linear impacts of two oscillators. Earthq Eng Struct Dynam 2001;30:633–51.
[6] Liu Chengqing, Yang Wei, Yan Zhengxi, Lu Zheng, Luo Nan. Base pounding model and response analysis of base-isolated structures under earthquake excitation. Appl Sci 2017;7:1238. https://doi.org/10.3390/app7121238.
[7] Baber TT, Wen Y-K. Stochastic response of multistory yielding frames'. Earthq Eng Struct Dynam 1982;10:403–16.
[8] Li J, Chen JB. Probability density evolution method for dynamic response analysis of stochastic structures. In: Zhu WQ, Cai GQ, Zhang RC, editors. Advances in stochastic structural dynamics. Proceedings of the 5th international conference on stochastic structural Dynamics−SSD03, Hangzhou, China. Boca Raton: CRC Press; 2003. p. 309–16.
[9] Anagnostopoulos SA. Pounding of buildings in series during earthquakes. Earthq Eng Struct Dynam 1988;16:443–56.
[10] Jankowski R, Wilde K, Fujino Y. Reduction of pounding effects in elevated bridges during earthquakes. Earthq Eng Struct Dynam 2000;29:195–212.
[11] Dimitrakopoulos EG. Seismic response analysis of skew bridges with pounding deck abutment joints. Eng Struct 2011;33(3):813–26.
[12] Ndy Von Kluge P, Djuidjé Kenmoé G, Kofané TC. Application to nonlinear mechanical systems with dry friction: hard bifurcation in SD oscillator. SN Appl. Sci. 2019;1:1140. https://doi.org/10.1007/s42452−019−0987−1.
[13] James H. Dieterich, time-dependent friction in rock. J Geophys Res july10,1972;77 (20).
[14] Rice JR, Ruina AL. Stability of steady frictional slipping. J Appl Mech 1983;50:343–9.
[15] Rice James R, Lapusta Nadia, Ranjith K. Rate and state dependent friction and the stability of sliding between elastically deformable solids. J Mech Phys Solid 2001;49:1865–98.
[16] Paz M. Structural dynamics: theory and computation. fourth ed. New York: Chapman and Hall; 1997.
[17] Chopra A. Dynamics of structures: theory and application to earthquake engineering. second ed. Upper Saddle River: Prentice-Hall; 2001.
[18] Chau KT, Wei XX. Pounding of structures modelled as non-linear impacts of two oscillators. Earthq Eng Struct Dynam 2001;30:633–51.
[19] Jean-Pierre Magnan, Description, identification et classification des sols. Doc. C 208.
[20] Jankowski Robert. Non-linear viscoelastic modelling of earthquake-induced structural pounding. Earthq Eng Struct Dynam 2005;34:595–611.
[21] Chopra A. Dynamics of structures: theory and application to earthquake engineering. second ed. Upper Saddle River: Prentice-Hall; 2001.
[22] Zhu P, Abe M, Fujino Y. Modelling three-dimensional non-linear seismic performance of elevated bridges with emphasis on pounding of girders. Earthq Eng Struct Dynam 2002;31:1891–913.
[23] Annual Geophysics, 4, B,6,11, August 1986, pp.679 − 702.
[24] Cornell, 1968.
[25] Trifunac and Brady, 1975.
[26] Maison BF, Kasai K. Dynamics of pounding when two buildings collide. Earthq Eng Struct Dynam 1992;21:771–86.

[27] Anagnostopoulos SA, Spiliopoulos KV. An investigation of earthquake induced pounding between adjacent buildings. Earthq Eng Struct Dynam 1992;21:289–302.

[28] Zakharova A, Vadivasova T, Anishchenko V, Koseska A, Kurths J. Stochastic bifurcations and coherence like resonance in a self−sustained bistable noisy oscillator. Phys Rev 2010;81. 0111061 − 6.

[29] Xu Y, Gu RC, Zhang HQ, Xu W, Duan JQ. Stochastic bifurcations in a bistable Duffing-Van der Pol oscillator with colored noise. Phys. Rev. E 2011;83:056215.

[30] Mbakob Yonkeua R, Yamapi R, Filatrella G, Tchawoua C. Stochastic bifurcations induced by correlated noise in a birhythmic vander Pol system. Commun Nonlinear Sci Numer Simulat 2016;33:70–84.

[31] Hao H, Zhang SR. Spatial ground motion effect on relative displacement of adjacent building structures. Earthq Eng Struct Dynam 1999;28:333–49.

[32] Jankowski R, Wilde K. A simple method of conditional random field simulation of ground motions for long structures. Eng Struct 2000;22:552–61.

[33] Lin JH, Weng CC. Probability analysis of seismic pounding of adjacent buildings. Earthq Eng Struct Dynam 2001;30(10):1539–57.

[34] Lin Jeng-Hsiang, Weng Cheng-Chiang. A study on seismic pounding probability of buildings in Taipei metropolitan area. J Chin Inst Eng 2002;25(2):123–35. https://doi.org/10.1080/02533839.2002.9670687.

[35] Lin JH, Weng CC. Seismic pounding risk analysis of adjacent buildings. In: Proceedings, Conference on Computer Applications in Civil and Hydraulic Engineering. 2; 2000. p. 2049–58.